CHARACTERIZATION AND GROUND-WATER FLOW MODELING OF THE MINT

WASH / WILLIAMSON VALLEY AREA, YAVAPAI COUNTY


By Luis Fernando Navarro


A Thesis

Submitted in Partial Fulfillment

of the Requirements for the Degree of

Master of Science

in Geology


Northern Arizona University

May 2002


Approved:


<u>Abraham E. Springer, Ph.D., Chair</u>


<u>Paul J. Umhoefer, Ph.D.</u>


<u>Charles M. Schlinger, Ph.D.</u>

ABSTRACT

CHARACTERIZATION AND GROUND-WATER FLOW MODELING OF THE MINT

WASH / WILLIAMSON VALLEY AREA, YAVAPAI COUNTY

LUIS FERNANDO NAVARRO

The characterization of the Mint Wash / Williamson Valley System (MWWVS) is a

combination of geological and hydrogeological characterization of the Mint Wash / Williamson

Valley area. The characterization was used to construct a ground-water flow model, used to

research the water supply of the area.

The geological characterization included data from previous investigations as well as

data gathered through this study. The results include a geologic map, cross sections throughout

the site, a synopsis of the known geological history of the area, including the identification of

lithologies, and a description of the tectonic history of the area.

The hydrogeological characterization included analyses of existing data, and collection

and analyses of new data. A conceptual model was developed from preliminary analyses of

data, then modified as more data was gathered.

The characterization was used in the development of a three-dimensional finite-

difference ground-water flow model. The model was calibrated to both the steady-state and

transient conditions. The calibrated model was used to simulate MWWVS using several

different water use scenarios and to compare these scenarios to the concept of sustainable

yield. Sustainable yield was defined as yield that would not significantly affect the availability of ground water to riparian habitat and perennial springs.

The results of the model indicates that the system currently does not exceed sustainable yield. Some of the water use scenarios that represent regulatory limits as well as potential future water use in the MWWVA did exceed the sustainable yield criteria.

ACKNOWLEDGEMENTS

TABLE OF CONTENTS

LIST OF TABLES

# LIST OF FIGURES

LIST OF APPENDICES

## CHAPTER ONE

## INTRODUCTION

**Purpose and Objectives**

The purpose of this study of the Mint Wash and Williamson Valley system (MWWVS) and aquifer (MWWVA) was to determine a sustainable yield for the ground-water system. The focus was to use field investigations to characterize the geology of the area including previously documented work, as well as the current hydrological and hydrogeological systems. The characterization was the foundation for a numerical finite-difference three-dimensional ground-water flow model.

The objectives of this study were to characterize the geology and hydrogeology of the MWWVS (chapters 2 and 3) and to create a three-dimensional framework model of the study, conduct sensitivity analyses of the ground-water conditions using the ground-water flow model, and create predictive simulations using a transient model to investigate water use scenarios (Chapter 4). Other objectives included estimating the volume of water stored within the aquifer during the time of study, determining the amount of water that could be discharged anthropogenically over the study period without exceeding sustainable yield, determining the location of  natural discharge  of the Mint Wash / Williamson Valley ground-water system, and

1

investigating connections to adjacent ground-water basins.


**Location**

The Mint Wash and Williamson Valley area is located in the Transition Zone physiographic province in central Arizona. The site is approximately 10 miles northwest of the City of Prescott (Figure 1). The region encompasses approximately 480 square kilometers (175 square miles) of semi-arid grassland. The project site is bound to the south by Granite Basin, to the east by a discontinuous linear range comprised of the Sullivan Buttes and Table Mountain, to the west by the foothills of the Santa Maria Mountains, and to the north by the confluence of the Big Chino and Williamson Valley sub-basins (Figure 1). The southern boundary is a surface and ground-water divide (Figure 2). The eastern boundary represented by the Sullivan Buttes and Table Mountain is a surface-water divide and is assumed to be the ground-water divide between the Mint Wash / Williamson Valley aquifer and the Little Chino aquifer in a study conducted by the Arizona Department of Water Resources (Corkhill and Mason 1995). The crest of the Santa Maria mountain range to the west is a surface-water divide and in this study is assumed to be the ground-water divide. The northern boundary is a surface-water and ground-water confluence, where the water from the Mint Wash / Williamson Valley ground-water system joins the water from the larger Big Chino Valley ground-water system.

**Significance of Problem**

Central Yavapai County has a rapidly growing population, which has more than doubled since the 1980 census (Arizona Department of Economic Security 1999). The population in Yavapai County in 1980 was 68,145, increasing to 142,075 by 1997 (Arizona Department of Economic Security 1999). The cities of Prescott and Prescott Valley and surrounding areas are being developed to accommodate the increase in population, which is occurring mostly in this region of central Yavapai County. Mining of central Yavapai County's ground-water supply has become a major concern due to this increase in population and development. Water resource development in the Mint Wash and Williamson Valley area will rely exclusively on ground water, as there are very limited perennial surface water supplies, and no water is imported to the area from the Colorado River or any other external source.

Most of the ground-water supply in the area of Chino Valley, Prescott and Prescott Valley is protected by the Prescott Active Management Area (AMA). It is an area overseen by a state regulatory agency run by the Arizona Department of Water Resources to regulate the rate of ground water pumping to "safe yield" (Corkhill and Mason 1995). "Safe yield" is the condition where the amount of ground water pumped out of an aquifer each year does not exceed the amount of water that is naturally recharged to the aquifer during that year. The Ground Water Act of 1980 proposed safe yield for all AMA's in Arizona by the year 2025 (Corkhill and Mason 1995).

The Mint Wash / Williamson Valley Aquifer (MWWVA) is outside of the Prescott

AMA. This aquifer is not protected by any state agencies against ground-water mining, so development on the Mint Wash / Williamson Valley area has proceeded without regard for exceeding "safe yield". Any restrictions on development in the Prescott AMA may be compensated for by increased development in the surrounding areas such as Mint Wash and Williamson Valley. Residents of the MWWVS have expressed concern about how quickly water will be mined due to recent development in the area.

Wildlife and vegetation in the region are dependent on ground water, as well. The MWWVA is unique in central Arizona due to the shallow water table (0.10 meters to 3.0 meters) in the Valley and along the major washes. The ground water has provided water resources for riparian ecosystems dependent on the shallow water table. The riparian habitat found in the area is one of the aspects that makes this ground-water basin unique. Less than 1% of the land in the state of Arizona contains riparian habitat (Briggs 1996). Many reaches of the major washes have perennial springs where the water table intersects land surface. These springs are a water resource for wildlife such as antelope, javelina, migrating Canadian geese, mountain lions, and many others (Maslansky 2000). The process of ground-water mining over time will lower the water table, depleting and possibly removing the ability of the aquifer to support the riparian ecosystem as well as the perennial springs.

Natural resources need to be considered to successfully introduce long term human development into any natural setting. The project study area is a region that depends on it's water resources to maintain the ecosystem that has evolved. Characterizing the ground-water system through field observations and sensitivity analyses will provide insight on the water

4

resource that is crucial to the ecosystem in this area. Ground-water flow modeling provided a

platform to produce predictive results to interpret how the ground-water system would react to

different water use scenarios.


**Previous Investigations**

The amount of published work on the study area is limited. There is only one published

hydrological study within the MWWVS. This Water Resources Investigation produced maps

for the ground water conditions in Williamson Valley alluvial basin during 1975 (Wallace and

Laney 1976). Other hydrological studies (e.g. The Ground Water Supply of Little Chino Valley

(Matlock and Davis 1972), etc.) described basins surrounding the Prescott area. The only

published geological studies within the field area are reconnaissance geologic maps of the

project and surrounding areas at a 1:62,500 scale (Krieger 1967a and 1967b). These were

referred to and field checked as part of the creation of the geologic map (Plate 1).

The map for this study has one improvement in the lithological classification presented in

the geologic map developed by Krieger. Current literature describes the Tertiary andesite found

in this area to be Tertiary latite (Krieger et al. 1971).

Two ground-water models have been produced for the Prescott AMA, which includes

the Little Chino Basin and the Upper Agua Fria Sub-basin. These studies were completed by

the Arizona Department of Water Resources (Corkhill and Mason 1995) and Southwestern

Ground-water Consultants, Inc. (Wellendorf 1998) and produced ground-water models for the

Prescott AMA to quantify "safe yield". A subsequent study by Woessner (1998) compared the

accuracy of the two models, which had produced different results.  The comparison of the two models described the significance of the input parameters, and how they affect the ability of the models to simulate various stresses on the system. The studies provide a basic understanding of ground water systems in the general area.

Other studies in the Prescott vicinity include "Little Chino Valley, Artesian Area and Groundwater Basin" (Schwalen 1967). The Little Chino Basin is to the east of the MWWVS. The basins are separated by a discontinuous north-south trending range composed of Tertiary volcanic rocks (Table Mountain and Sullivan Buttes), uplifted Paleozoic Redwall and Martin Formations (Sullivan Buttes), and Proterozoic schist and gneiss (Plate 1). These basins are very similar due to their proximity, geomorphic similarity and the regional tectonics responsible for their formation.

Little Chino Valley was characterized in other studies such as "The Groundwater Supply of Little Chino Valley" (Matlock and Davis 1972) and "Definition and paleogeographic significance of Cenozoic stratigraphic units, Chino-Lonesome Valley, Yavapai County, Arizona" (Buren 1992).

These publications provide an understanding of the Chino Valley geology and hydrogeology, similar to the geology and hydrogeology of the MWWVS. The literature available for the Little Chino and Upper Agua Fria Sub-basins provides a framework for the general geology and hydrogeology of the Prescott area.
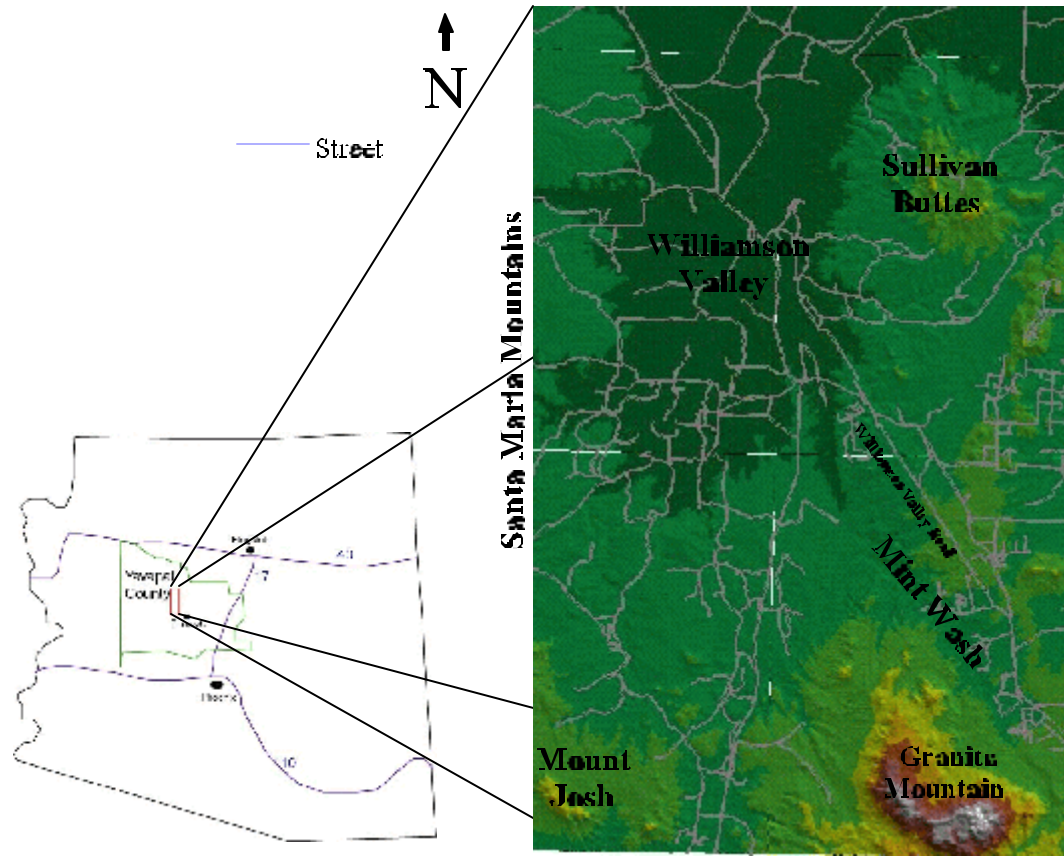
**Figure 1.** Map showing the location of the Mint Wash / Williamson Valley system, and shaded relief of the topography.

# CHAPTER TWO

## GEOLOGICAL CHARACTERIZATION

**Purpose and Objectives**

An important component of this study was to summarize the geology of the Mint Wash / Williamson Valley System (MWWVS). Geologic studies for the study area available to the public are limited. The results of this study have been combined with the results of previous studies to provide a cumulative summary of the known geology of the area. This study describes the basic geology of the Mint Wash / Williamson Valley area, including lithologies, structure and basin formation.

The geological characterization includes a geologic map (Plate 1), cross sections throughout the study area (Figures 5-9), fracture orientations of the Proterozoic granite (Figure 10), fault orientation, tectonic classification of the basin, a stratigraphic column (Figure 11), and stream bed mapping. These features provide insight on the geologic history of the area, as well as the causes for the formation of the basin.

**Introduction**

      The MWWVS is located within the Transition Zone physiographic province (Figure 2). The Transition Zone represents a gradation from the Colorado Plateau to the Basin and Range physiographic province. The basin in the MWWVS shows morphological trends similar to those common in the Basin and Range (Figure 1).

      The MWWVS has rocks from the Proterozoic eon, and Paleozoic and Cenozoic eras (Krieger 1967a and 1967b). The Mesozoic Era appears to have been a time of erosion or no active deposition for the area, as there are no lithologies of Mesozoic age (Krieger 1967a and 1967b).

**Methods**

*Geologic Map*

      A geologic map was created and revised using traditional field mapping techniques as well as aerial photography. Aerial photography was available for the southern half of the field area and was provided by the National Forest Service (NFS 2000). Field mapping was conducted on 1:24,000 USGS quadrangles using a Brunton transit and a protractor to map the location of contacts relative to landmarks.

      Krieger's (1967) 1:62,500 scale maps were used during several reconnaissance trips to verify the contacts that were easily accessible. Areas that were difficult to access were mapped during two, week-long field trips, and subsequently compared to the maps produced by

Krieger. Most of the alluvium was mapped in the field. Areas that were inaccessible were

mapped using aerial photography. There were several areas where alluvium was not mapped

by Krieger but was included in the map produced in this study due to the difference in scale

between the two maps. Krieger's (1967) maps were found to be accurate and not many

alterations were made except for some detail of the contacts along the Sullivan Buttes.

Most of the field mapping was completed during a week long field trip in August, 1999.

Accessible areas were visited during monitoring trips. The geologic map was finalized during a

week long field trip in July, 2000 and subsequent aerial photo interpretation in the office.

The geologic map was digitized in ArcView (ESRI 1999), using a large digitizing tablet

and the hard copy quadrangles that were used in the field. The lithologies were represented as

geo-referenced polygons in ArcView.  Digital Elevation Models (DEM) for the area were

provided by the Arizona Land Resource Information System (ALRIS 2000). The DEMs were

imported to ArcView and contoured. The contoured surfaces were overlain by the digitized

polygons representing the lithologies.

Cultural feature GIS data was also provided by the Arizona Land Resource Information

System. These coverages were imported into ArcView, and overlay the contoured surface as

well as the lithology coverages. The digital cultural feature data used in this map include washes,

faults, and Universal Transverse Mercator (UTM) coordinates. These data provide landmark

references for the lithologic mapping.

*Cross Sections*

The cross sections were created from surface maps and lithologic information recorded

on driller's logs for several wells throughout the study area. The location of the wells were

found using the ADWR well registry CD (ADWR 2000). The UTM coordinates for each of the

wells were imported into ArcView and plotted on the contoured surface of the DEMs with a

contour interval of 5 meters. The proximity of the wells to the contours was calculated, which

gave a precision of 2.5 meters for the well elevations.

The lithologic changes identified in the driller's logs were interpreted using knowledge

of the local geology provided by previous studies (Kreiger 1967). The stratigraphy between the

wells along the section line was assumed using the stratigraphic relation of the wells and

assuming that extensional tectonics were responsible for basin formation in the Tertiary.

*Fracture Orientation*

The average orientation of three sets of fractures within the granite was measured at

several points throughout the Granite Mountain Wilderness Area. The measurements were

taken to the north of the pluton apex at three sites where large outcrops of autochthonous

granite were found (Figure 4). The measurements were taken

to the north of the pluton apex because these sites are in the direction of the field area relative

to Granite Peak. The dominant fractures in a granite pluton are tension fractures and strike

radially from the apex of the granite pluton (Castro 1984). Tension fractures provide insight on

the emplacement of the granite pluton by striking radially from the granite pluton apex, and are

the major conduit for fluid flow within a granite pluton (Larsson 1972). Shear fractures tend to

have a smaller aperture than tension fractures and are usually less laterally extensive. Shear

fractures usually strike perpendicular to tension fractures, and are responsible for dispersive

fluid flow between the tension fractures (Larsson 1972).

*Stream Bed Mapping*

Grain-size analyses of the material within the washes were conducted. The sampling sites chosen are along the major washes within the study area. The sites within   each wash were chosen based on proximity to the sediment source and the accessibility of the desired sites.

The samples were collected by digging a 2 foot hole in the middle of the wash. The stratigraphy of the material was described, then samples were collected representative of the described section. The samples were then dry sieved and weighed to determine the percent grain-size distribution of the material.
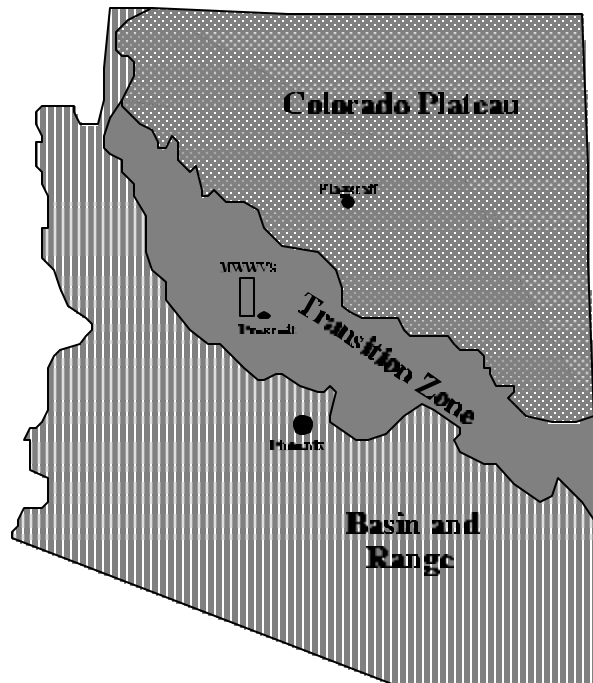
**Figure 2.** Physiographic provinces map of Arizona showing the location of the MWWVS.



**Figure 3.** Outcrop of Tertiary conglomerate in the MWWVS. Notice the cross bedding typical of fluvial environments. A-A' is approximately 20 feet.

**Results**

The results of the geological characterization include a geologic map of the study area (Plate 1), cross sections throughout the study area (Figures 5-9), a stereonet of the fracture orientations for portions of the granite pluton (Figure 10), a stratigraphic column of the MWWVS (Figure 11), and a map showing the sampling locations for the grain-size distribution analyses within the major washes of the Mint Wash / Williamson Valley area (Figure 26).

*Geologic Map*

The geologic map is included as Plate 1. The map displays the lithologies found within the study area, and land surface contours at a 40 meter interval.

The areal distribution of the lithologies is clear in the geologic map. There are distinct zones of lithologies based on age and morphology. The southern portion of the study area is mainly Proterozoic granite (pCg), Proterozoic gneiss and schist (Yavapai Series) (pCy), or a combination of the two (pCgy), with some volcanic deposits to the east and west of Granite Mountain. The existing apex of the granite pluton is the crest of Granite Mountain. Granite Mountain has been specifically identified as a porphyritic quartz monzonite (Krieger 1967b). A recent age of 1.72 Ga was measured using U-Pb dating of zircon (Dewitt 1999). To the north and west of Granite Mountain (Plate 1) is a metamorphic belt, which is the location of most of the Yavapai metamorphic series (pCy) present in the MWWVS (Kreiger 1967b).

Williamson Valley begins to the northwest of the metamorphic belt. The dominant lithology within Williamson Valley is a Tertiary conglomerate that consists of the Paulden Formation and Perkinsville Unit. The conglomerate is fluvial based on common cross bedding

14

(Figure 3) (Buren 1992). The clasts in the conglomerate consist mainly of Proterozoic granite, gneiss, and schist, consistent with the description of one of the facies within the Paulden Formation.

Volcanic deposits are common in the northern portion of the MWWVS and consist of latite (Tl) and basalt (Tb) of Tertiary age. Volcanic deposits are centralized along the eastern boundary of the study area.

The concentration of Tertiary volcanic deposits and faults along the eastern boundary of the study area indicates that there was tectonic activity in this area during the Tertiary. The deposits are linear, and in the northern half of the area are coincidental with topographic relief. Previously mapped and inferred faults trend parallel to the topographic relief (Plate 1). The previously documented faults are defined as normal, which is consistent with the inferred faults, determined to be normal through the documented tectonic history, as well as the topographic relation and age of the units in contact at the faults.

The Sullivan Buttes represent the remnants of Tertiary volcanism. The dominant lithology of the buttes is Tertiary latite (Krieger 1967a and Krieger et al. 1971). At the surface the latite is highly eroded, however outcrops of Tertiary latite are visible along the flanks of the Sullivan Buttes.

Within the topographically higher Sullivan Buttes there are outcrops of Paleozoic and Proterozoic rocks. Williamson Valley consists of Tertiary conglomerate and Quaternary alluvium. Older lithologies along the buttes are topographically higher than younger lithologies in the basin, a scenario commonly related to extensional tectonism, mechanics that are known to

15

occur in the region during the Tertiary.

*Cross Sections*

The location of the section lines are plotted on Figure 4. The cross sections include two section lines that trend along the main washes, one along Williamson Valley Wash (Figure 5) and the other along Mint Wash (Figure 6). Three more cross sections were created traversing the valley and the general direction of surface-water flow (Figures 7, 8 and 9). The location and extent of the section lines are based on the availability of subsurface data provided by well logs and interpretation of the geological conceptualization.

Section lines A-A' and B-B' show the transition from a complex geologic setting influenced by the granite pluton in section B-B', to a flat "layer cake" type of stratigraphy in Williamson Valley along A-A'. The granite underlies the Tertiary conglomerate in Williamson Valley, but there are no wells that penetrate the entire thickness of the conglomerate to the depth of the contact between the granite and the conglomerate in the lower half of Williamson Valley. Initial interpretation of aero-magnetic data indicates that a dense rock underlies the conglomerate at approximately 274 meters / 900 feet. It is inferred that this lithology is the Proterozoic granite. No Paleozoic rocks have been identified within Williamson Valley. The lower half of Williamson Valley may contain Paleozoic rocks that have not been exposed within the existing wells. Wells in the upper half of Williamson Valley indicate an unconformity with Proterozoic units in contact with Tertiary units. The thickness of the Paulden Formation in the MWWVS has been estimated at 900 feet (274 meters) based on an initial interpretation of aero-magnetic data

16

recently collected by the United States Geological Survey (USGS) (Woodhouse 2000).

Williamson Valley has been the site of fluvial deposition since the Tertiary Period (Buren 1992).

Tertiary conglomerate is found stratigraphically higher than the Tertiary volcanics as shown in Figures 7 and 8. This is likely the equivalent of the Perkinsville unit, which is younger than the Paulden Formation and the Tertiary volcanics (Buren 1992). The conglomerate within Williamson Valley may be a combination of the Paulden Formation and the Perkinsville unit. Tertiary volcanics can be used to differentiate between the Paulden Formation and the Perkinsville unit, but no volcanics have been identified within Williamson Valley to distinguish which conglomerate unit is present in the valley.

Section line C-C' shows the subsurface from Williamson Valley to the Sullivan Buttes (Figure 8). The cross section supports the hypothesis of extensional tectonics occurring between the buttes and the valley. Devonian Martin Formation and Mississippian Redwall Limestone have been documented to be tilted in the area. The orientation of the dip is towards the east on the eastern range bounding Williamson Valley. The tilt of the Martin Formation and the Redwall Limestone is consistent with the topographical dip along the western range bounding Williamson Valley. The stratigraphically lowest plane (oldest) along the tilted block is in contact with younger units, which is indicative of extensional tectonics. There are inferred normal faults which serve as indicators of extensional tectonics in cross sections D-D' and E-E' (Figures 9 and 10). The faults mapped on the cross sections have a general strike to the north, which is similar to orientations of normal faults in the adjacent Basin and Range physiographic province (Plate 1). Several of the faults in the Sullivan Buttes area were mapped by Krieger

17

(1967), the inferred faults throughout the rest of the study area were mapped in this study.

*Fracture Orientation*

A stereonet was created of the fractures that were measured in the Granite Mountain Wilderness (Figure 11). The three tension fractures that were measured in the field consistently have a strike to the northwest with high angle dips to the northeast. The three shear fractures are relatively perpendicular to the tension fractures with high angle dips to the southeast. These results were expected given the location of the sample sites relative to the apex of the pluton. The fault orientations that were measured are representative of the fractures at the outcrops where they were measured. The locations where the orientations were measured were selected based on the outcrop. Most of the granite at the surface of Granite Mountain is colluvium. The locations selected represent outcrops of autochthonous granite. A radial pattern of fractures would be concentric on a stereonet if there were fault orientation sites completely around the pluton apex. The sites of fracture orientation for this study were located only to the north of the pluton apex (Figure11) and therefore only show tension fracture orientations to the north. The tension fractures generally had larger apertures and were laterally more extensive then the shear fractures, but tend to be less abundant (Table 1).
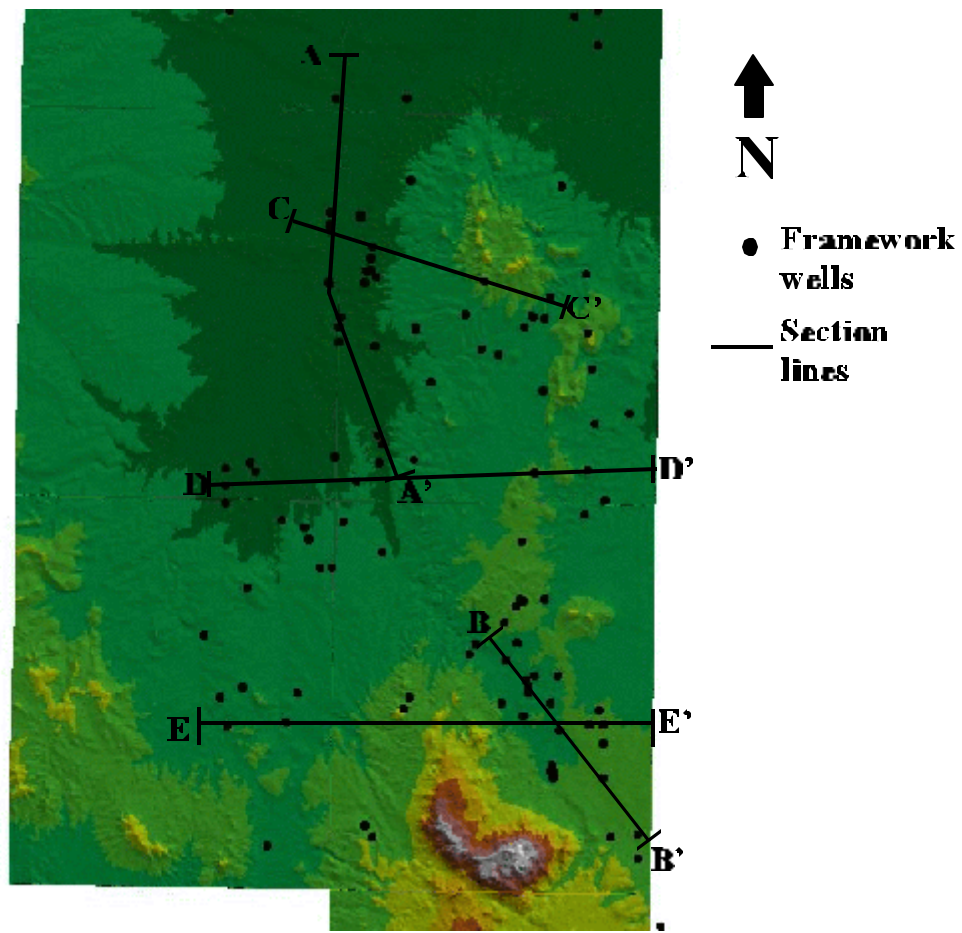
**Figure 4.** Location of the section lines in the MWWVS. AA' and BB' trend along the strike of the basin, and CC', DD' and EE' traverse the basin. Refer to Figure 19 for georeference.
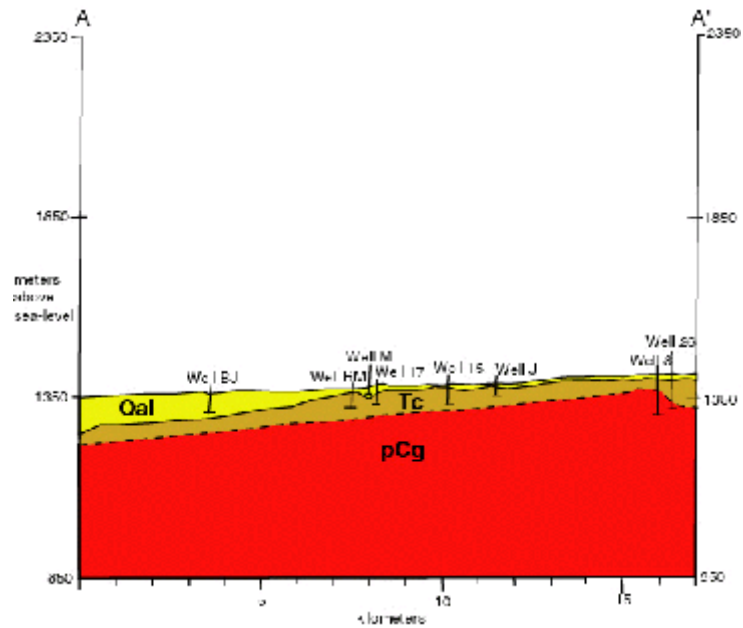
Figure 5 - Cross section A-A', MWWVS. Vertical exaggeration = 10X.
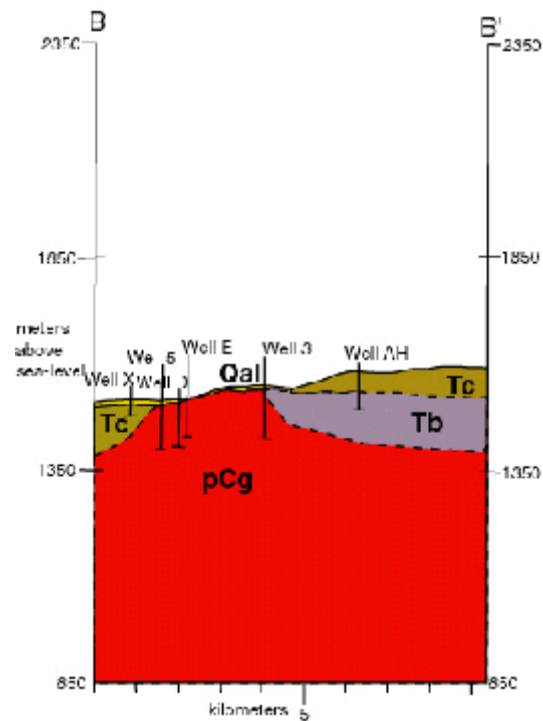


Figure 6 - Cross section B-B', MWWVS. Vertical exaggeration = 10X.

20
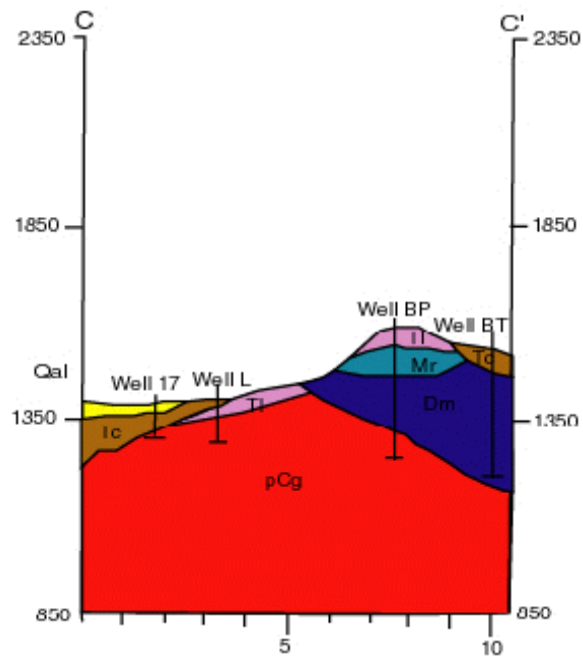
Figure 7 - Cross section C-C', MWWVS. Vertical exaggeration = 10X.
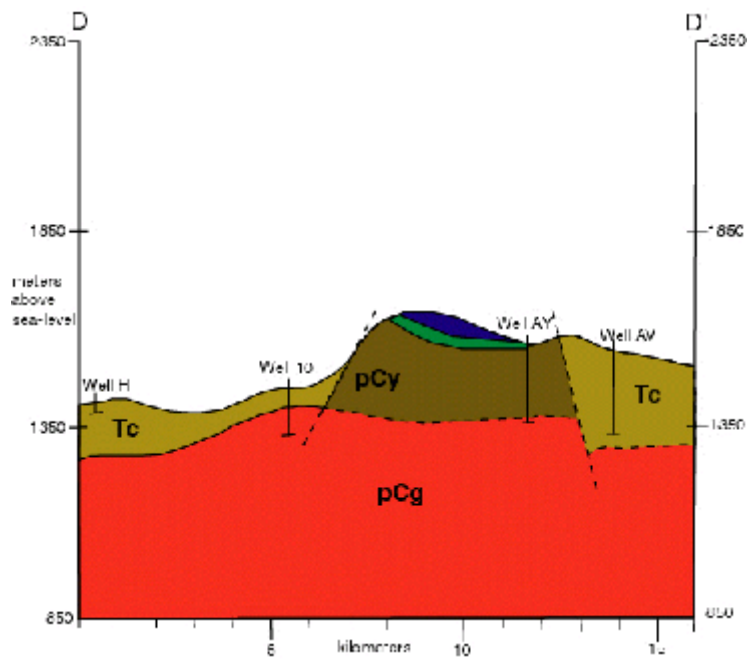


Figure 8 - Cross section D-D', MWWVS. Vertical exaggeration = 10X.

21
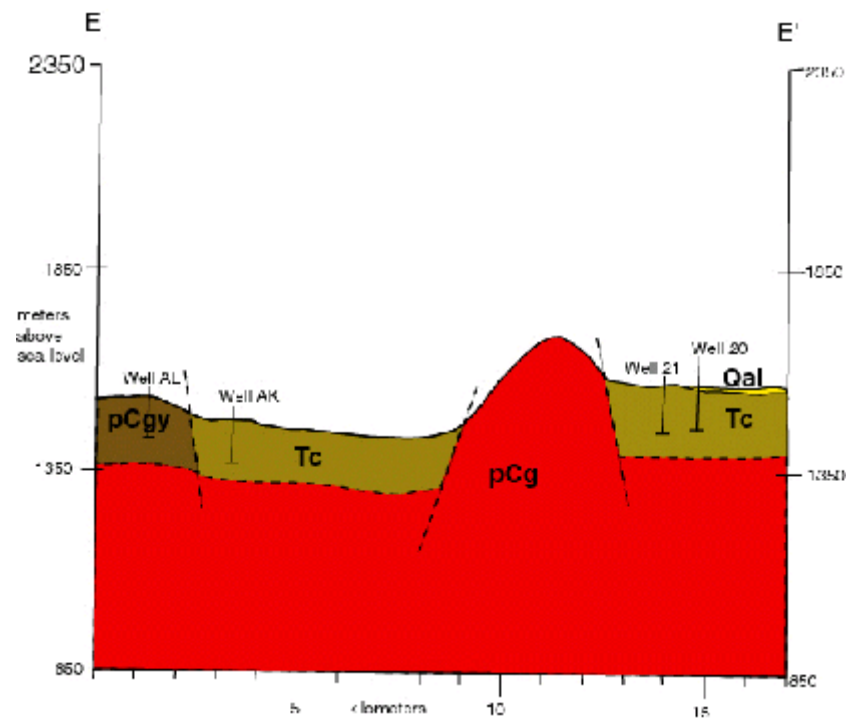
Figure 9 - Cross section E-E', MWWVS. Vertical exaggeration = 10X.

*Stream Bed Mapping*

The results of the grain size analysis are included in Table 3. The sample sites are shown in Figure 26. Cobbles, pebbles and sand form the majority of the material at the sites closer to areas of high relief. The distribution grades towards finer grained materials away from the high relief, towards the valley. This distribution was expected due to the mechanics of sediment transport. Higher relief creates more kinetic energy with fluid motion, making the fluid capable of transporting larger material.

**Conclusions**

The geologic history of the area includes emplacement of a granite pluton into what is currently a metamorphic complex of gneiss and schist during the Proterozoic, at approximately 1.72 Ga (Dewitt 1999). There was a marine environment in the study area during the Paleozoic as demonstrated by the Devonian Martin Formation and Mississippian Redwall Limestone. The Martin Formation and Redwall Limestone units have been identified as marine environments in the area by several workers (Celestian 1979, Meader 1977, Smith 1974, Gutschick 1943 and Kent 1975). The geologic history of the area is summarized in a stratigraphic column showing lithologies present in the MWWVS (Figure 11).

Within Williamson Valley there are no outcrops of lithologies from the Mesozoic era, so there may have been a non-depositional setting during the Mesozoic, or post-depositional erosion. A fluvial environment was present during the Tertiary (Buren 1992). Volcanic activity and northeast-southwest extensional tectonics also occurred in the middle of the late Tertiary

23

(Krieger 1967 a and b, Krieger et al. 1971). The Quaternary is marked by alluvial deposition only within the active washes.

Normal faults are present throughout the MWWVS. Normal faults are most commonly found at gradient changes in the topography, and strike parallel to Williamson Valley. Several faults are found around Granite Mountain, and may be related to the granite emplacement.

Analyses of fracture orientations were measured at three outcrops exposing autochthonous granite. The orientation of the tension fractures trend radially from the crest of Granite Mountain, which is assumed to be the pluton apex. The fracture orientation is consistent with a model developed for fracture orientation resulting from pluton emplacement (Larsson 1972).

The basin morphology would suggest that Williamson Valley basin is a half graben. The half graben is formed by the normal fault between the Sullivan Buttes and Williamson Valley, and the low gradient slope from the apex of the basin up to the west

forming the eastern flank of the Santa Maria Mountains (Plate 1). This basin is in the Transition Zone bounding the Basin and Range physiographic province. The tectonics that occurred in the region during the Tertiary supports the theory that Williamson Valley is a half graben.

**Table 1.** Fracture measurements from the Proterozoic granite in the Granite Mountain Wilderness Area, MWWVS.

| Site Tension Fracture | Orientation | Dip | Relative Aperture Size | Concentration (fracture/meter) |
|---|---|---|---|---|
| 1 | 67º | 76º | large | 6 |
| 2 | 10º | 84º | small | 13 |
| 3 | 32º | 71º | large | 5 |
| Site Shear Fracture | Orientation | Dip | Relative Aperture Size | Concentration (fracture/meter) |
| 1 | 129º | 80º | small | 11 |
| 2 | 122º | 61º | large | 7 |
| 3 | 114º | 84º | small | 6 |
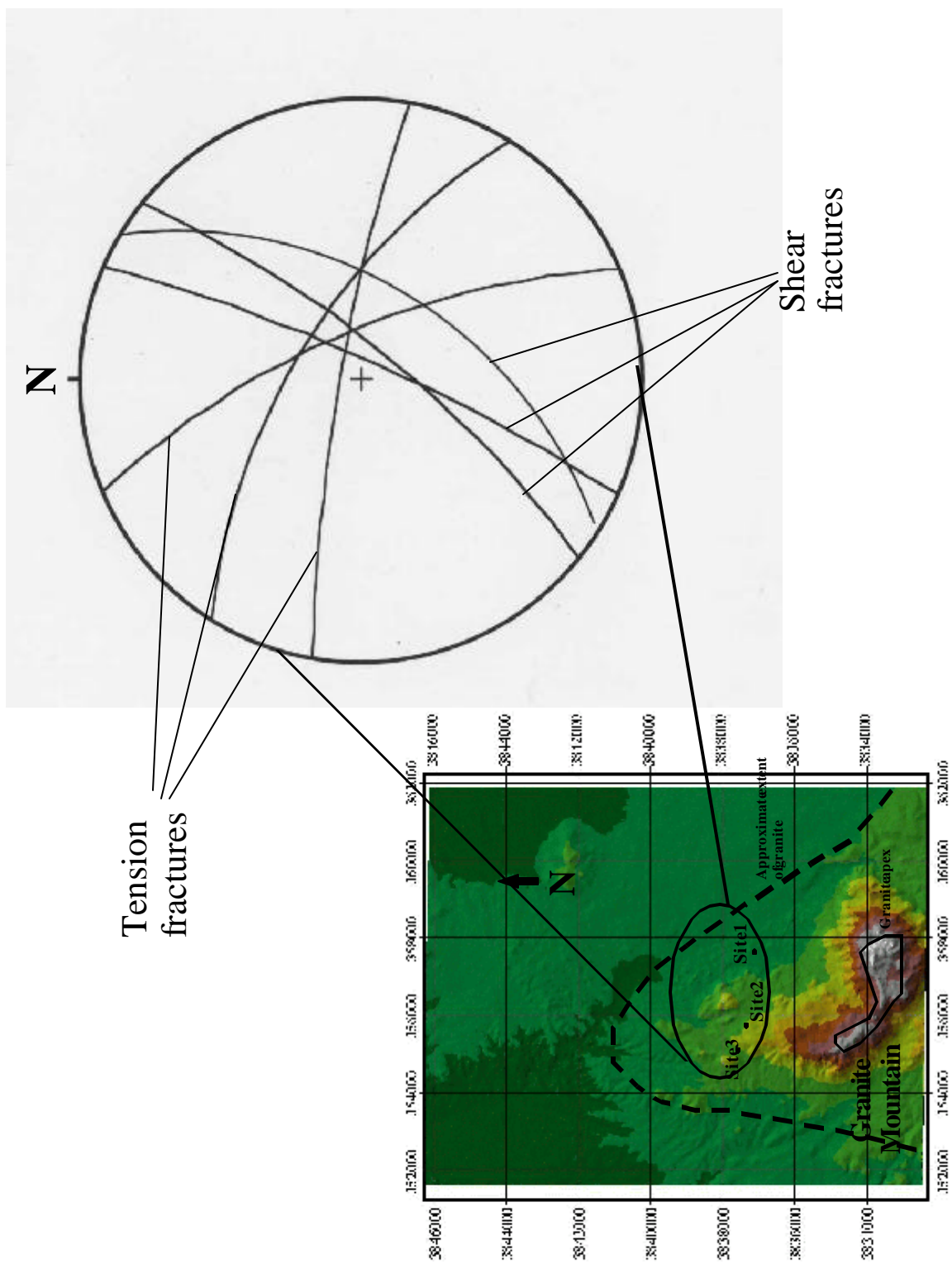
Figure 10 – Stereonet of the fracture orientations measured in the Proterozoic granite in the MWWVS.
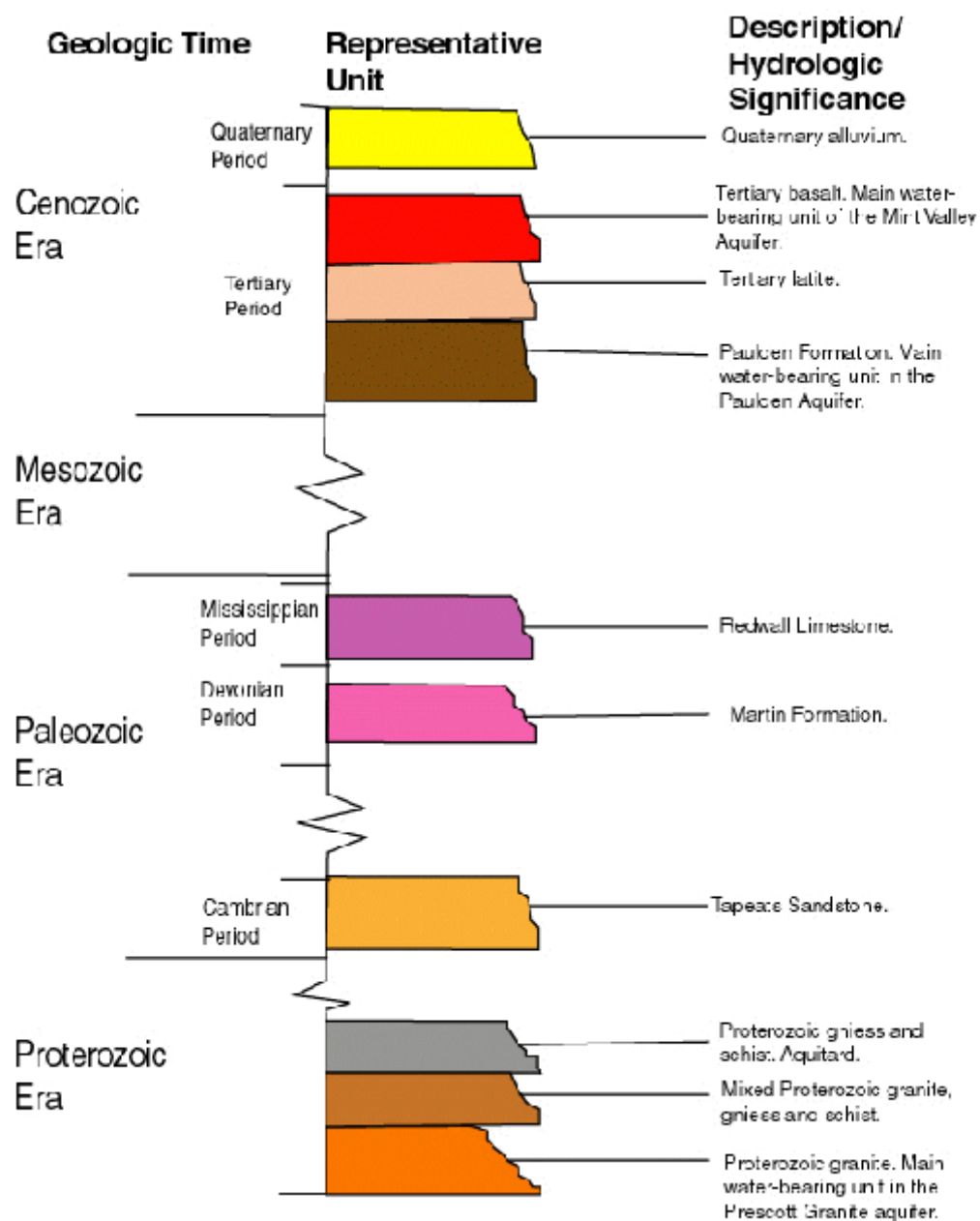
Figure 11 - Stratigraphic column for the MWWVS.

# CHAPTER THREE

# HYDROGEOLOGICAL CHARACTERIZATION

## Purpose and Objectives

A detailed study of the hydrogeology of the Mint Wash / Williamson Valley area has

not been published. The few reconnaissance-level studies that have been conducted for the

area and are available to the public are outdated, and have no written documentation of the

study methods. The hydrogeology of the Mint Wash / Williamson Valley area  has been

characterized in this study in greater detail than previous studies and using updated methods.

The characterization of the area includes a conceptual model, hydrographs of water-

levels in wells and a dynamic steady-state potentiometric surface map, permeability

measurements, aquifer tests, and a conceptual water budget. These tools were used to build a

numerical model of the ground water of the MWWVS.

## Introduction

The MWWVS is an area with complex geology, making the accurate creation of a

conceptual model integral in understanding the hydrogeology. The conceptual model was

created using the known geology of the area, assumed qualitative values for the major

hydrostratigraphic units for recharge and hydraulic conductivity, the topography of the area, and

basic hydrogeologic concepts.

The conceptual model displays the main areas of recharge, major areas of discharge,

the hydraulic headwaters and discharge boundaries, and the general direction of flow for the

regional ground-water system (Figure 12). Granite Mountain, located in the southern region of

the study area, forms the hydraulic headwaters for the entire system. Granite Mountain

produces the largest amounts of recharge due to the high elevation of the mountain and the

highly fractured granite, which is highly permeable (Larsson 1972). High levels of recharge also

occur along the washes which receive additional precipitation from runoff (Simmers 1997). The

Santa Maria Mountains are not included in the study area, but are responsible for a large inflow

of ground water from the west. The main discharge areas due to pumping in housing

developments occur to the east and north of Granite Mountain in Mint Valley, and on the

western flanks of the Sullivan Buttes. There is pumping in central and western Williamson

Valley, though most of that pumping is seasonal, for irrigation. The main natural discharge

boundary for the system is the northeastern corner of the study area, north of the Sullivan Buttes

through ground-water flow.

The southern boundary for the MWWVS is defined as Granite Basin in the

southeastern region, and Mount Josh in the southwest. The western boundary is formed by the

foothills of the Santa Maria Mountains. The eastern boundary, which forms the

surface-water divide, is formed by a discontinuous range consisting of the Sullivan Buttes and

29

Table Mountain. The Williamson Valley Wash and Big Chino Wash surface water confluence is assumed to be the confluence for the ground-water flow systems from Williamson Valley and Big Chino Valley.

The main hydrostratigraphic units in the MWWVS include the Paulden Conglomerate (Tc), the Prescott Granite (pCg), and the Mint Valley Basalt (Tb) (Plate 1) (Figures 5 - 9). The Prescott Granite is volumetrically the largest hydrostratigraphic unit in the southern half of the study area, and forms the basement for the overall system. Tension fractures are the dominant conduit for fluid flow in the granite. The Mint Valley Basalt occurs in the southern portion of the field area, and is a relatively thin layer in which fractures are also responsible for fluid flow. The Paulden Conglomerate is volumetrically the largest water-bearing unit in Williamson Valley, and covers most of the surface of the field area. Pore space allows for fluid flow in the Paulden Conglomerate.

## Background

Water use in the Mint Wash / Williamson Valley area was predominantly for irrigation prior to the sub-division and development of several ranches, and thus seasonal. The only other water use was domestic use for ranchers.

Land subdivisions of the ranches began to occur in the second half of the 1900s. Several ranches were sold and subdivided by developers in the 1980s. The recent population boom in central Yavapai County has created demand for more development in the area.

Presently there are over four ranches which have been subdivided creating several hundred single family home sites in the Mint Wash and Williamson Valley area.

The hydrography of the area is rare in central Arizona. The shallow water table has created several perennial springs and extensive riparian vegetation in the area (Figure 13). Sustainable yield must be addressed for the MWWVS to protect the ecosystem that has formed, which is dependent on the availability of shallow ground water. Sustainable yield is water use to support human communities without degrading the hydrological cycle and the ecosystems that depend on water (Gleick 1998). A sustainable yield for the MWWVS is defined and further addressed in the sensitivity analyses produced by the ground-water flow model.

**Methods**

*Well Network Monitoring*

A monitoring network of 12 wells was established in August of 1999, and for the first several months of measurement several additional existing wells were added to the network to a total of 17 wells to fill in gaps in spatial coverage. Water levels in the wells were measured using a Solinst ground-water sounder with a maximum range of 150 meters and an accuracy of +/- 0.01 meter (Solinst 2000). The probe was triple washed with bleach, non-phosphate soap, and distilled water. The 15th of every month was established as the date of measurement to avoid conflicts with any major holidays, in which the well owners would not be able to provide access.

The distance from the top of the well casing to land surface was measured for every well. The well casings were marked so every reading was consistently measured from the same point on the well casing. The elevation and location of each well was measured using a Trimble GPS receiver with an external antenna and a Trimble Pathfinder field computer. The rover station readings were differentially corrected using the Prescott National Forest Service base station available through the Trimble Pathfinder software. The average horizontal 95% confidence precision was approximately +/- 1.5 meter, while the average 95% confidence precision for the vertical dimension was approximately +/- 2.5 meters. Appendix 1 lists the wells used as monitoring wells, and the wells added for the synoptic water-level reading, their locations, as well as the 95% confidence precision of their location.

Water-level data was entered into a spreadsheet in meters above sea-level. Hydrographs were produced for each hydrostratigraphic unit in Grapher 2.0 (Golden Software 2000) (Figures 14-18). The hydrographs for each unit were used to qualitatively compare the storativity of the different hydrostratigraphic units.

*Potentiometric Surface Map*

A potentiometric surface map (Figure 19) was created using data collected during a synoptic water-level reading on the 14th and 15th of July, 2000. The month prior to the synoptic water level reading was free of rainfall or any other major climatic events. The 17 monitoring wells used to create the hydrographs were used along with 19 extra wells that were added to fill gaps in the water level data. All pumps were shut down 1 hour prior to measurement to allow for recovery of any drawdown. This recovery time was determined from aquifer test data:

all of the wells fully recovered within 1 hour during the aquifer tests, and the wells that were stressed only enough to simulate average discharge from a domestic well recovered within 10 minutes.

The water level data was plotted on a TIN (Triangular Irregular Network) surface of the study area. A topographic contour map was created in ArcView (ESRI 1999) using 1:24,000 quadrangle Digital Elevation Models provided by the Arizona Land Resource Information System (ALRIS 2000).The water-level contour interval is 20 meters. Most of the ground-water contours are dashed due to the uncertainty of the location of the ground-water contours. Adequate spatial distribution of wells were lacking in most of the study area and the water-level could not be determined for large areas (Figure 19). Most of the study area is either rural, National Forest land, or undeveloped. The potentiometric surface map was analyzed to determine ground-water flow paths, ground-water divides, and delineate aquifers.

*Permeability*

Recharge to ground water is concentrated along the washes in the MWWVS. Saturated hydraulic conductivity was measured at several points within the major washes to determine the saturated infiltration capacity of the material. The hydraulic conductivity measurements provided recharge rates for the washes during saturated conditions.

A Guelph Permeameter was used to measure the saturated vertical hydraulic conductivity of the washes. The Guelph Permeameter has a limited to a range of $10^{+1}$ to $10^{-3}$ meters/day for hydraulic conductivity (Soilmoisture Equipment Corp. 1986). The permeability of several points along the washes exceeded the capability of the Guelph Permeameter. The

33

range provided a minimum for the value of the permeability of those points along the washes.

The successful measurements were compared to the infiltration rates reported within the Soil

Survey of the western part of Yavapai County (Wendt et al. 1976). The rates measured

matched the range of infiltration rates reported by the soil survey. The areas that had hydraulic

conductivity values too high for the permeameter to measure were reported in the survey as

having possible hydraulic conductivity values exceeding the range of the Guelph Permeameter.

The permeabilities reported in thesoil survey of the western part Yavapai County were assumed

to be accurate, and were used to estimate the hydraulic conductivity values of the sections of

the washes that had hydraulic conductivities out of the range of the Guelph Permeameter.

Permeability measurements and grain size analyses of the wash material were

conducted at the same sites. Permeability of sedimentary materials is controlled by the grain size

distribution. The grain-size analyses were used to map out the sites where permeability would

be most likely to vary.

*Aquifer Tests*

Aquifer tests were conducted and analyzed on several wells within the study area to

calculate values for transmissivity and storativity. Existing well pumping test data were available

for three wells within the Prescott granite, and one within the Paulden conglomerate. Values for

transmissivity and storativity were estimated for the Mint Valley basalt using the Theis method

for transmissivity and storativity estimation using specific capacity (Wellendorf 2000).

An aquifer test for the Prescott granite was conducted as part of this study on well

34

number 2 (location of RS-2, Figure 24). Discharge was induced through a submersed pump, approximately 44 meters below land surface. Discharge was measured every 5 minutes during the first hour of the test, then every half hour for the remainder of the test and the mean of the discharge values was used in the aquifer property calculations. The schedule for water level measurement is outlined in "A Manual of Field Hydrogeology" (Sanders 1998).

All of the wells were screened in an unconfined aquifer, and the Neuman (1975) method of aquifer test analysis was used for the pumping well. The Neuman method was the most accurate analytical method for pumping test analysis based on the unconfined nature of the aquifer and the assumptions and limitations of the method and aquifer test.

The recovery for well 2 was analyzed using the Theis (1936) straight line method;

$$T = 264Q/Delta(s\text{-}s')$$

(Driscoll, 1986). Theis' corollary to the non-equilibrium equation and Jacob's modification to the non-equilibrium equation are analytical methods available in the current literature for well recovery analysis.

*Water Budget*

A water budget was calculated using precipitation data from three rain gauges distributed throughout the field area (Figure 31) for recharge estimates, well registration data for pumping estimates (ADWR 2000), and Darcy's Law for an estimate of natural discharge (Fetter 1996) (Domenico and Schwartz 1998). The water budget provides a quantitative comparison of total discharge and recharge to the system, which was used to check the

"goodness" of the mass balance created in the model output.

Darcy's Law is mathematically represented by the following equation:

$$Q = -KA(dh/dl)$$

where Q = discharge ($m^3$/yr), K = horizontal hydraulic conductivity (m/yr), A = cross sectional

area ($m^2$), and dh/dl = ground-water gradient (dimensionless). Darcy's Law was applied to

estimate the natural discharge by using the potentiometric surface map to find the gradients

along inflow and outflow boundaries, and the results of the aquifer tests to estimate values for

hydraulic conductivity. The conceptual model and data from well logs provided information

enabling an estimation of the saturated thickness to calculate the cross sectional area.

The storage within the aquifer was calculated with the numerical ground-water flow

model because no multiple-well aquifer analysis data were available. The transient simulation

included storage parameters to estimate volumes of water change in storage.
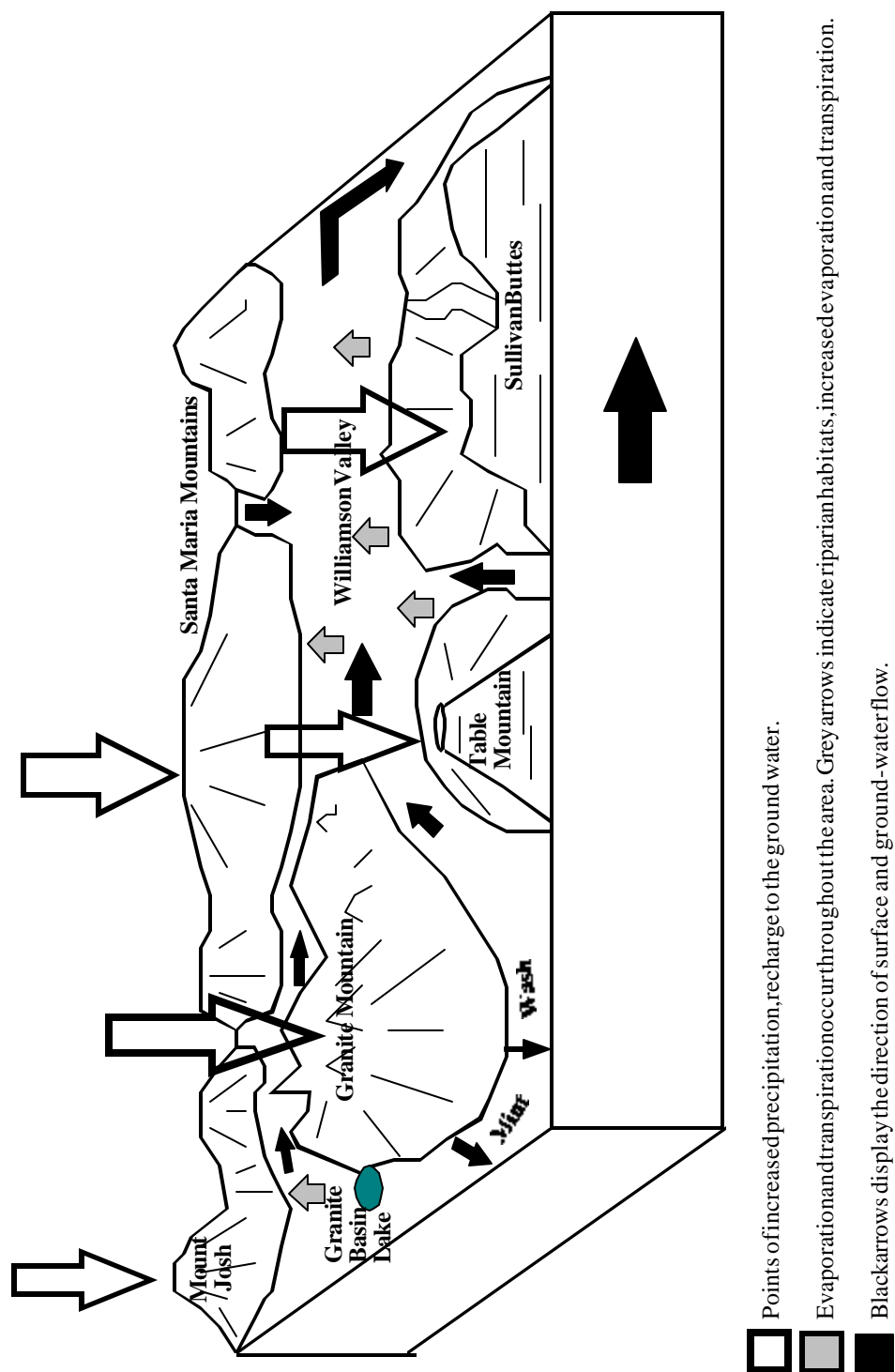
Figure 12 - Conceptual model for the MWWVS.

Points of increased precipitation, recharge to the ground water.

Evaporation and transpiration occur throughout the area. Grey arrows indicate riparian habitats, increased evaporation and transpiration.

Black arrows display the direction of surface and ground-water flow.

37

a.                                                    b.

**Figure 13a.** Riparian vegetation dependent on a shallow ground-water supply. The site is shown on Figure 19.


**Figure 13b.** Perennial springs supplied by shallow ground water. The site is shown on Figure 19.

**Results**

*Hydrographs*

Hydrographs for all of the wells within each hydrostratigraphic unit (Figures 14-18) were compiled from the water level data collected the 15th of every month, and show the responses of the water table to stresses throughout the year. The magnitude of the response for a given well provides qualitative information on the storativity of the unit.

The climate in the region of Yavapai County has seasonal precipitation; the wet monsoon seasons in the late summer / early fall, and in late winter / early spring snow melt. The 1999-2000 water year had below average precipitation as compared to precipitation data reported in the western part Yavapai County soil survey (Appendix 3) (Wendt et al. 1976). The long term average for the area as reported in the Soil Survey for Western Part of Yavapai county is 18.24 inches (Wendt et al. 1976). The ground-water levels showed minimal response to the wet seasons during the study period. The hydrograph of the well within the Mint Valley basalt showed a continual decline in water level throughout the year. The degree of water-level change at this well location was high, relative to the wells found in the other hydrostratigraphic units. This high magnitude of water-level change represents low storage values for the Mint Valley basalt.

The water levels in wells in the Prescott granite exhibited large fluctuations of the water-table relative to those in the Paulden conglomerate. The storage values of the granite are apparently lower than those of the conglomerate.

The wells in the conglomerate were graphed separately by location in the valley or

along the range within the study area (Figures 17 and 18). One of the composite hydrographs for the conglomerate includes the wells that are in the Williamson Valley basin, and the other wells that are on the slopes of the Sullivan Buttes. These locations had different levels of response to the stresses, though both had fluctuations of lesser magnitude than Mint Valley basalt or Prescott granite wells. The wells in the conglomerate in Williamson Valley exhibited the least amount of water-table fluctuation. This is most likely due to the distance from major sources of recharge. The wells along the Sullivan Buttes show a higher degree of fluctuation due to their proximity to major recharge areas along the topographic highs.

*Potentiometric Surface Map*

The potentiometric surface map was constructed using the synoptic water-level readings from the July 14th-15th, 2000 measurements (Figure 19). The data were placed on a composite TIN surface of the DEMs available for the field area.

The hydraulic headwaters for the entire system are Granite Mountain. There is radial ground-water flow from the mountain to the surrounding topographic depressions. Ground-water divides extend in the directions of the ridge of Granite Mountain. The ground-water divide splays to the north at the aquitard created by the metamorphic rocks. The area of the aquitard has been drilled several times with little significant water productivity (Figure 20).

At least three distinct aquifers can be identified on the potentiometric surface map (Figure 19). The upper Granite Basin aquifer flows from granite mountain toward the southeast and consists of Mint Valley basalt above Paulden conglomerate.   Depending on the exact

location of the ground-water divide, one to three of the wells measured yield water from this aquifer.

The second distinguishable aquifer flows from the concave side of Granite Mountain toward the northeast. The upper Mint Wash aquifer is composed of highly fractured Prescott granite, while the lower aquifer has Paulden conglomerate above the granite.  The upper Mint Wash discharges to the east of the study area towards the Little Chino aquifer. Most of the flow in this aquifer occurs through fractures.

The third aquifer is the most extensive in the MWWVS. The Las Vegas aquifer extends from west of Granite Mountain up north through Williamson Valley, and discharges out of the system  north of the Sullivan Buttes to the adjacent, Big Chino aquifer, which is down-gradient. The main water-bearing unit in this aquifer is the Paulden conglomerate. This is volumetrically the largest aquifer. Most of the wells in this study yield water from this aquifer.

The potentiometric surface map (Figure 19) suggests that the different aquifers are hydraulically connected and all have the same hydraulic headwaters. The aquifers flow in different directions and discharge to different sub-basins, which is important to consider when managing aquifers.

*Permeability*

The limited range of measurement of the Guelph Permeameter resulted in two successful permeability measurements (Table 2). The successful measurements were compared to the measurements reported in the Soil Survey of the western part of Yavapai County (Wendt et al., 1976).

Saturated hydraulic conductivity measured in the field fit near or within the range of

infiltration rates reported by the soil survey. The sites where the permeability values exceeded

the range of the permeameter were also compared to the data in the soil survey, and the

possible permeability values reported were out of the range of the Guelph permeameter (Table

2). The sites that indicate that no measurement was conducted with the Guelph Permeameter

are sections along the wash where it was determined through failed permeability measurement

attempts that the soil was out of the range of the Guelph Permeameter.

The limited results of the permeability study were considered during the calibration of

the ground-water flow model to estimate recharge through the washes during saturated

conditions. Saturated conditions in major washes is felt to be a major component of recharge in

a semi-arid ground-water basin.
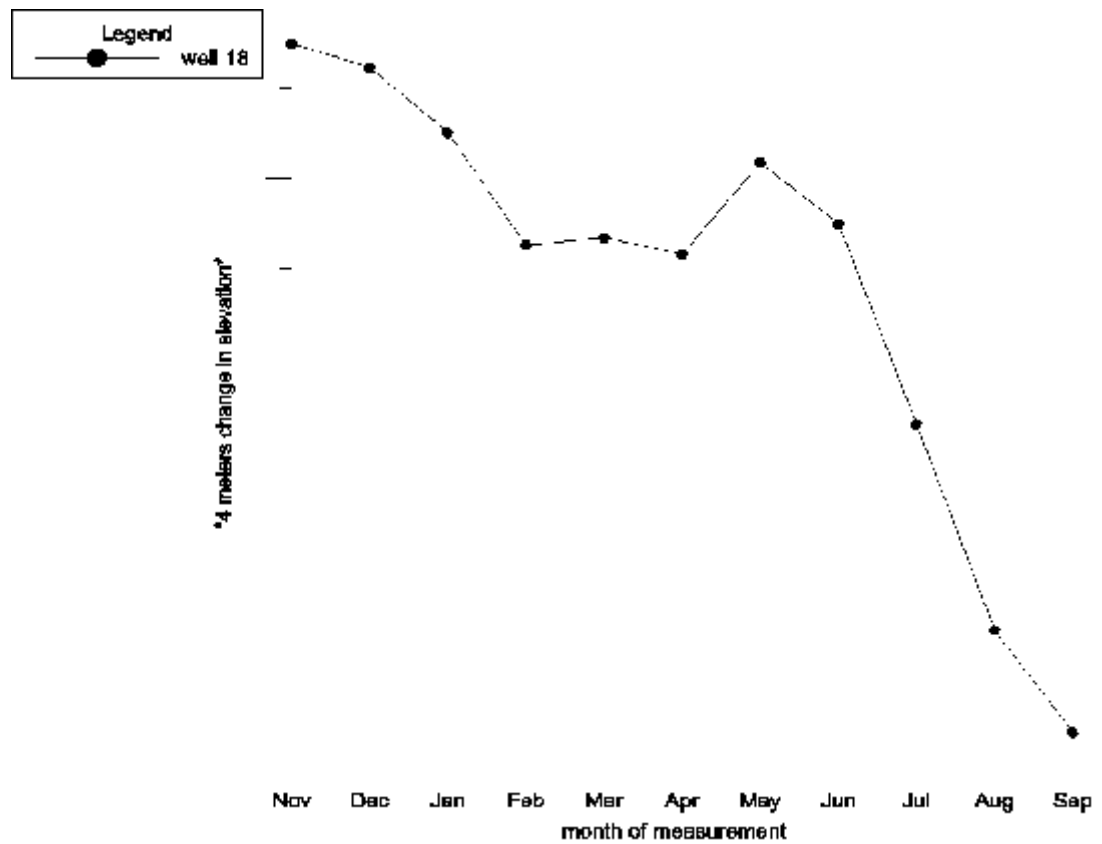
**Figure 14.** Hydrograph for well 18 in the Proterozoic gneiss and schist (Yavapai Series) from Aug '99 through Sep '00, MWWVS.
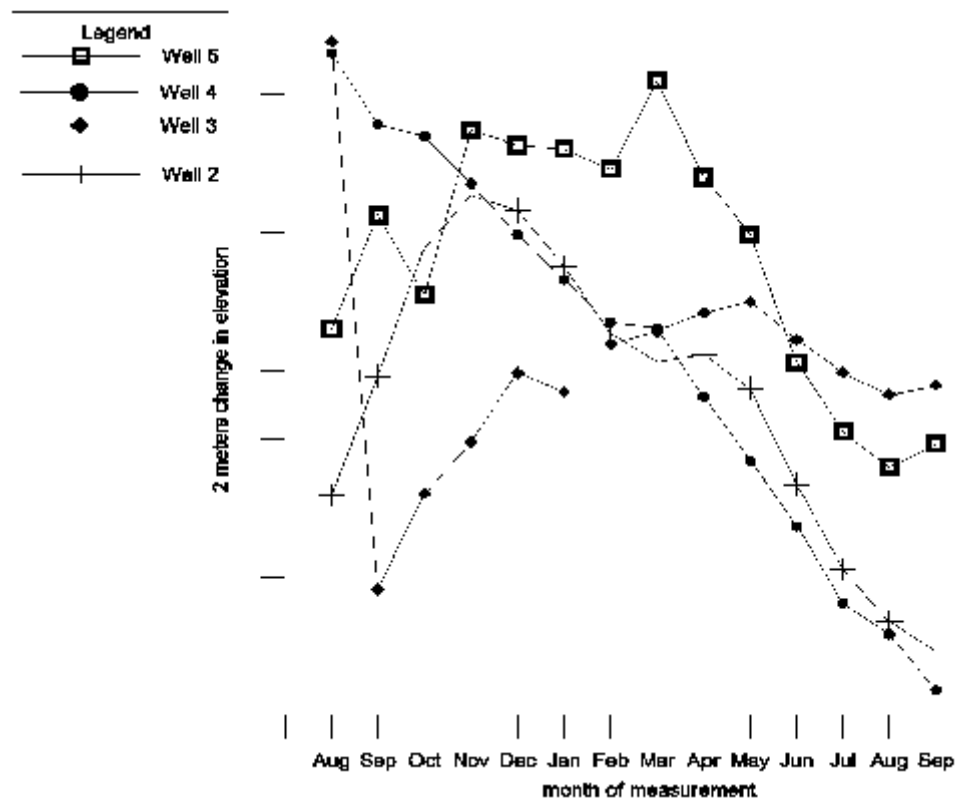
**Figure 15.** Hydrograph for wells 2, 3, 4, and 5 in the Prescott Granite from Aug '99 through Sep '00, MWWVS.
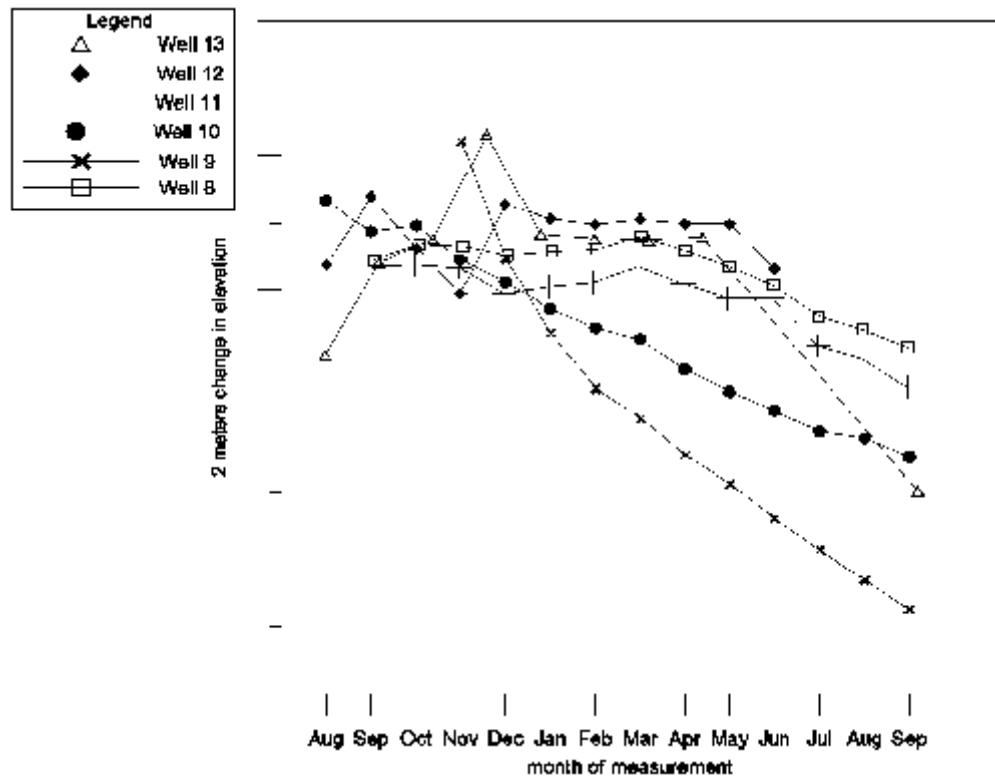
**Figure 16.** Hydrograph for wells 8, 9, 10, 11, 12, and 13 in the Paulden Conglomerate from Aug '99 through Sep '00, Williamson Valley, MWWVS.
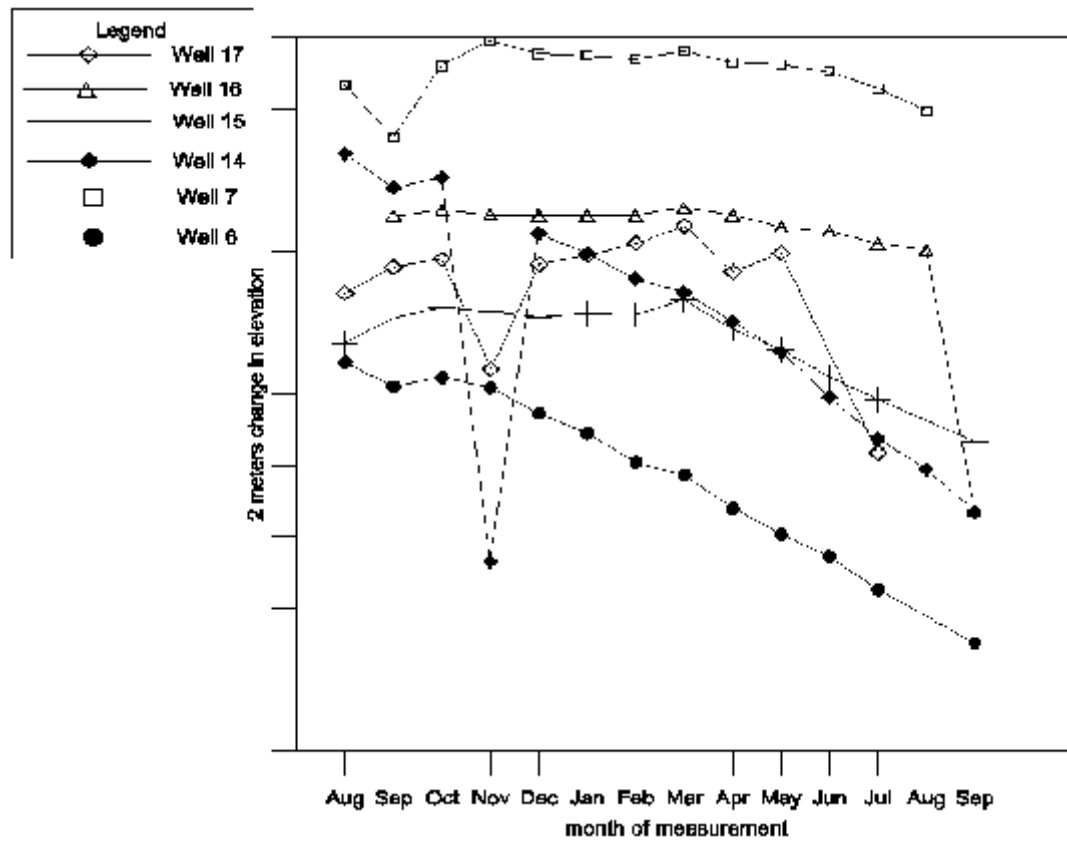
**Figure 17.** Hydrograph for wells 6, 7, 14, 15, 16, and 17 in the Paulden Conglomerate from Aug '99 through Sep '00, Sullivan Buttes, MWWVS.
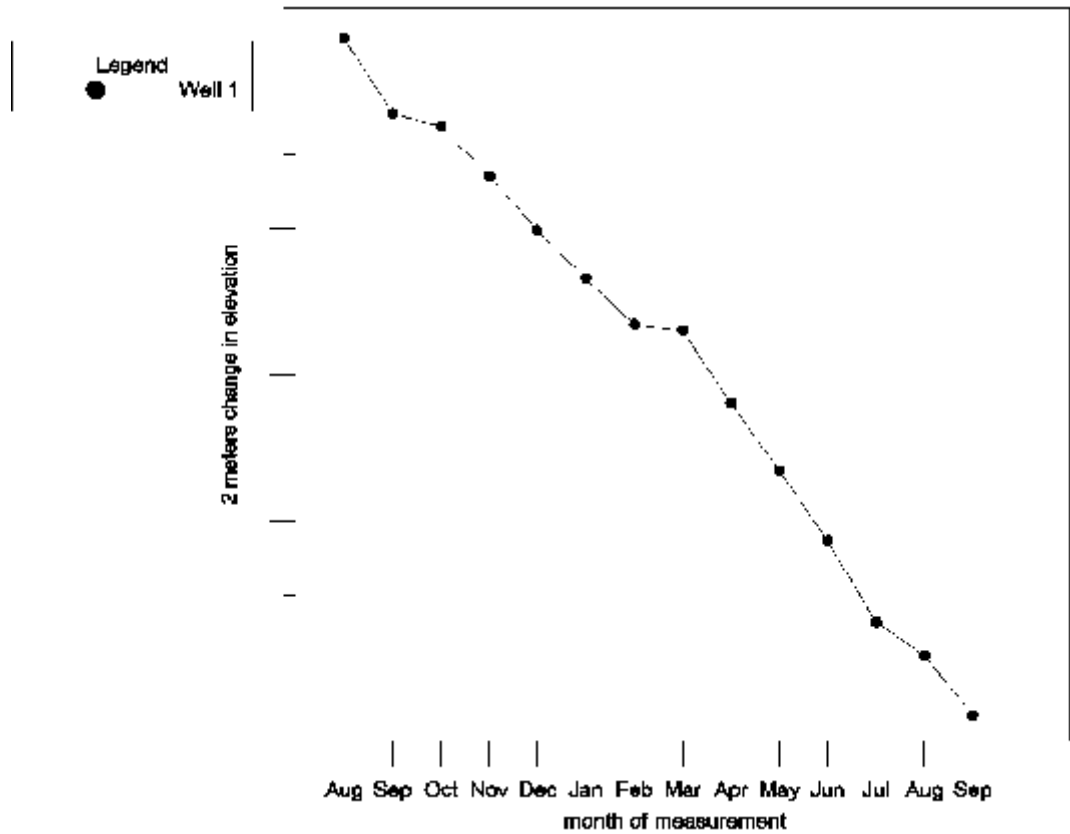
**Figure 18.** Hydrograph for well 1 in the Mint Valley Basalt from Aug '99 through Sep '00, MWWVS.
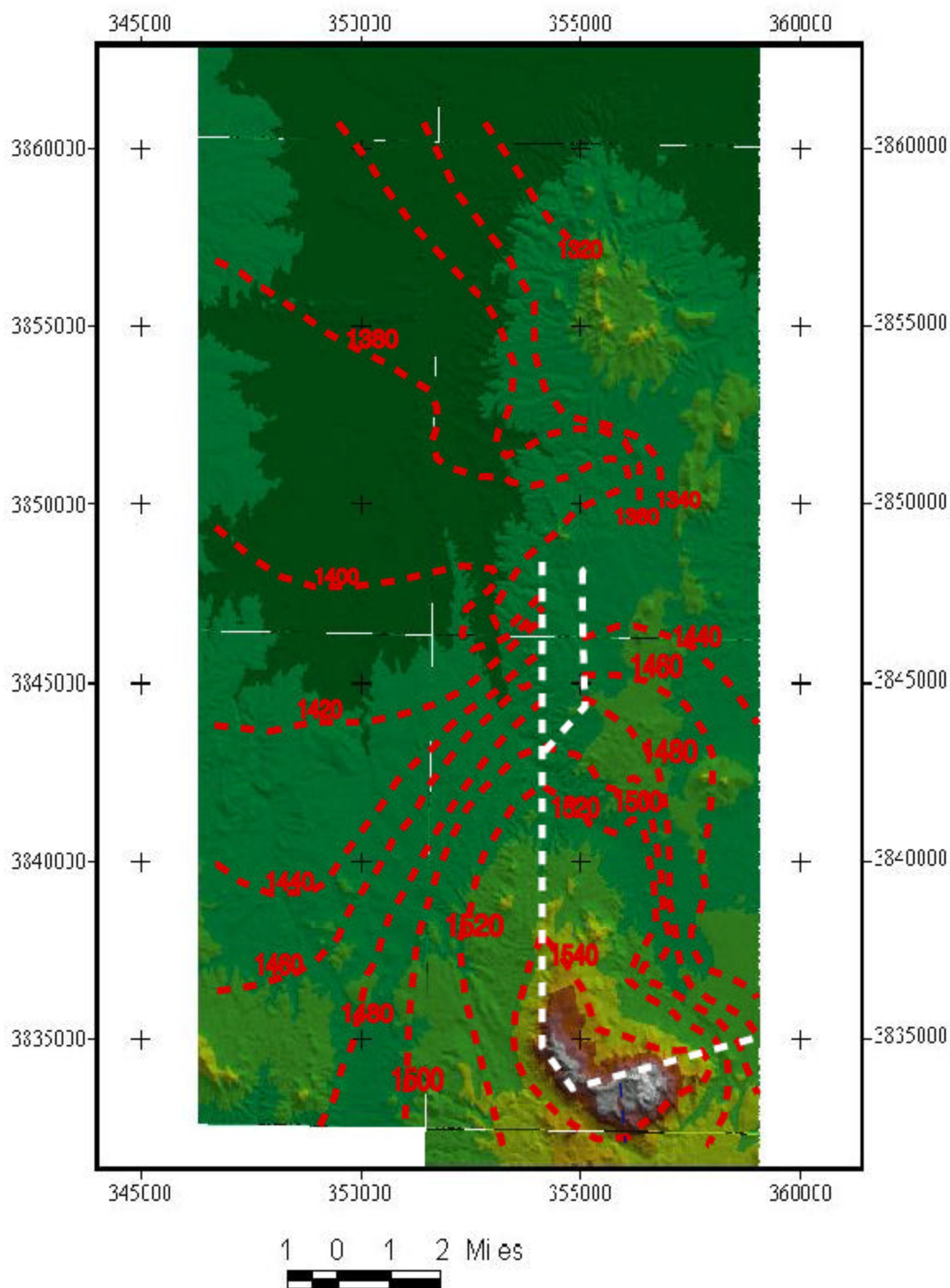
Figure 19 - Potentiometric surface map of the MWWVS. Water level data was collected July 14&15, 2000. Red lines represent ground-water contours. The white lines are ground-water divides. Grid is UITM Easting and Northing.

48
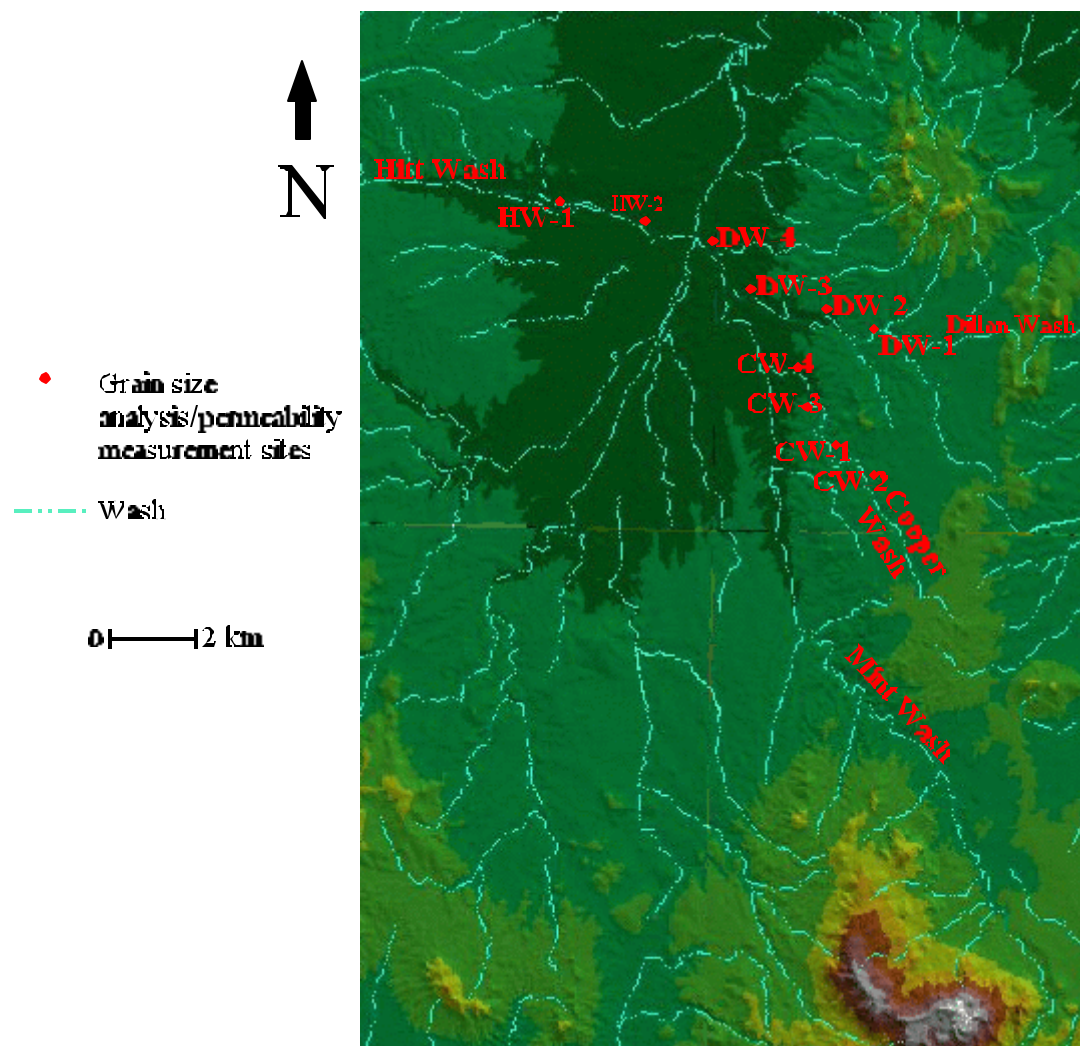
**Figure 20.** Sites for grain-size analyses and permeability measurements for the MWWVS.

**Table 2.** Results of the grain-size analyses and permeability measurements. See Figure 26 for location of measurements.

| Site | Guelph Permeameter measurement (cm/sec) | Grain-Size Analyses (% of sample) | | | Permeability reported by Soil Survey (cm/sec) |
|------|------|------|------|------|------|
| | | Gravel | Sand | Fines (silt and clay) | |
| CW-1 | Out of Range | 33 | 66 | 1 | 0.0014-0.0042 |
| CW-2 | Out of Range | 25 | 74 | 1 | 0.0014-0.0042 |
| CW-3 | Out of Range | 28 | 72 | 1 | 0.00042-0.0014 |
| CW-4 | No Measurement | 19 | 81 | 0 | 0.00042-0.0014 |
| DW-1 | No Measurement | 71 | 29 | 0 | 0.00042-0.001 |
| DW-2 | No Measurement | 30 | 70 | 0 | 0.00014-0.00042 |
| DW-3 | Out of Range | 64 | 35 | 1 | 0.00014-0.00042 |
| DW-4 | 0.00013 | 34 | 64 | 2 | 0.00014-0.00042 |
| HW-1 | Out of Range | 21 | 79 | 0 | 0.00014-0.00042 |
| HW-2 | 0.00021 | 29 | 65 | 6 | 0.00014-0.00042 |

*Aquifer Tests*

The data from several aquifer tests were analyzed using graphical analysis methods. The aquifer tests available included one aquifer test in the Paulden conglomerate (Las Vegas aquifer), and three aquifer tests in the Prescott granite (Mint Wash aquifer). Transmissivity and storativity were estimated for the Mint Valley basalt using average specific capacity values (Wellendorf 2000) and the Theis equation for estimating transmissivity and storativity from specific capacity data (Fetter 1994).

The pumping data for the aquifer test on the Navarro conglomerate were plotted semi-logarithmically with drawdown on a linear y-axis and time on a logarithmic x-axis (Appendix 3). The Neuman analytical method (Neuman 1975) for an unconfined aquifer was used to analyze the data. The early time data fit well on the $' = 0.01$ Neuman type curve. There was no late time data evident to match to the Neuman late time curve nor was there an observation well, so an estimation of specific yield was not attained. The results produced are reported in Table 3. The same method was used for the pumping data for all of the aquifer tests available for the Prescott granite (Table 3).

The aquifer test for well-2 is the only test conducted as part of this study. All of the assumptions for the Neuman analytical method were met to secure a valid aquifer test. The test did not last long enough to produce late time data to estimate specific yield.

The aquifer test for well 52 was deemed invalid, though the results are still reported. The total drawdown exceeded 20% of the assumed saturated thickness of the aquifer. Analytical methods are only valid for aquifer tests in which the drawdown does not exceed

51

10% of the saturated thickness.

Specific yield was estimated using the late time data from the aquifer test on well 51. The test on well 51 was the most complete of the tests. All of the assumptions for the Neuman method were met. The initial hydraulic conductivity value in the ground-water flow model is based on this aquifer test.

**Table 3.** Aquifer parameters for the major hydrostratigraphic units using aquifer tests and specific capacity estimates.

| Aquifer Test | Hydrostrat. Unit | T(m2/yr) | Thickness (m) | K(m/yr) | Storativity |
|---|---|---|---|---|---|
| ARwell-51 | Prescott pCg | 69000 | 152 | 460 | n/a |
| ARwell-52 | Prescott pCg | 10000 | 152 | 69 | n/a |
| ARwell-54 | Prescott pCg | 15000 | 152 | 95 | 0.00035 |
| Well-2 | Prescott pCg | 18000 | 152 | 120 | n/a |
| Well-2 (recovery) | Prescott pCg | 440000 | 152 | 2900 | n/a |
| Well W-1 | Paulden Tc | 44000 | 44 | 990 | n/a |
| Tb-specific capacity | Granite Basin Tb | 4400 | 50 | 88 | 0.0004 |

The recovery data for well-2 were analyzed using the Theis straight line recovery method (Driscoll 1986). Residual drawdown after the cessation of pumping is measured at a logrithimic interval until full recovery. The calculated recovery is plotted on a linear y-axis, while the time since pumping stopped $t'$ is the logarithmic x-axis (Table 3) (Figure 21).

The transmissivity and storativity of the Mint Valley basalt were estimated using an

equation created by Theis (1963) for specific capacity measurements:

$$T=(Q/(h_o-h))(2.3/4\mathbf{B})\log(2.25Tt/r^2S)$$

where $Q/(ho-h)$ is the specific capacity of the well (m$^3$/day/m), $t$ is the period of pumping (day),

$r$ is the radius of the pumping well (m), $T$ is aquifer transmissivity (m$^2$/day), and $S$ is aquifer

storativity (dimensionless). Storativity and transmissivity are both variables for the specific

capacity equation, so an accurate approximation of either values must be determined to

accurately estimate the other.

Aquifer tests provide values for aquifer parameters, but the major limitation is that it is a

local value, and may not be representative of the entire hydrostratigraphic unit. Aquifer test

analysis is best used in local studies, or regional studies when sufficient aquifer tests are

available to use statistics to create semi-variograms. For the purpose of this study, the limited

data were applied as initial values in the ground-water flow model, and the parameter values

were varied through the calibration process and representative values for the hydrostratigraphic

units were determined.

*Water Budget*

The water budget includes estimates of discharge and recharge to the MWWVS

utilizing limited data and several assumptions. Recharge was estimated from precipitation data

from three rain gages stationed at different locations in the study area (Figure 31) (Appendix 3).

A percentage of 4 to 5% has been estimated to be the amount of total precipitation that goes to

recharge the ground-water in this region (Corkhill and Mason 1995). Precipitation was

assumed to vary with elevation throughout the study area. Areas that were lacking in precipitation data were assigned approximate values based on the nearest precipitation data source and the assumption that in Arizona there is an additional 1.5 inches (3.8 cm) of precipitation per year per 1,000 feet (300 meters) of additional elevation (Allen 1995). Initial recharge values were estimated throughout most of the study area using this assumption. Recharge through washes is a combination of direct precipitation recharge and the permeability of the washes during saturated conditions multiplied by the amount of time during the study period that the washes were saturated. Mint Wash adjacent to Granite Mountain was assumed to be saturated approximately 30 to 45 days during the study period (Maslansky 2000) at approximately 40% of the wash area. Washes along the Sullivan Buttes, Santa Maria Mountains, and Williamson Valley were assumed to be saturated due to precipitation events approximately 2 to 3 days (Maslansky 2000) during the study year at 10% of the wash area. The use of percentages of precipitation values for recharge can produce errors and should not be used by practitioners to calculate recharge values (Watson et al. 1976, Gee and Hillel 1988), so the calibrated values in the ground-water flow model are assumed to be the most accurate recharge values for the MWWVS.

Natural discharge through sub-surface flow in or out of the MWWVS was estimated using Darcy's Law (Domenico and Schwartz 1998). Discharge due to pumping was estimated using the Arizona Department of Water Resources Well Registry CD to find the number of wells within the study area (ADWR 2000). Using the same database, the wells were differentiated by use: domestic, irrigation, and second family home, based on the well owner's

address. The rule of thumb for the region on values for water use were used to find the average water use per well per year. These assumptions include 180 gallons/day/person and 2.3 people per home (Wellendorf 2000). Second family homes were assumed to use the same quantity of water, but only for half of the year.

The results of the water budget are included in Table 4. This conceptual water budget is used to help calibrate the mass balance of the steady-state model. The inflows and outflows reported by the model should be within the same order of magnitude as the values reported in the water budget.

There are discrepancies in the water budget due to the uncertainty in the recharge value and the inflow and outflow through the boundaries of the study area. Many of the boundaries were assumed in the potentiometric surface map due to the lack of available water-level data. The gradient and saturated thickness of the aquifer at these boundaries could vary from the actual values. The uncertainty of the inflow value and the recharge value could both introduce error in the water budget. The recharge value seems the most likely cause for the error in the water budget due to it's high value relative to the other components in the water budget.

**Table 4.** Initial water budget for the MWWVS.

| Ground-Water Movement | Inflow (m³/yr) / (ac-ft/yr) | Outflow (m³/yr) / (ac-ft/yr) | Difference / (ac-ft/yr) (m³/yr) |
|---|---|---|---|
| Recharge | $2.9 \times 10^7$ / $2.4 \times 10^4$ | ------------------ | ------------------ |
| Inflow | $1.1 \times 10^7$ / $8.9 \times 10^3$ | ------------------ | ------------------ |
| Pumping | ------------------ | $4.5 \times 10^5$ / $3.6 \times 10^2$ | ------------------ |
| Outflow | ------------------ | $1.6 \times 10^7$ / $1.3 \times 10^4$ | ------------------ |
| Total | $4.0 \times 10^7$ / $3.2 \times 10^4$ | $1.6 \times 10^7$ / $1.3 \times 10^4$ | $2.4 \times 10^7$ / $1.9 \times 10^4$ |

# CHAPTER FOUR

## GROUND-WATER FLOW MODELING

**Model Purpose**

Ground-water flow through the Mint Wash and Williamson Valley System (MWWVS) was simulated using a three-dimensional finite-difference ground-water flow model (Figures 21, 22 and 23). The purposes of the ground-water flow model were to quantify sustainable yield for the ground-water flow system, create sensitivity analyses of the MWWVS aquifers' properties, produce predictive modeling results based on safe yield and sustainable yield water use scenarios, and predictive results to the current pumping condition and the proposed American Ranch Build Out condition. The sustainable yield was determined to be ground-water yield through pumping without significantly affecting the perennial springs nor the riparian habitat of the area. The sensitivity analyses quantified the uncertainty of the calibrated model by quantifying the effects that uncertainty in the aquifer parameters had on the model (Anderson and Woessner 1992), and provided insight to how the aquifers might react to changes in recharge, e.g. due to climatic changes. The predictive modeling results were compared to the concept of sustainable yield.

**Model Objectives**

The objectives for this ground-water flow model included calibrating the model to a steady-state condition using the geological and hydrogeological characterization to establish an interpretive model. Additionally, the model was calibrated to the transient condition using the established steady-state calibration and hydrographs. The model results document a method to quantify the sustainable yield of a ground-water flow system using a numerical ground-water flow model. The transient calibration was used to simulate potential future water use scenarios. A final objective was to document the effects that current water usage is having on the hydrological system of the Mint Wash and Williamson Valley Area.

**Methods**

*Conceptual Model*

The Paulden Conglomerate and the Prescott Granite are volumetrically the most extensive hydrostratigraphic units in the MWWVS, and therefore have the greatest storage of the active model area. Cross sections show that the Paulden Conglomerate is approximately 900 feet (252 meters) thick (Woodhouse 2000) in the Williamson Valley Basin (Figures 6, 8, 9). The conglomerate is the main unit in the northern half of the study area at land surface (Plate 1). The southern half of the study area is predominantly Prescott Granite and Yavapai Series Metamorphic rocks, or a combination of the two.

The layers of the model were established based on the conglomerate and the granite. The granite is assumed to be 400-500 feet (120-150 meters) thick as a water bearing unit due to the overburden of the rock sealing most fractures below that depth (Driscoll 1986, Freeze

57

and Cherry 1979, Meinzer 1923). Depth of granite fractures for use as a ground-water flow

conduit has been determined for several plutons through case studies. Many of the studies were

conducted in granite located in areas that do not have a history of extensional tectonics.

Extensional tectonics would likely increase the depth of granite fractures that contribute to

ground water flow. The assumed 400-500 feet thickness of the Prescott Granite

hydrostratigraphic unit may be conservative due to the extensional tectonics that have been

documented in the area.

The conglomerate was assumed to be approximately 900 feet (274 meters) thick based

on preliminary analyses of geophysical data for the area (Woodhouse 2000). The layers for the

model were descritized by the assumed thicknesses of these two units.

Two layers of equal thickness were created to simulate the vertical distribution of

hydrostratigraphic units. Each layer was set at 450 feet (137 meters) thick. Areas that were

composed of fractured Proterozoic media were represented by the top layer, while layer two

was set as a no flow or inactive area (Figures 22 and 23). The areas that had conglomerate at

the surface were modeled using a combination of both layers to represent the assumed 900 feet

(274 meters) thickness.

The other hydrostratigraphic units that were modeled include the Mint Valley Basalt,

Yavapai Series schist and gneiss, and the Mixed granite/gneiss/schist hydrostratigraphic unit.

The Mixed granite/gneiss/schist hydrostratigraphic unit (Mixed unit) is located towards the

center of the field area north-northwest of the Yavapai Series metamorphic complex and west

of Table Mountain (Plate 1).The Mixed unit was treated as a fractured medium, and was

58

simulated in the first layer only, based on the same assumptions used for the Prescott granite.

The areas that were simulated in both layers include the northwestern portion of the model area representing Williamson Valley, and the lower half of the Mint Wash and Granite Basin aquifers. These regions represent mapped conglomerate and associated alluvium (Plate 1). The area where conglomerate is exposed was modeled using both layers.

Recharge zones were distributed throughout the model based on the permeability of the lithologies, and the elevation of the region. The assumption that precipitation increases 1.5 inches (3.8 cm) per 1,000 feet (305 meters) elevation increase was used when assigning recharge zones to the model grid (Springer 1998). Recharge zones were delineated along lithological contacts due to the different permeabilities between fractured media (Larsson 1976) versus sedimentary media, and was concentrated along washes due to the saturated conditions caused by runoff from precipitation events.

*Water Budget*

Inputs of water to the MWWVS include direct recharge, flow from the hydraulic headwaters at Granite Mountain, and flow from the Santa Maria Mountains. The outputs include pumping for irrigation and residential use, discharge through baseflow, and evapotranspiration.

The inflows and outflows of the ground-water system influenced the model design. Model boundaries were set at areas of baseflow, inflow and outflow. Specified flows were defined at cells located with wells. The total value for discharge due to pumping was evenly distributed through the specified flow cells by taking the calculated pumping value defined in

Chapter Three and distributing it evenly to each cell assigned to represent pumping wells.

Recharge was distributed throughout the study area to account for the recharge value reported

in the water budget.

*Software Selection*

The processor software chosen for this model is MODFLOW, a three-dimensional

finite-difference ground-water flow model (McDonald and Harbaugh 1996). Though the

geology and topography of the study area are complex, a finely spaced finite-difference grid

was used to simulate the system.

MODFLOW is the standard finite-difference model code used today. It is free and

widely used, making the MWWVS model easy to replicate. Updated versions of MODFLOW

have improved many limitations of the original code, and have made the software more

versatile. The most up to date version available with the selected pre and post-processor is

MODLFOW[win32] (ESI 1998), and was used for this modeling effort.

MODFLOW is solved using a finite-difference governing equation. Hydraulic head is

calculated at the node in the center of each cell, and is the average value calculated from the

adjacent cells (McDonald and Harbaugh 1988). All of the hydraulic properties are constant

throughout the cell.

The pre and post processor used for the model was ESI's Groundwater Vistas version

2.x (ESI 1998). Groundwater Vistas version 2.0 is constantly being updated with patches

available on the internet as errors are encountered by users, making the software versatile and

up to date.

ESI's Groundwater Vistas has a highly developed graphical user interface making it user friendly. Errors found in the MODFLOW output file are easy to fix due to Groundwater Vistas' file structure and graphical user interface. Groundwater Vistas has an effective import/export utility compatible with widely available GIS software allowing for the creation of figures displaying the modeling output as well as georeferenced surfaces of the study area created in the GIS software.

ESI's Groundwater Vistas provides it's own version of MODFLOW as well as the USGS version of the modeling code (ESI 1998). ESI has created a Windows version of MODFLOW called MODFLOW[win32] (ESI 1998) which is a Windows platform (Microsoft 2000) based version of MODFLOW. The Windows version of MODFLOW allows Microsoft Windows to communicate to Groundwater Vistas when a simulation is terminated, so Groundwater Vistas can automate the modeling process.

Automated sensitivity analyses and automated calibration are options available on Groundwater Vistas due to MODFLOW[win32]. The modeler can write a text file listing changes in parameter values for automated modeling runs in Groundwater Vistas. The results are presented by Groundwater Vistas as text files, graphs, and contoured hydraulic head files produced for each run. Both the automated calibration and the automated sensitivity analyses functions were used in the creation of the MWWVS model. The results of the automated sensitivity analyses were used to determine the most sensitive parameters to help attain calibration. The automated calibration was not very useful for this study because it was used while the model was still numerically unstable, which did not allow the automated calibration

61

attempts to converge.

*Spatial Descritization*

The region was divided into a grid with two layers of cells. Each layer has 156 columns and 272 rows of cells (Figures 22 and 23). Each cell represents 125 meters in the x-direction, 125 meters in the y-direction, and 137 meters in the z-direction. The model contains 84,864 total cells with 43,410 active cells. The total model surface area is 663 km$^2$, the total model volume is 182 km$^3$ with an active model volume of 94 km$^3$.

Inactive areas were established where no water level data could be collected due to lack of wells. Layer 2 also has inactive cells that underlie the fractured media due to the assumed thickness of the hydrostratigraphic units in the fractured crystalline rock.

Elevation of the model grid was imported from Digital Elevation Models (DEM) made available by ALRIS (2000). The elevation data in the DEMs were imported as top elevation zones to layer 1 in Vistas. The elevation databases were set to 1 meter accuracy for the elevation value assigned to each cell from the imported DEM.

The top elevation of layer 2 and the bottom elevation of layer 1 were both 137 meters below the top of layer 1. The top elevation zones from layer 1 were copied into the bottom of layer 1 and the top of layer 2 with a zone decrement of 137 meters. This set layer 1 to be exactly 137 meters thick at each cell.

The bottom elevation of layer 2 was set the same way as the bottom elevation of layer 1. The zones from the top elevations of layer 2 were copied into the bottom of layer 2 with a zone decrement of 137 meters. This made layer 2 exactly 137 meters thick at each cell.

*Boundaries*

The boundaries for the numerical model are similar to the boundaries of the MWWVS conceptual model and are shown in Figures 22 and 23. The boundaries are physical, hydrological, or based on the availability of data. The boundaries were altered throughout the modeling process as areas of numerical instability were identified.

The northern boundary is the confluence of the Williamson Valley surface water flow system with the Big Chino Valley flow system (Figure 21). The confluence is located just north of the Sullivan Buttes, and is parallel to the UTM northing base line. The boundary is a hydrologic boundary.

The eastern boundary is the western base of the Sullivan Buttes, and extends farther east, south of the Sullivan Buttes to include Table Mountain and the residential developments east of Mint Wash. The boundary was determined by the availability of data as well as a surface-water divide. The boundary at the Sullivan Buttes was established due to a lack of wells within the buttes and is not the physical divide represented by the crest of the Sullivan Buttes. The southern portion of the eastern boundary is a very subtle physical divide as represented by the surface hydrology. The area adjacent to this boundary within the model drains into Mint Wash, the adjacent area outside of this model boundary drains into Little Chino Valley.

The southern boundary was determined by the availability of water level data. Granite Mountain was excluded from the model area due to the lack of wells and water-level data. The southern boundary is set at the base of Granite Mountain. Mixed hydraulic head boundary cells were placed around Granite Mountain and represent mountain front recharge (Figure 22).

The southern boundary west of Granite Mountain was also established by the availability of data. The area excluded from the model is either National Forest or minimally developed, and wells were not available to collect water level data.

The western boundary is set at the foothills of the Santa Maria Mountains. The western boundary represents the physical boundary present at the crest of the Santa Maria Mountains. The western boundary is linear, parallel to the UTM Easting base line, similar to the linear crest of the Santa Maria Mountains.

An internal boundary is present extending north from the southern boundary covering Granite Mountain connecting to the eastern boundary of the model area representing the Sullivan Buttes (Figure 21). This boundary represents the ground-water divide indicated on the potentiometric surface map of the MWWVS (Figure 19), and was inserted during the calibration process to optimize the calibration of the model.

*Parameter Values - Hydraulic Conductivity*

Initial estimates of hydraulic conductivity values for the hydrostratigraphic units were developed from aquifer tests and specific capacity estimates (Table 5). The values attained in the hydrogeological characterization of the MWWVS were used as initial parameter values for the model (Table 3). The values were altered through trial and error during calibration.

The limited aquifer test and specific capacity data for each hydrostratigraphic unit made it difficult to create an error limit for the values of the parameters. Variograms are commonly used in modeling to create error limits for parameter values based on the variability of the values in space. Heterogeneous materials will produce different parameter values based on the location of the measurement. Several measurements of the same parameter at different points within a heterogeneous material will provide a range of values for that parameter. Variograms quantify the uncertainty of parameter values based on heterogeneity. The uncertainty can provide an allowable error range, which can be used to validate the final calibrated property values. The only measure of the validity of the final calibrated hydraulic conductivity values is a range of measured values for different lithologies as reported in hydrogeology text books (Table 5) (Domenico and Schwartz 1998).

Initial values for the vertical anisotropy of the hydraulic conductivity (K) were assumed to vary between 3:1 (horizontal K:vertical K) and 100:1. The initial values were not considered to be representative of the actual values, and calibration was the process responsible for attaining representative values of vertical anisotropy.

Anisotropy was not available through any of the aquifer tests. Neuman's (1975)

unconfined analytical method provides anisotropy estimates for aquifer tests where water level

is monitored at an observation well. The only aquifer test with water level data from an

observation well was the test performed on ARwell 52 with observation well ARwell 54, but

the test was deemed invalid due to significant dewatering of the aquifer during the aquifer test,

and $k_x$:$k_z$ could not be determined.

*Parameter values - Recharge*

Initial estimates of recharge were calculated using the precipitation data from three rain

gages located throughout the study area (Figure 25). Two methods for estimating recharge from

precipitation data were used.

A previous study in the vicinity of the MWWVS assumed that 4% to 5% of total

precipitation forms direct recharge (Corkhill and Mason 1995). This assumption was used as

an initial estimate of the recharge values for the different zones in the MWWVS model.

The other method for calculating recharge was by using an equation developed by

Rabinowitz et al. (1977) for a precipitation-recharge relationship. Rabinowitz estimated the total

amount of recharge to an aquifer in New Mexico from precipitation by measuring tritium

concentrations of the water discharging from the aquifer. The equation is:

$$\mathbf{R} = f\mathbf{P}_i \quad \text{where:} \quad f = k(\mathbf{P}_i/\mathbf{p})$$

and R = annual recharge, $P_i$ = annual precipitation of the ith year, $f$ = proportionality factor, p =

mean annual precipitation (all in the same units), and $k$ = normalizing factor. These values are

reported along with the values attained using the 4% to 5% precipitation assumption and the

final calibrated values (Table 6).

As can be noted from Table 6, the two methods of recharge estimation from precipitation data overestimated the representative recharge values attained through calibration. Methods of recharge estimation based on percentages of precipitation data can be misleading and should not be used by practitioners (Watson et al. 1976, Gee and Hillel 1988). Empirical precipitation-recharge expressions can be useful estimates of recharge if the constants have been derived from careful observation and measurement, and should not be used on any other ground-water basin for recharge determination (Simmers 1997). The values calculated using these different methods of recharge estimation were used to provide initial values to the recharge zones, but calibration was used to provide representative values of recharge for the zones and conceptual water budget.

The recharge values used in the model account for natural recharge, recharge induced anthropogenically through septic systems, and evapotranspiration caused by features other than riparian vegetation or perennial springs. Septic systems are a variable that could not be accounted for in this recharge model due to the limited septic return data available for the MWWVS. This may have been another factor contributing to the discrepancy between the calculated recharge values and the calibrated recharge values. Evapotranspiration that was not caused by perennial springs or riparian vegetation was included in the recharge parameter to minimize the number of variables presenting uncertainty to the calibration process. No measurements of field evapotranspiration were collected, and no values for average field evapotranspiration representative of the climate at the study area were found in the existing literature.

67

*Parameter Values - Storage/Specific Yield/Porostiy*

Storage, specific yield and porosity were modeled in the transient condition (Figure 24). No valid absolute storage data was available for the MWWVS, so the constraint on the values used were based on literature values. A qualitative relation of the storage values between the lithologies was established through analysis of the hydrographs included as Figures 14 through 18. Average absolute storage values for lithologies found in the MWWVS were estimated (Domenico and Schwartz 1998), and are in Table 7.

Initial storage, specific yield, and porosity values were adjusted through the transient model calibration process. The storage parameters affected the magnitude of water level change with time. These values were adjusted until the simulated hydraulic heads hydrograph had a similar degree of water-level change over the study period to the observed hydraulic head hydrographs. The storage/specific yield/porosity values used in the calibrated model fall within the range indicated in Domenico and Schwartz (1998).

*Parameter Values - Evapotranspiration*

Zones of active evapotranspiration were modeled in areas of observed perennial or ephemeral springs and riparian vegetation (Figure 26). Values of evapotranspiration and extinction depths were established from a previous water use study by Wright (1997). Wright's study established water use by riparian plants in central Arizona. The study established average water use for mature cottonwood, young cottonwood, and mesquite. Wright also established values for pan evaporation in semi-arid central Arizona. The pan evapotranspiration value was modeled in areas of observed perennial springs. Wright also established the extinction depths

for evapotranspiration along springs and for different species of riparian vegetation. The extinction depths were incorporated into the model simulations.

Evapotranspiration was not altered during model calibration process from the values that Wright established. Evapotranspiration was a negligible percent of the total water budget, and it was assumed that any alteration of these values would not create a significant change in the modeling results (Table 8).

*Parameter Values - Drains*

Drain cells were input to the calibrated steady-state and transient models to dewater the area where the simulated water levels exceeded the top elevation of layer one. This occurred in the model grid that represented perennial springs in the MWWVS. The cells where the simulated water levels exceeded the top of layer one had to be dewatered until the water table was at or below the top of layer one so MODFLOW would account for all of the water in the mass balance.

The conductance of the drain cells were altered until the values were optimized by assigning the lowest value of conductance to the cells to dewater the cells to the level of the top of layer one. The drain cells were only activated to attain the mass balance / water budget output of the model simulations. No drains were active when the water table was modeled so as to not affect the modeled water table with drains that were input as a tool to correct the water budgets. The drains are virtual dewatering features that affect the modeled water table.

The water budgets were altered as a result of the introduction of drain cells. The conductance was minimized so the drains would have a minimal affect on the simulated water budgets. The drains affected the evapotranspiration (ET) and flux out values in the MODFLOW mass balance. The volumes of water discharged through the drain cells are likely a combination of water removed from ET and flux out. For the purposes of this study the volumes of water discharged through drains was assumed to be removed entirely from ET. The ET rates listed in Table 11 - Table 14 include the value of water discharged through the drain features. This assumption altered the water budgets because the water accounted for through the drains is a combination of ET and flux out.

*Sustainable Yield Estimation*

Sustainable yield has been defined as water use to support human communities without degrading the hydrological cycle and the ecosystems that depend on water (Gleick 1998). Sustainable water yield for the MWWVS was determined to be a yield above which perennial springs would dry out or the root zone of the riparian habitat would significantly dewater through ground-water drawdown due to pumping. Most of the perennial springs within the

70

MWWVS have water levels within 1 foot (0.30 meters) of land surface. Lowering the water table one foot (0.30 meters) would dry out the springs located in the MWWVS, and may significantly dewater the root zone of the riparian habitat.

Virtual Observation wells were placed in model cells representing springs and riparian communities within the MWWVS (Figure 28). Discharge rates were varied to create different drawdown scenarios at the observation cells. Sustainable yield was defined as a well discharge that created 1 foot (0.30 meters) of drawdown from the non-pumping condition to the respective pumping condition at any of the observation cells.

The model area was divided to represent the three aquifers identified in the hydrogeological characterization (Figure 29). Zone water budgets were produced for the Granite Basin Aquifer, Mint Wash Aquifer, and Las Vegas Aquifer (Table 12 - Table 14). The zone budget for the whole model area is included as Table 11 for a comparison of the individual aquifers versus the MWWVS..
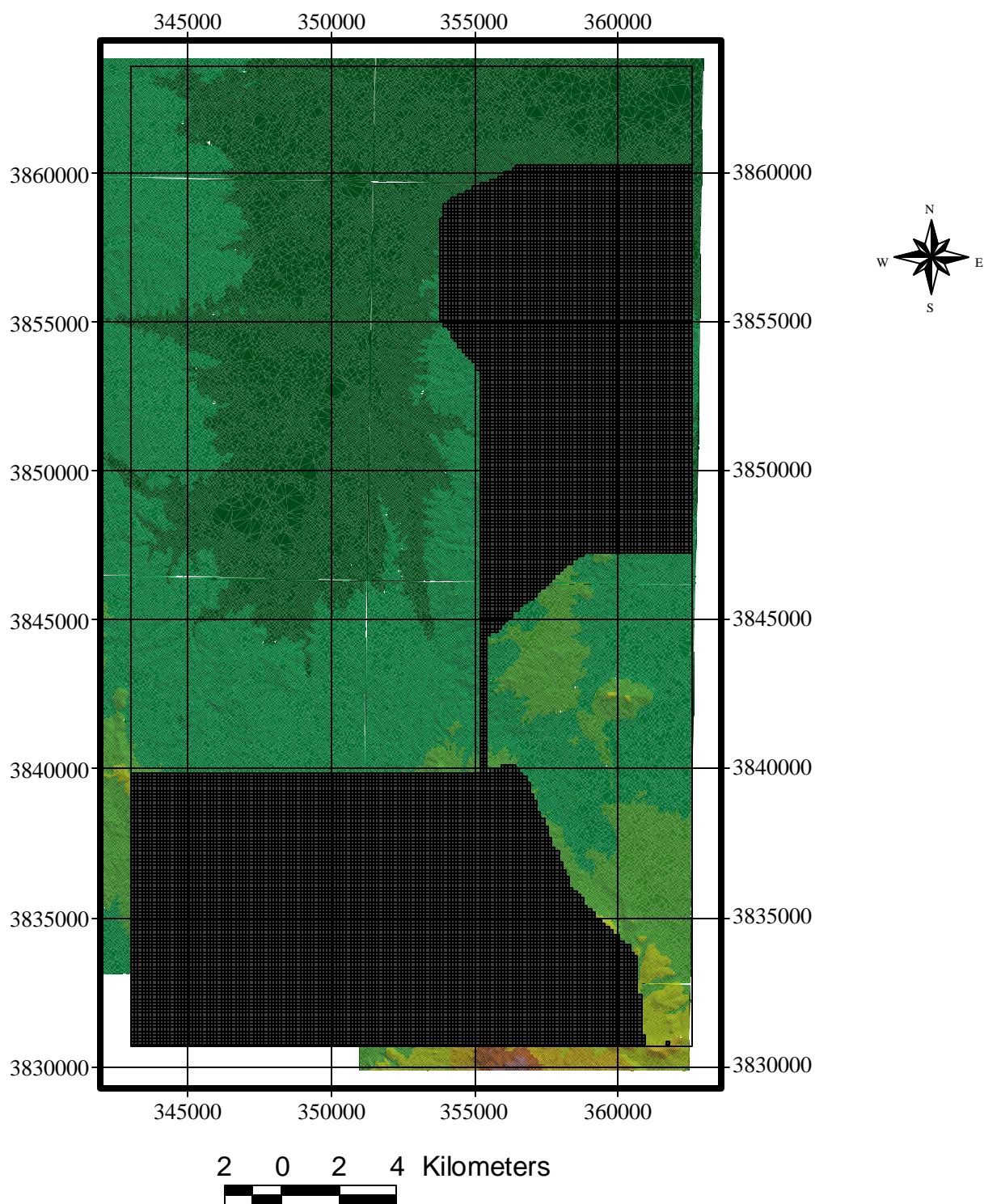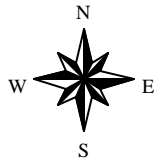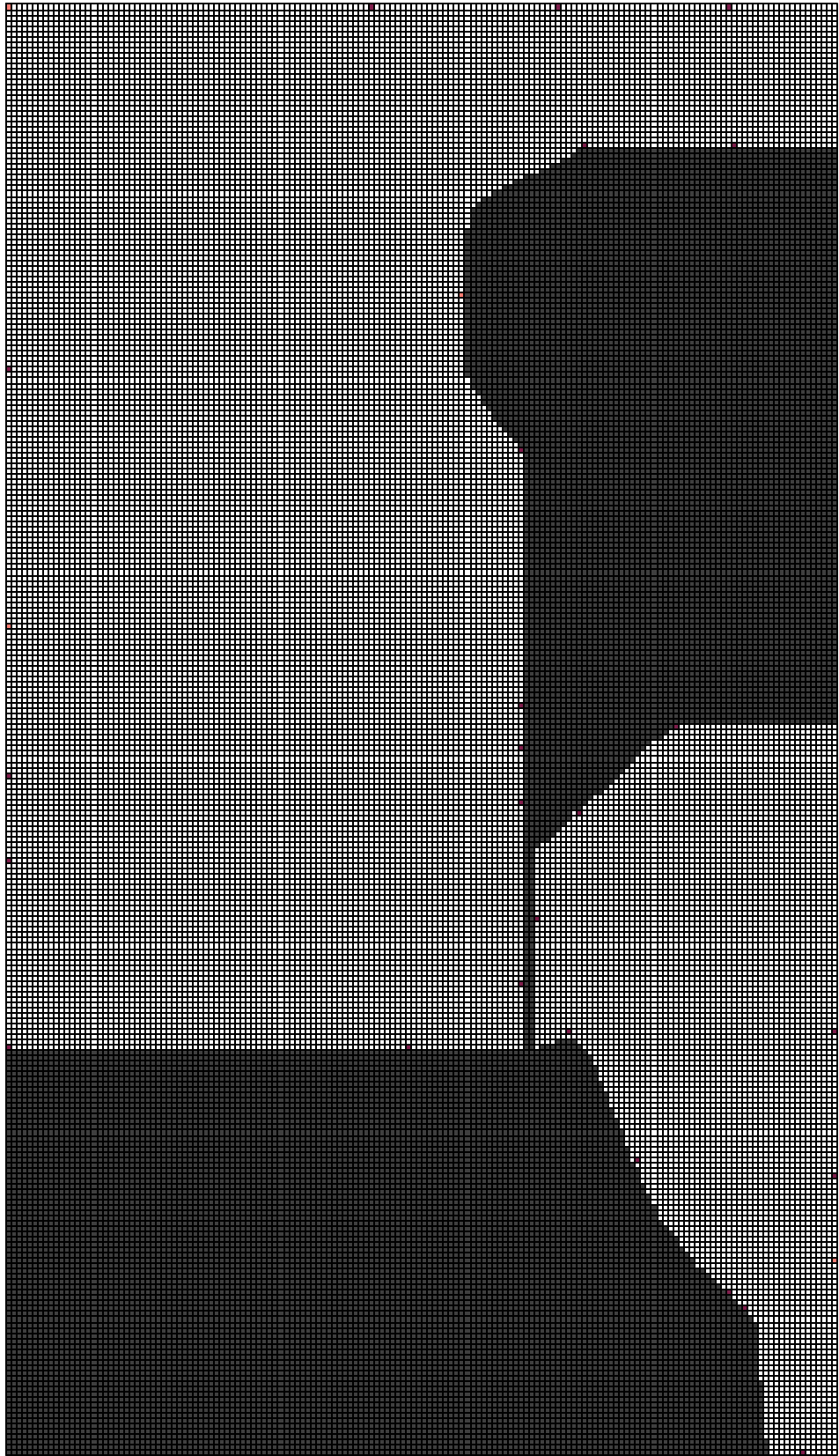
Figure 21 - Triangular Irregular Network (TIN) of the MWWVS
overlain by the active and inactive model area.
Coordinate grid is UTM Northing and Easting.

## Legend

■ Noflow zone

☐ layer1

## Legend

- ■ Constant Head Boundary cells
- ■ General Head Boundary cells
- ■ Noflow zone
- □ Grid cell

Figure 22 - Layer one grid with boundary condition    cells. Refer to Figure 21 for georeference.
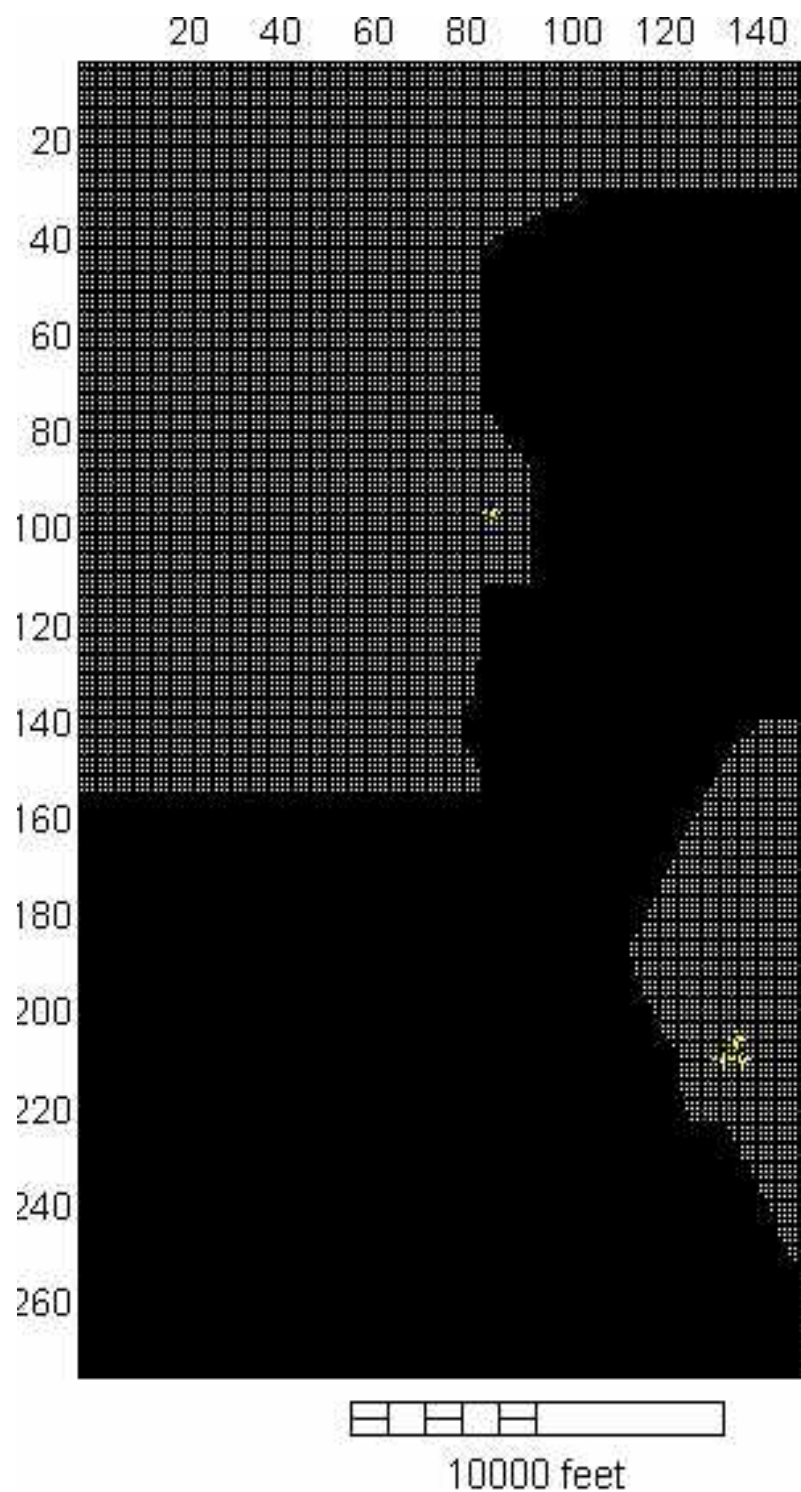
Figure 23 - Layer two model grid. Row and column numbers are listed on the left and top boundaries of the grid.

74

Figure 24 (a) - Zone distributions of horizontal and vertical hydraulic conductivity, storage, specific yield, and porosity in layer 1. The three
RS locations indicate the approximate location of the rain stations. Data collected from the rainstations are included in appendix 3.
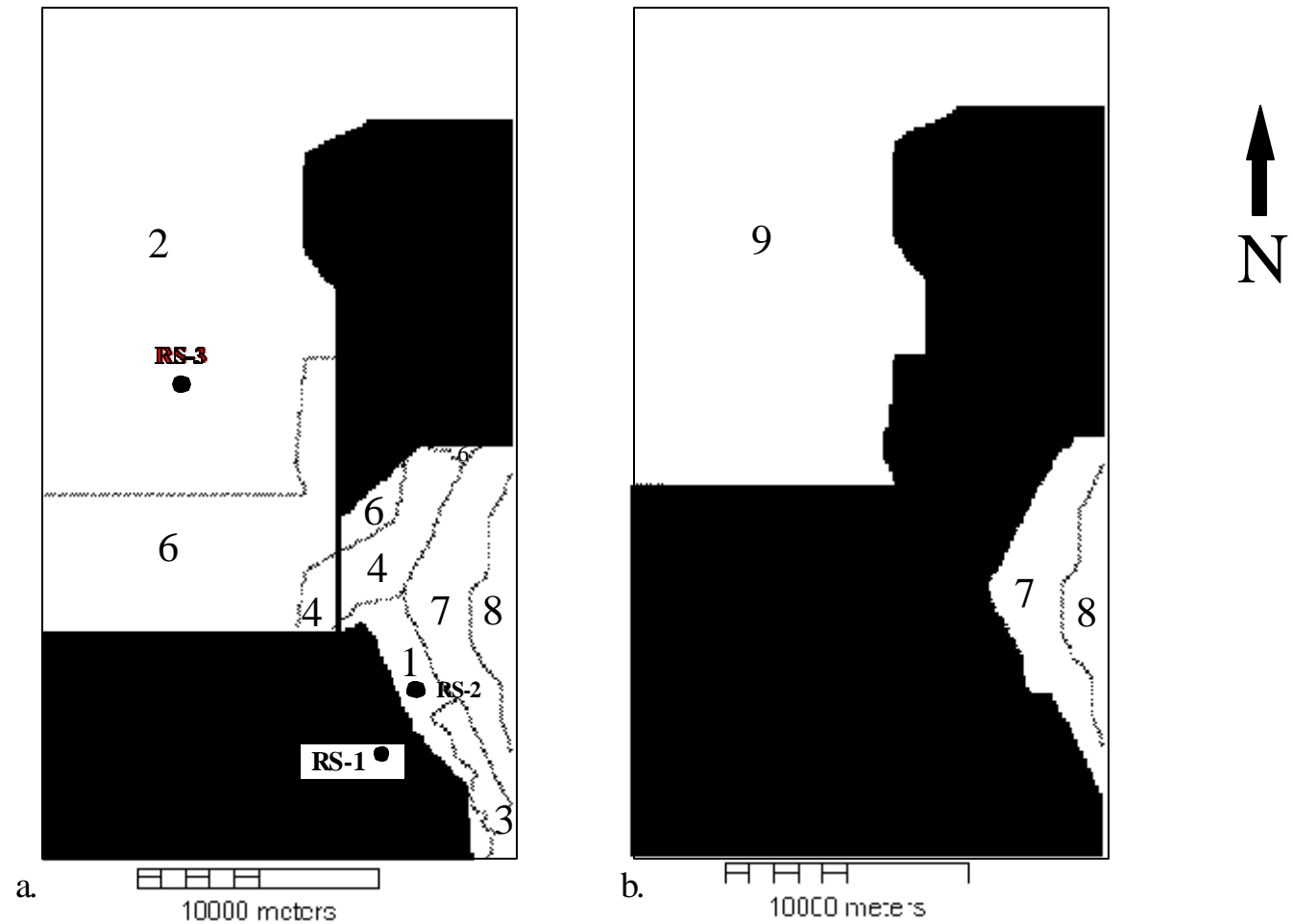Figure 24 (b) - Zone distributions of horizontal and vertical hydraulic conductivity, storage, specific yield, and porosity in layer 2 .
Refer to Table 5 for Zone values. Refer to Figure 21 for georeference.
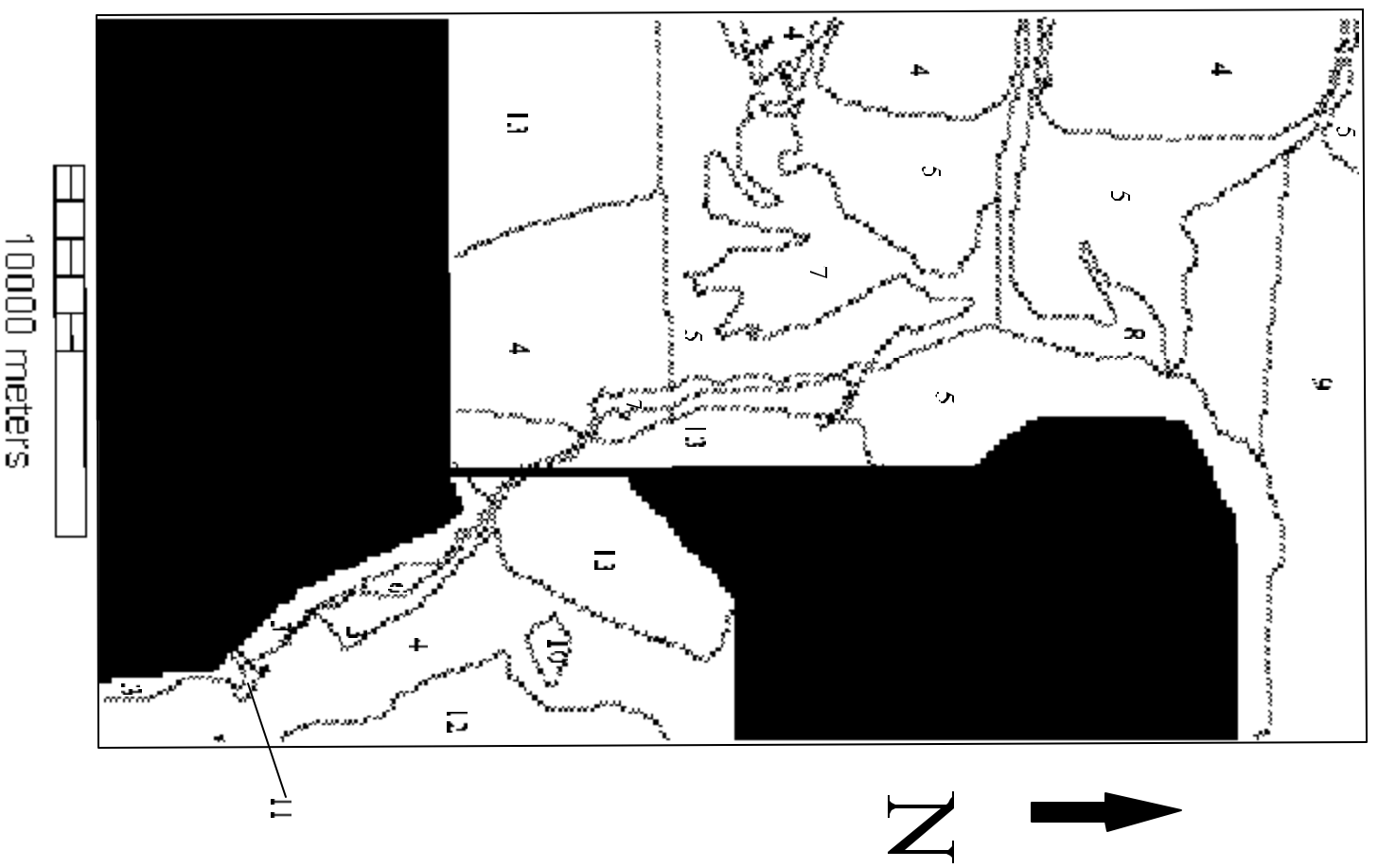
Figure 25 - Zone distribution for recharge in layer 1.
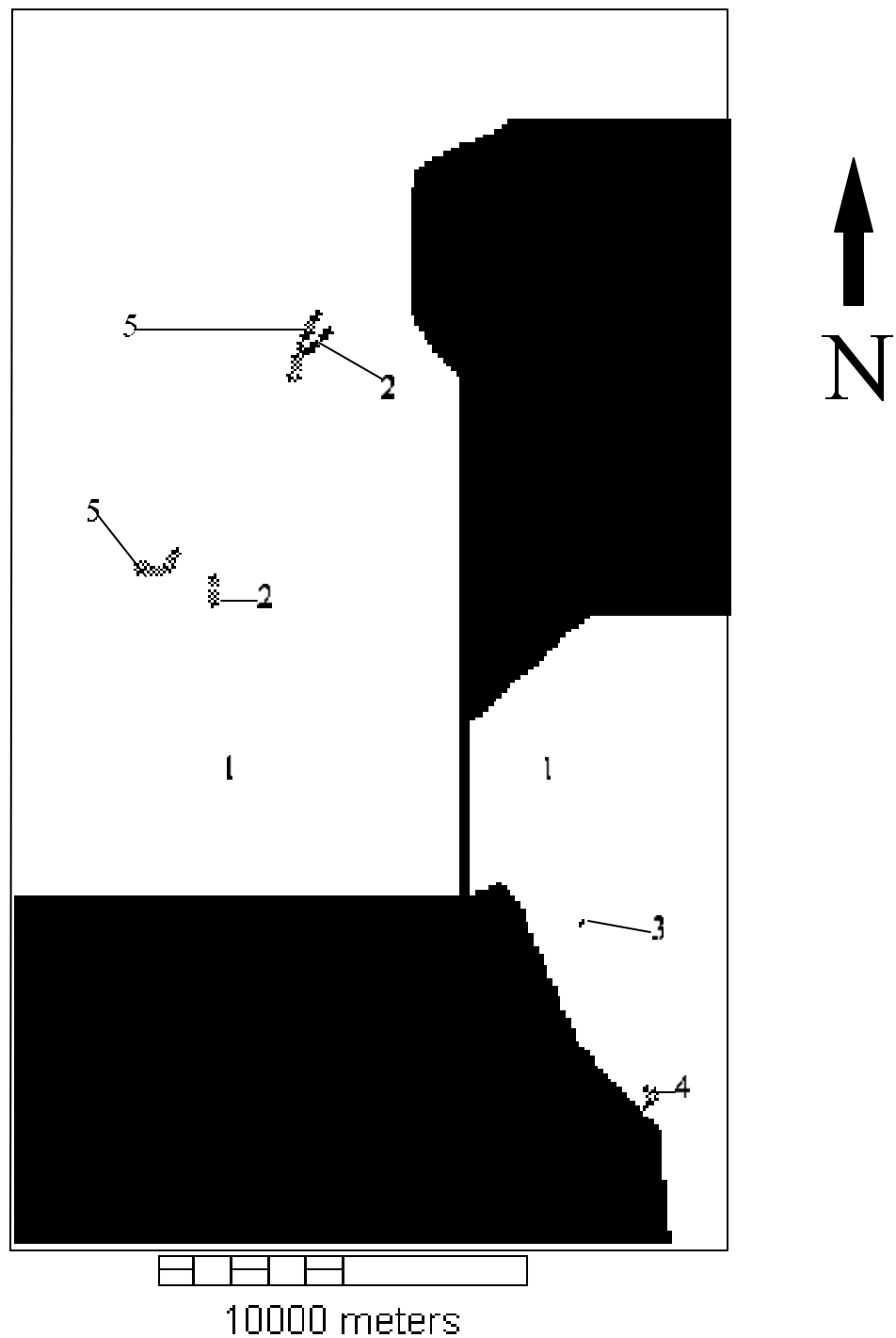Refer to Figure 21 for georeference.

76

N

5

2

5

2

1

1

3

4

10000 meters

Figure 26 –Zone distribution for evapotranspiration in layer 1.
Refer to Figure 21 for georeference.

**Results**

*Steady-State Calibration*

Steady-state model calibration was initiated using the initial parameter values estimated from the aquifer tests and specific capacity values discussed in Chapter Three. The model was calibrated using 24 targets representing wells where monthly water-level measurements were collected and additional wells to provide more targets for the calibration. The water-level data were collected at the end of the study period in August, 2000.

The model was calibrated through trial and error parameter adjustment. The most sensitive parameters were identified through an initial sensitivity analysis, and these parameters were adjusted until the model approached calibration. Changes were made in the grid cell spacing as well as the active versus inactive regions.

When the model approached the calibration criteria, parameter values in problem zones were altered through trial and error to improve calibration. The ground water divide between the Las Vegas aquifer and the Mint Wash aquifer was modeled as an inactive boundary. The model could not be calibrated without the simulation of the ground-water divide as an inactive area unless the $k_x = k_y$ (horizontal hydraulic conductivity) and $k_z$ (vertical hydraulic conductivity) zone values were changed to unrealistic values.

Two statistical measures of the calibration of a model are the root mean square error (RMSE) and the mean absolute error (MAE). The mean absolute error is the mean of the absolute value of the difference between measured and simulated hydraulic heads. The root mean square error is the average of the squared difference in measured and simulated hydraulic

78

heads (Anderson and Woessner 1998):

$$MAE = \frac{1}{n} \sum_{i=1}^{n} \left| (h_m - h_s)_i \right|$$

$$RMSE = \left[ \frac{1}{n} \sum_{i=1}^{n} (h_m - h_s)_i^2 \right]^{0.5}$$

where n is the number of observations, $h_m$ is the measured hydraulic hydraulic head, and $h_s$ is

the simulated hydraulic hydraulic head.

The calibration criteria for the steady-state model was established using the criteria

outlined in Anderson and Woessner (1992). The criteria outlined for a steady-state model

include a Root Mean Squared Error (RMSE) of observed versus simulated hydraulic heads no

greater than 5% of the total hydraulic head change across the model. A model that reaches this

criterion is considered a "good model" (Anderson and Woessner 1992) (Figures 30 and 31).

Another criterion for steady-state as well as transient calibration is how well it's simulated water

budget compares to the conceptual water budget. A condition of a ground-water model is that

all water in and out of the system is accounted for, as well as any change in the storage.

Therefore the mass balance for any time step in a model should have less than a 1%

discrepancy (Table 9).

After the steady-state model was calibrated, the transient model was calibrated. The

transient calibration involved altering several model parameters, including parameters that had

been established through the steady-state calibration. Upon the calibration of the transient

condition, the steady-state condition was re-calibrated with the transient parameter values to

79

assure that the model satisfied the calibration criteria for both the steady-state and transient

conditions.

*Transient Calibration*

The transient model was calibrated using a semi-quantitative calibration. The calibration

criteria included maintaining the mass balance requirements for each time step (less than 1%

discrepancy), but the hydraulic heads were not validated quantitatively. The qualitative criteria

for the transient calibration was to create simulated hydraulic heads which had the same trends

and the same magnitude of change as the observed hydraulic heads.

The transient calibration had two objectives. The first was that the transient calibration

would serve as a validation of the steady-state calibration. The transient calibration would also

establish the framework for the creation of predictive scenarios, which is an objective of this

study of the MWWVS. The predictive scenarios had different pumping scenarios to simulate

potential water use in the area. All of the other model parameters remained constant for the

predictive scenarios.

The stresses included in the steady-state model were broken down into 12 time steps

that were used in the transient design. The boundary conditions included recharge,

evapotranspiration, and discharge wells.

Recharge was distributed throughout the stress periods to reflect the precipitation

throughout the study area. The calibrated steady-state recharge values (Table 6) were

distributed throughout the stress periods to represent the percentage of total precipitation during

the respective month (Appendix 3), based on the data gathered at the nearest rain gauge.

Periods of increased recharge were modeled to reflect the late summer during the monsoon season, and winter. The distribution of recharge was based on precipitation data collected at three rain gages distributed throughout the study area.

Discharge of the domestic pumping wells was temporally divided to represent the assumptions of water use that were described in Chapter Three. Twenty percent of the wells reflected field observed pumping schedules for irrigation wells, with discharge occurring in the spring and early summer. The remaining 80% were modeled as domestic wells, with continuous water use year round. The distribution of water well use was established from the ADWR well registry for the area (ADWR 2000).

Evapotranspiration was modeled in cells representing areas of surface water or riparian habitat (Figure 26). Evapotranspiration was distributed throughout the stress periods to represent the summer months where evapotranspiration would be greatest. No evapotranspiration was modeled for the winter months from October '99 through March '00. Though there may be evapotranspiration during the winter, this amount was assumed to be negligible in the scope of the water budget.

*Sensitivity Analyses*

Sensitivity was defined as an absolute value of the calibrated versus observed hydraulic head residuals for this model as a change in a parameter value to the extent that the model departs from the calibration criteria. Sensitivity was also defined qualitatively along a relative scale. The parameters that were analyzed for sensitivity were compared to each other and identified as the most or least sensitive parameter.

Sensitivity analyses were created for one parameter and one boundary condition at a time. Hydraulic conductivity for all active zones was analyzed for sensitivity in the steady-state condition (Figure 32). The analysis was quantified by using the calibration criteria. The variable was changed increasingly away from the calibrated value until the model no longer met the steady-state calibration criterion based on the RMSE value.

Recharge was analyzed for sensitivity in the steady-state condition (Figure 33). This variable was changed by orders of magnitude greater than, and less than, the calibrated value to quantify the sensitivity. As with hydraulic conductivity, recharge was varied until the model no longer met the steady-state calibration criterion based on the RMSE value.

Recharge and hydraulic conductivity have similar sensitivities. Sensitivity in this model is more a function of the zone than the parameter. Some of the zones for both recharge and hydraulic conductivity were highly sensitive relative to other zones that are not very sensitive over a parameter change of several orders of magnitude. Comparatively, recharge zones appear to be slightly more sensitive than the hydraulic conductivity zones, due to several recharge zones that make the model exceed the calibration criteria represented by the top of the graphs (Figures 32 and 33) with a relatively low variance from the calibrated value.

The recharge and hydraulic conductivity zones that were closer to the headwaters (Granite Mountain) appear to be more sensitive to changes in recharge and hydraulic conductivity values. The area closer to the headwaters have a higher ground water gradient (Figure 19), as well as more recharge (Figure 32 and Table 6). These factors may be responsible for the relatively high sensitivity of these zones to changes in parameter values.

82

Table 5 - Initial values, literature values, and calibrated values for hydraulic conductivity.

| Lithology | Initial Value (m/yr) | Literature Value (m/yr) | Calibrated Value (m/yr) | Calibrated Vertical Anisotropy |
|---|---|---|---|---|
| Granite (zone 1) | 460 | 0.2-9000 | 330 | 1.7:1 |
| Conglomerate (zone 2) | 990 | 30-20,000 | 990 | 1.4:1 |
| Basalt (zone 3) | 88 | 10-600,000 | 220 | 11:1 |
| Gneiss/schist (zone 4) | N/A | 0.2-9000 | 50 | 10:1 |
| Granite/Gneiss/ Schist (zone 6) | N/A | 0.2-9000 | 300 | 100:1 |
| Weathered Granite (zone 7) | N/A | 100-2000 | 300 | 150:1 |
| Conglomerate (zone 8) | N/A | 30-20,000 | 6,000 | 1:1 |
| Buried Conglomerate (zone 9) | N/A | 30-20,000 | 700 | 1:1 |

Table 6 - Initial values and calibrated values for recharge.

| Recharge Zone | Initial Values ($m^3$/yr/cell) | Calibrated Values ($m^3$/yr/cell) |
|---|---|---|
| 1 | 0.024 | 0 |
| 2 | 0.022 | 0 |
| 3 | 0.017 | 0.03 |
| 4 | 0.016 | 0.01 |
| 5 | 0.014 | 0.0005 |
| 6 | 4.82 | 2.5 |
| 7 | 0.3 | 0.001 |
| 8 | 0.3 | 0.0003 |
| 9 | 0.3 | 0.0001 |
| 10 | 3.2 | 0.2 |
| 11 | 6.8 | 3.6 |
| 12 | N/A | 0.001 |
| 13 | N/A | 0.04 |

Table 7 - Literature and calibrated values for specific yield and porosity.

| Lithology | Literature Specific Yield Range | Calibrated Specific Yield | Literature Porosity Range | Calibrated Porosity |
|---|---|---|---|---|
| Granite (zone 1) | N/A | 0.15 | 0.01-0.6 | 0.2 |
| Conglomerate (zone 2) | 0.35-0.03 | 0.2 | 0.01-0.4 | 0.2 |
| Basalt (zone 3) | N/A | 0.15 | 0.01-0.6 | 0.2 |
| Gneiss/schist (zone 4) | N/A | 0.1 | 0.01-0.6 | 0.15 |
| Granite/Gneiss/Schist (zone 6) | N/A | 0.1 | 0.01-0.6 | 0.1 |
| Weathered Granite (zone 7) | N/A | 0.2 | 0.01-0.6 | 0.3 |
| Conglomerate (zone 8) | 0.35-0.03 | 0.2 | 0.01-0.4 | 0.2 |
| Buried Conglomerate (zone 9) | 0.35-0.03 | 0.1 | 0.01-0.4 | 0.1 |

Table 8 - Evapotranspiration rates and extinction depths used in calibrated model.

| Evapotranspiration Zone | Evapotranspiration Value ($m^3$/yr/cell) | Extinction Depth (meters) |
|---|---|---|
| 1 | 0 | 0 |
| 2 | 3.68 | 3.0 |
| 3 | 2.06 | 1.8 |
| 4 | 2.8 | 1.0 |
| 5 | 3.74 | 3.0 |

Table 9 - Calibration statistics for the steady-state and transient models.

| Time (Stress) Period | Total Head Change Across Model (meters) | RMSE (meters) | RMSE % of Total Head Change (%) | Water Budget Error (%) |
|---|---|---|---|---|
| steady-state | 239.73 | 5.42 | 2.3 | 0.04 |
| Aug, 99 (1) | 240.04 | 7.87 | 3.3 | -0.11 |
| Sep, 99 (2) | 237.37 | 8.06 | 3.4 | -0.07 |
| Oct, 99 (3) | 234.03 | 8.14 | 3.5 | -0.10 |
| Nov, 99(4) | 234.85 | 8.10 | 3.5 | -0.12 |
| Dec, 99 (5) | 234.44 | 7.94 | 3.4 | -0.12 |
| Jan, 00 (6) | 239.68 | 8.10 | 3.4 | -0.13 |
| Feb, 00 (7) | 239.80 | 8.33 | 3.5 | -0.14 |
| Mar, 00 (8) | 238.67 | 8.46 | 3.5 | -0.14 |
| Apr, 00 (9) | 236.26 | 8.30 | 3.5 | -0.15 |
| May, 00 (10) | 234.83 | 7.30 | 3.1 | -0.17 |
| Jun, 00 (11) | 237.88 | 4.18 | 1.8 | -0.18 |
| Jul, 00 (12) | 239.93 | 4.40 | 1.8 | -0.18 |

Table 10 - Drawdown observations made at areas of interest (AOIs) representing springs and riparian habitat for comparison with the sustainable yield criteria.

| Observation Point | Current Condition Drawdown (meters) | Safe Yield Drawdown (meters) | Sustainable Yield Drawdown (meters) |
|---|---|---|---|
| 1 | 0.23 | 8.0 | 0.3 |
| 2 | 0.15 | 7.0 | 0.2 |
| 3 | 0.18 | 6.5 | 0.27 |
| 4 | 0.24 | 9.5 | 0.3 |
| 5 | 0.2 | 7.5 | 0.25 |
| 6 | -0.1 | 0.7 | -0.1 |
| 7 | -0.08 | 0.8 | -0.07 |
| 8 | -0.005 | 0.62 | 0.0 |
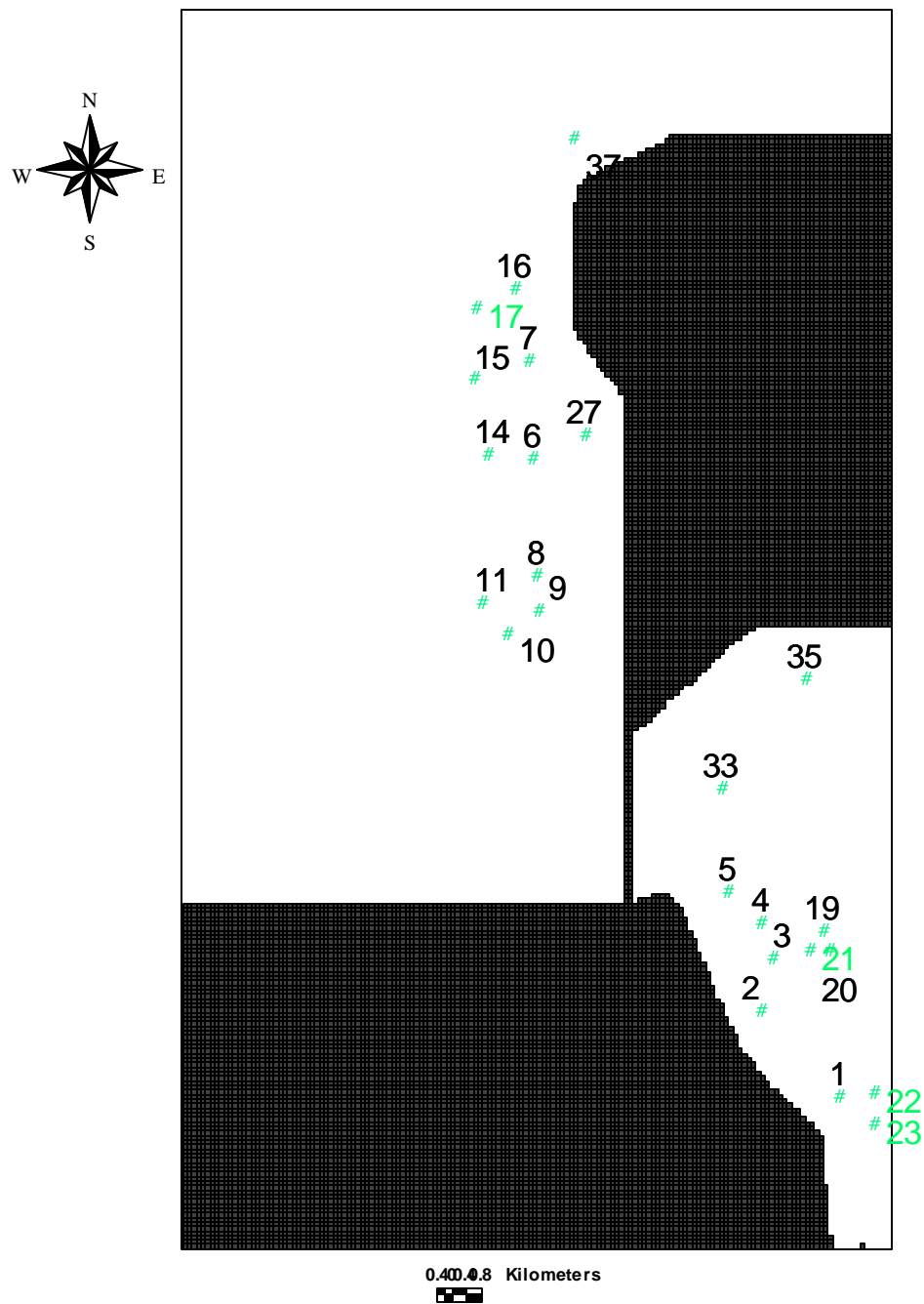
Figure 27 - Map showing the location of the steady-state and transient targets. Targets used in the transient condition include targets 1-17. Refer to Figure 21 for georeference.
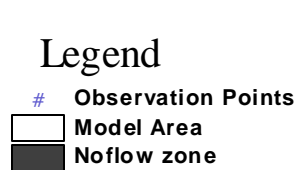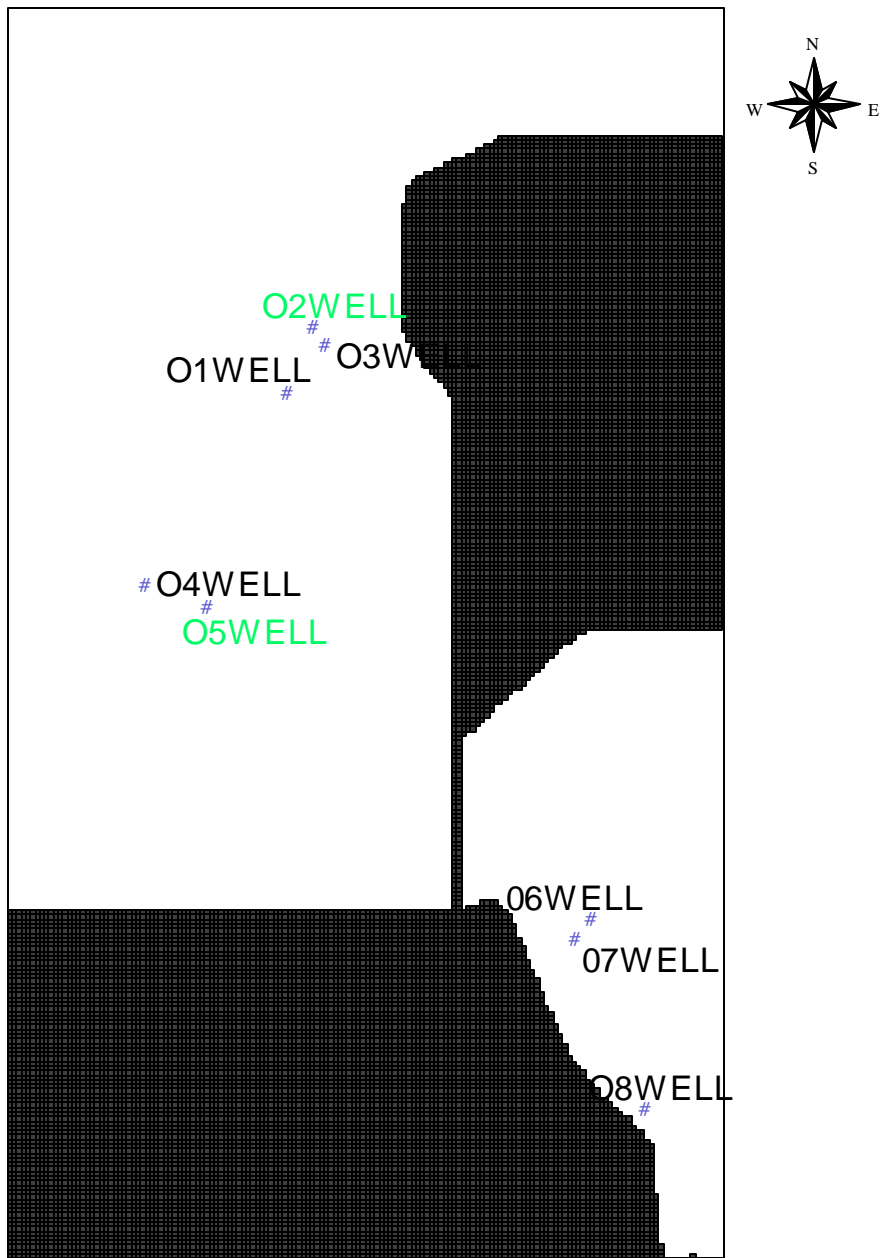
Figure 28 - Map showing locations of the Observation Points (virtual wells) used for analysis of the predictive scenarios. Refer to Figure 21 for georeference.

Las Vegas
Aquifer

Mint Wash
Aquifer

Granite
Basin
Aquifer

1   0   1   Kilometers
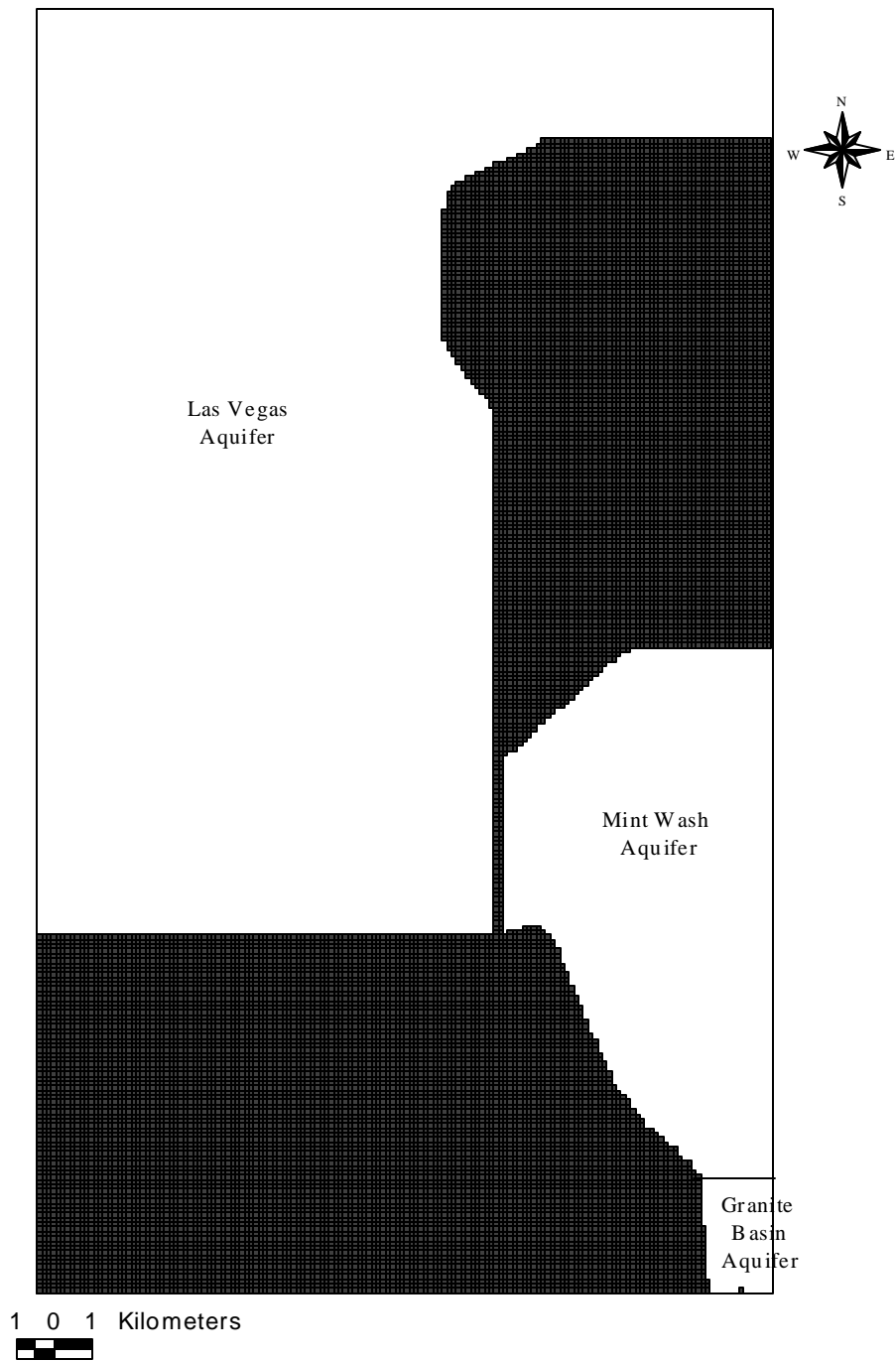
Legend

Model Area
Noflow zone

Figure 29 - Map showing seperate aquifers
where zone budgets were calculated for
steady-state, transient, and predictive models.
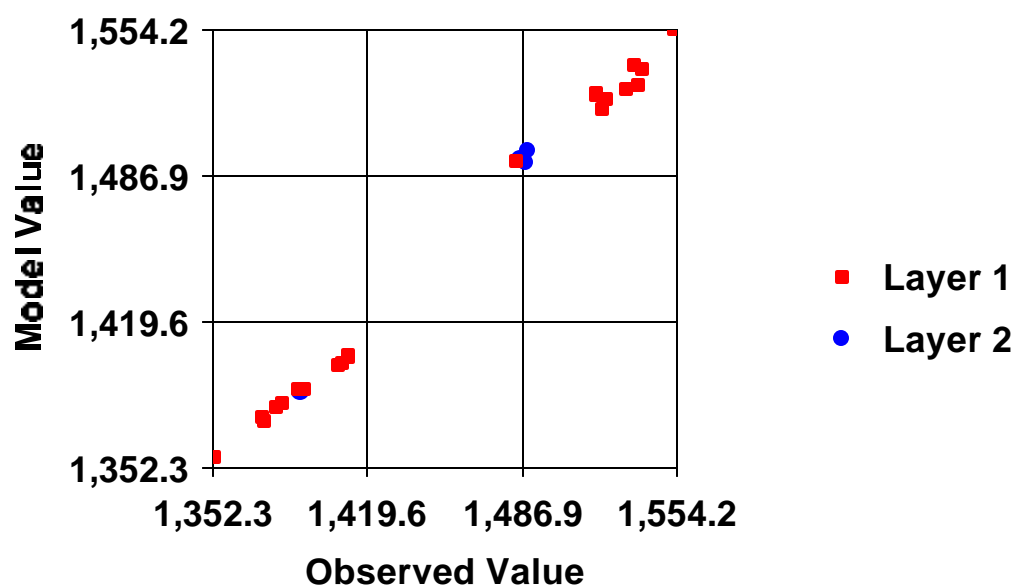Refer to Figure 21 for georeference.

**Observed vs. Computed Target Values**



Figure 30 - Observed vs. Computed target values for the steady-state calibration.
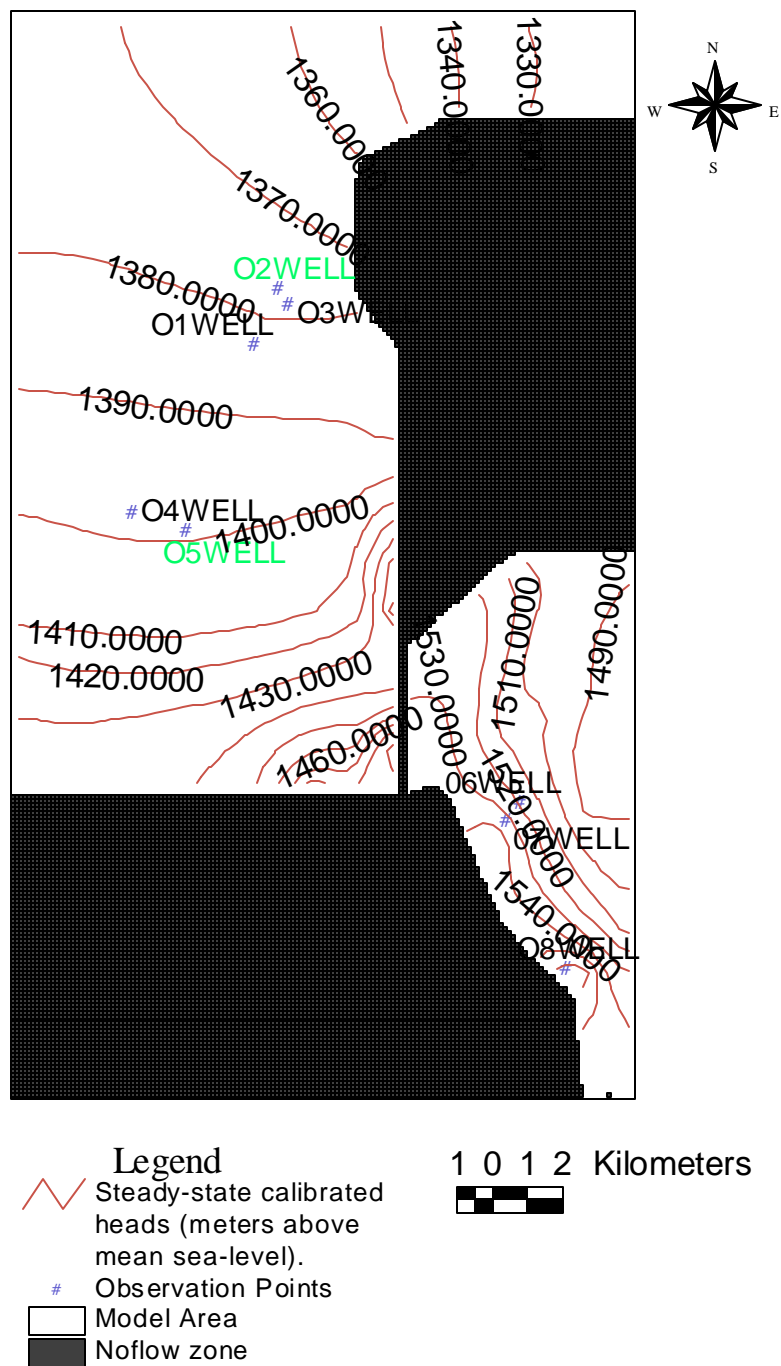
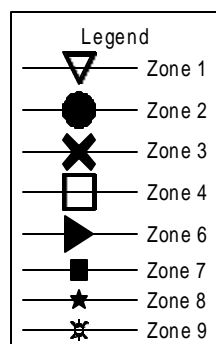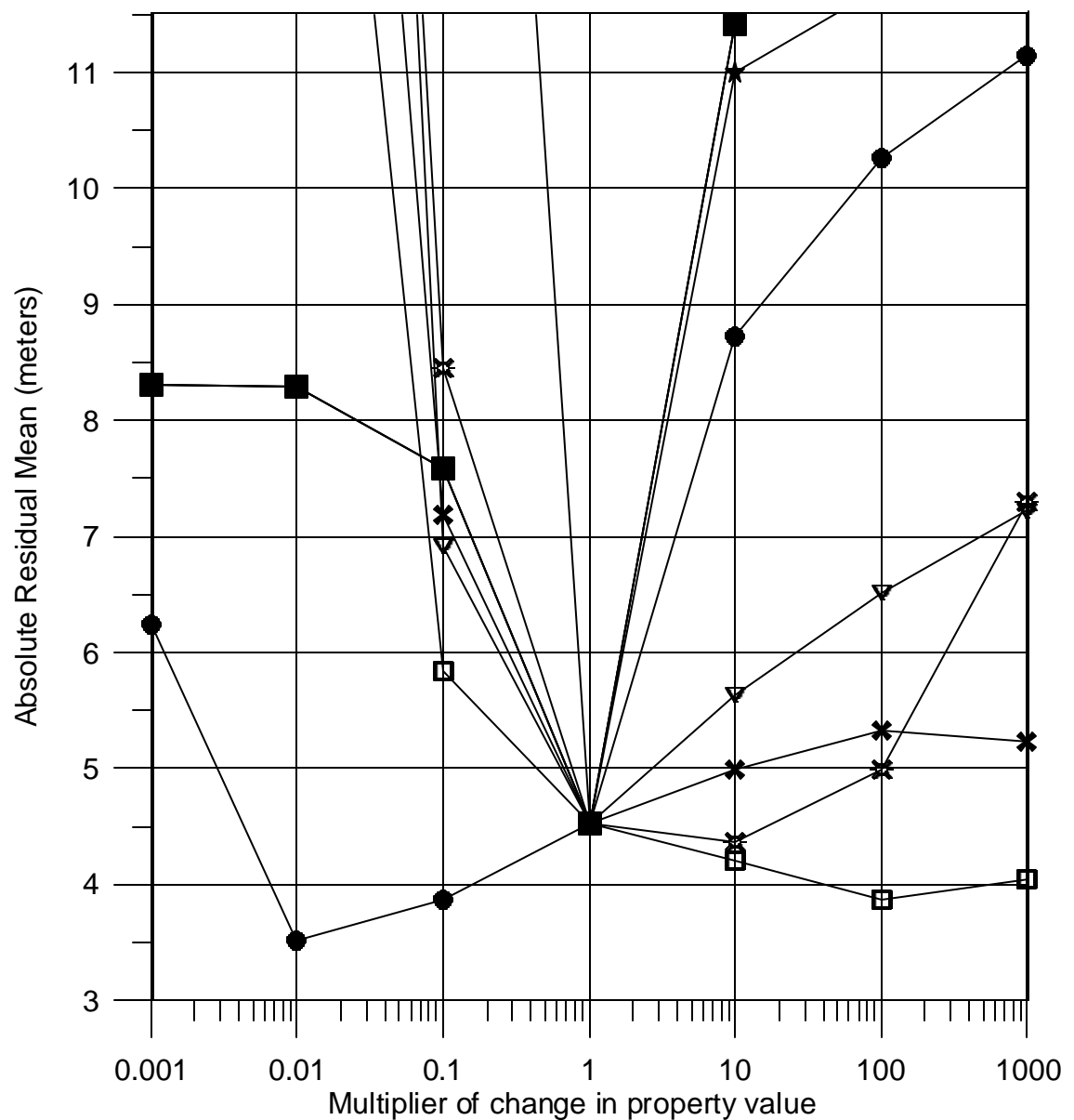Figure 31 - Contoured surface of the calibrated steady-state model.

Figure 32 - Absolute residual mean vs. sensitivity analyses multipliers for horizontal hydraulic conductivity zones.
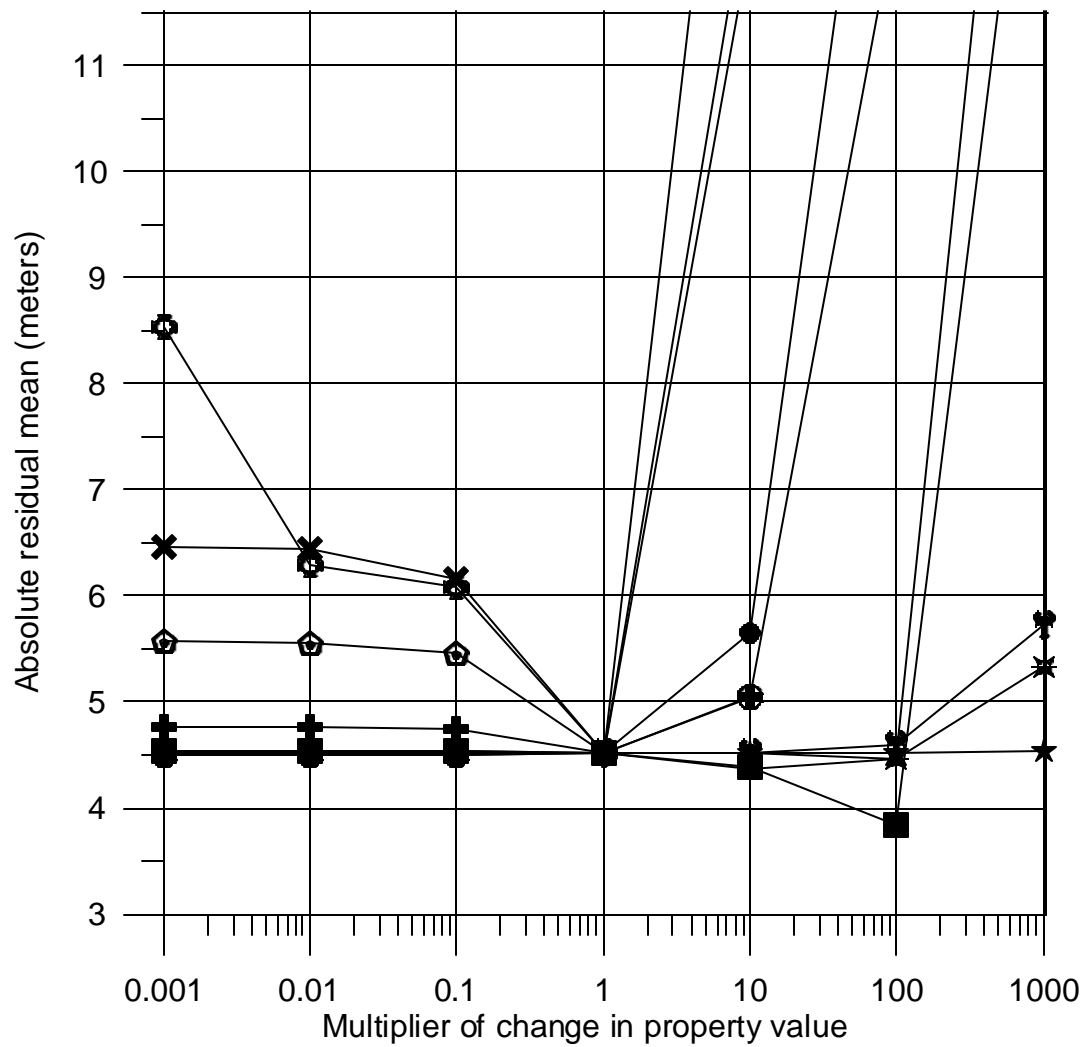
Figure 33 - Absolute residual mean vs. sensitivity analyses multipliers for recharge zones.

Legend
Zone 3
Zone 4
Zone 5
Zone 6
Zone 7
Zone 8
Zone 9
Zone 10
Zone 11
Zone 12
Zone 13

*Predictive Simulation Scenarios*

Safe Yield

Safe yield is a concept used by Arizona Department of Water Resources (ADWR) to manage ground water in the Active Management Areas (AMA) within Arizona. Safe yield is defined as a quantity of water use per year that does not exceed the amount of water that is naturally recharged to the ground-water system. The threshold for safe yield was modeled for this scenario. The total discharge out of the private and irrigation wells was set to equal the amount of recharge that was determined through calibration of the steady-state model. This recharge rate was applied for 10-year long stress periods in the transient, predictive scenario. The length of the stress periods was changed to ten years to examine the long term affects of these water use scenarios. The water budgets calculated by the model simulation for the predictive scenarios are included in Tables 10-13.

The results of the model simulation indicate that drawdowns for the safe yield scenario exceed the sustainable yield criteria (Figure 34, Table 10, Appendix 6). Drawdown at the modeled springs and riparian habitats (areas of interest, AOI) exceeds 0.3 meters (1 foot), and therefore exceeds sustainable yield. Drawdown averages 5.1 meters at the AOIs, which is an order of magnitude greater than the drawdown allowed by the sustainable yield criteria.

Sustainable Yield

The threshold of sustainable yield was modeled to be able to quantify the maximum yield that could still be considered sustainable. This was simulated using a trial and error method varying the pumping values at the wells until a stable hydrograph was produced. This was

determined to be the sustainable yield threshold. All of the other parameters were maintained at their respective calibrated values.

The sustainable-yield threshold was found to be greater than the current water use scenario, but less than the safe yield scenario (Figure 35, Appendix 7). The sustainable yield simulation had a maximum drawdown of 0.3 meters at an AOI, which is near the definition of sustainable yield for this system. The yield for this scenario is 15% greater than the yield used for the calibrated current water use scenario.

## *Calibrated Water Use*

A model scenario was created to examine the long-term impacts to the MWWVS of current amounts of water use. All parameter values derived during the steady-state calibration were used fir this scenario, except longer stress periods were applied. The stress periods were extended to ten years for each stress period. Ten stress periods were modeled to examine the potential effects of water consumption at the current rate over the next one hundred years.

The current water use scenario remained within the sustainable-yield criteria and therefore is considered sustainable (Figure 36, Appendix 5). Drawdown did not exceed 0.30 meters at any of the AOIs at any time throughout the 100 year, current-use scenario.

*American Ranch Build Out*

The American Ranch Build Out scenario was developed using the current-use scenario, with four additional pumping wells to simulate the proposed development at the American Ranch. The pumping values for the wells were established using water demand values that were reported in the ground-water study conducted by Clear Creek Associates (Glotfelty 2001).

The Clear Creek report provided water use values of 149.8 acre-feet / $1.84 \times 10^5$ meters$^3$ for the first year, 126.4 acre-feet / $1.55 \times 10^5$ meters$^3$ for the following nine years, and 109.9 acre-feet / $1.35 \times 10^5$ meters$^3$ for the remaining ninety years of a one hundred year period for the proposed development. This water use was divided between the four wells (Figure 37) added to the model for this scenario. Tables 11 through 14 display the output water budget calculated in the model simulation.

The hydrographs of observation points four and five in the Las Vegas Aquifer indicate that the water demand required for the American Ranch development exceeds the sustainable yield criteria established for the MWWVS (Appendix 8). Drawdown at two of the observation points within the Las Vegas Aquifer exceed 0.30 meters / 1 foot. Drawdown at these observation points exceeds the sustainable yield calibration by tenths of a meter.
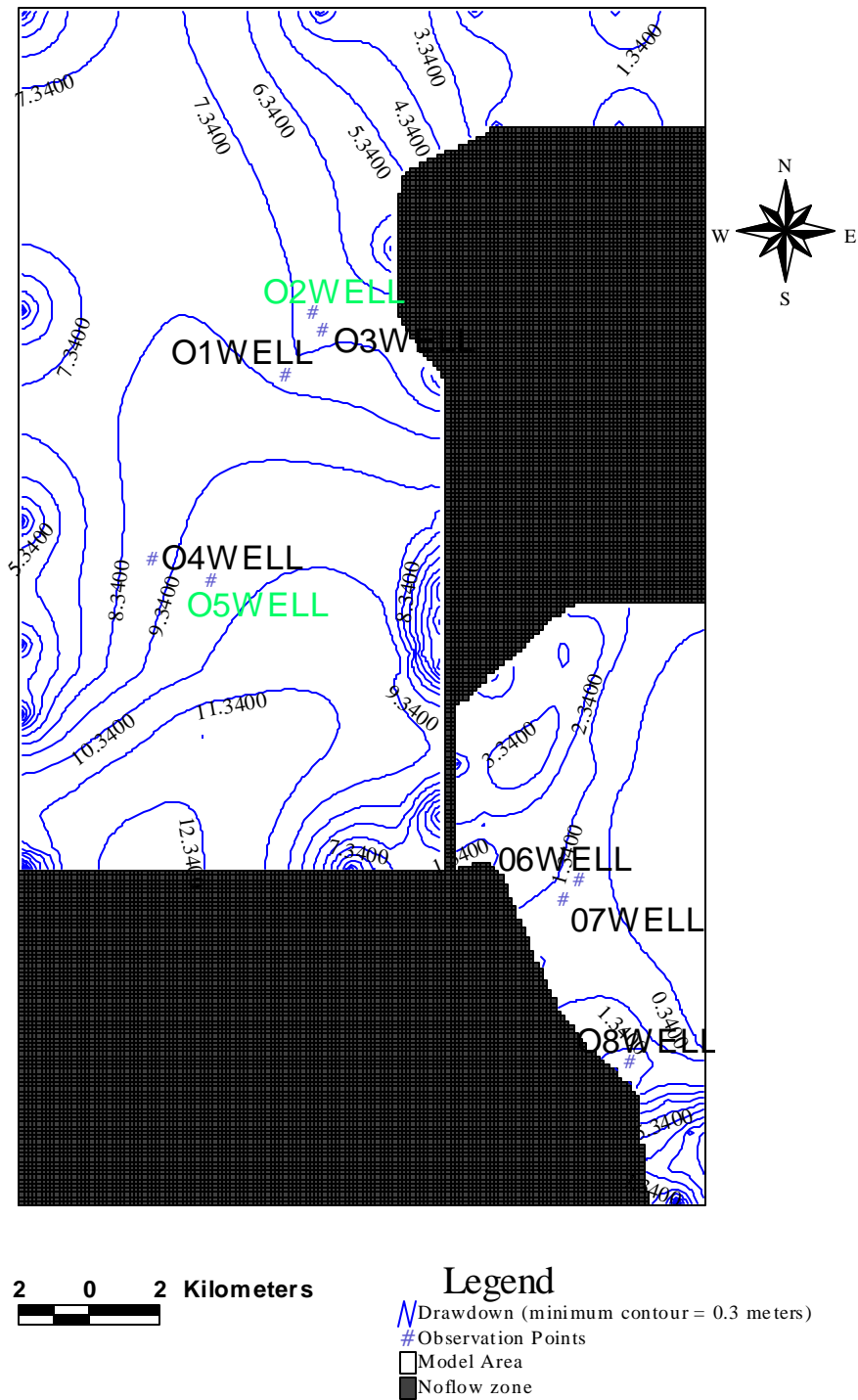
Figure 34 - Contoured model surface displaying drawdown after 100 years in the safe yield condition. Refer to Figure 21 for georeference.
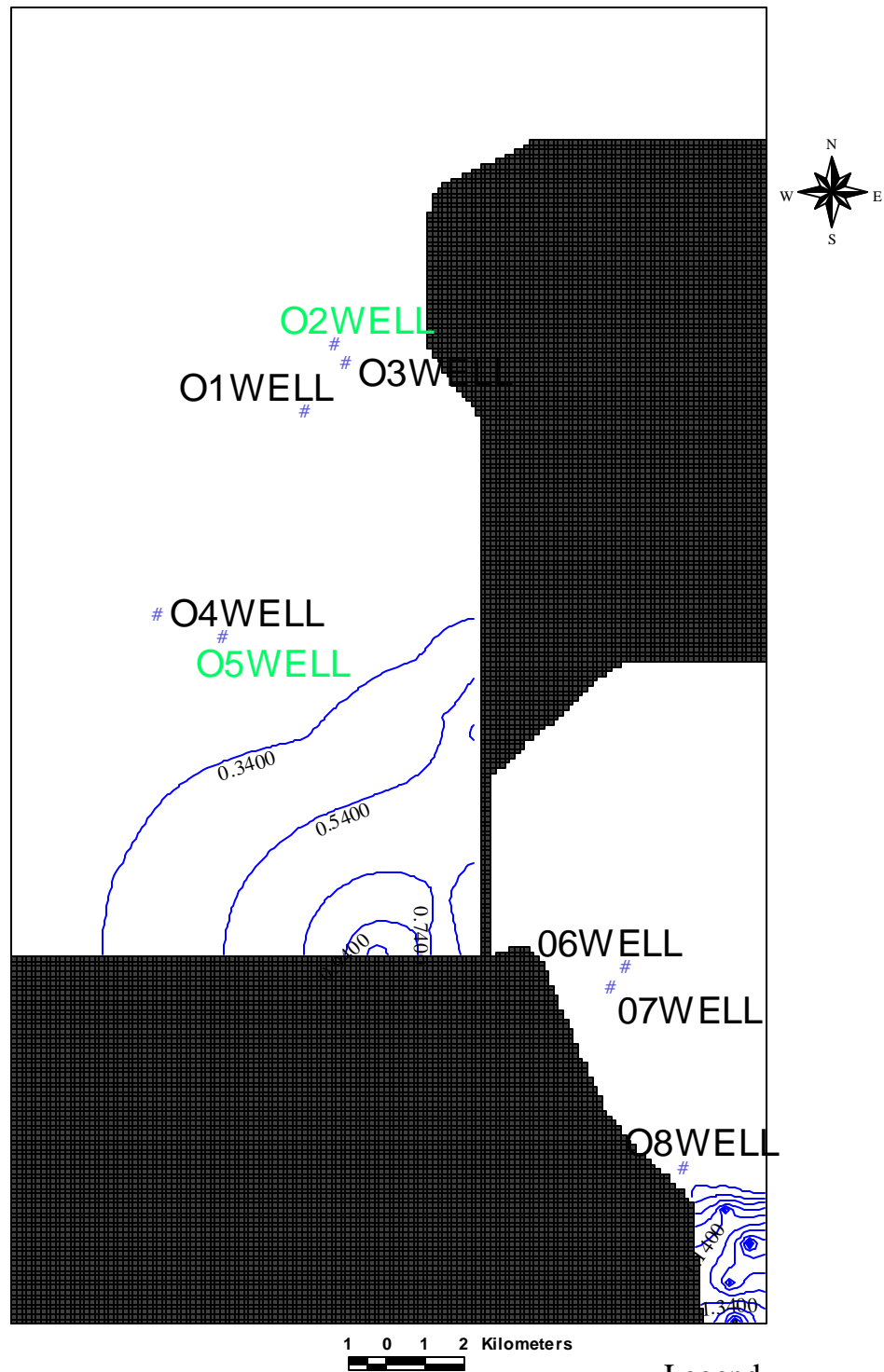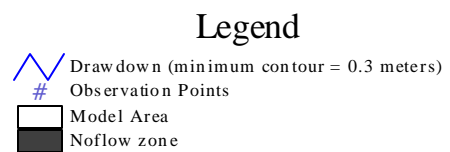
Figure 35 - Contoured model surface of drawdown after 100 years in the sustainable yield condition. Refer to Figure 21 for georeference.
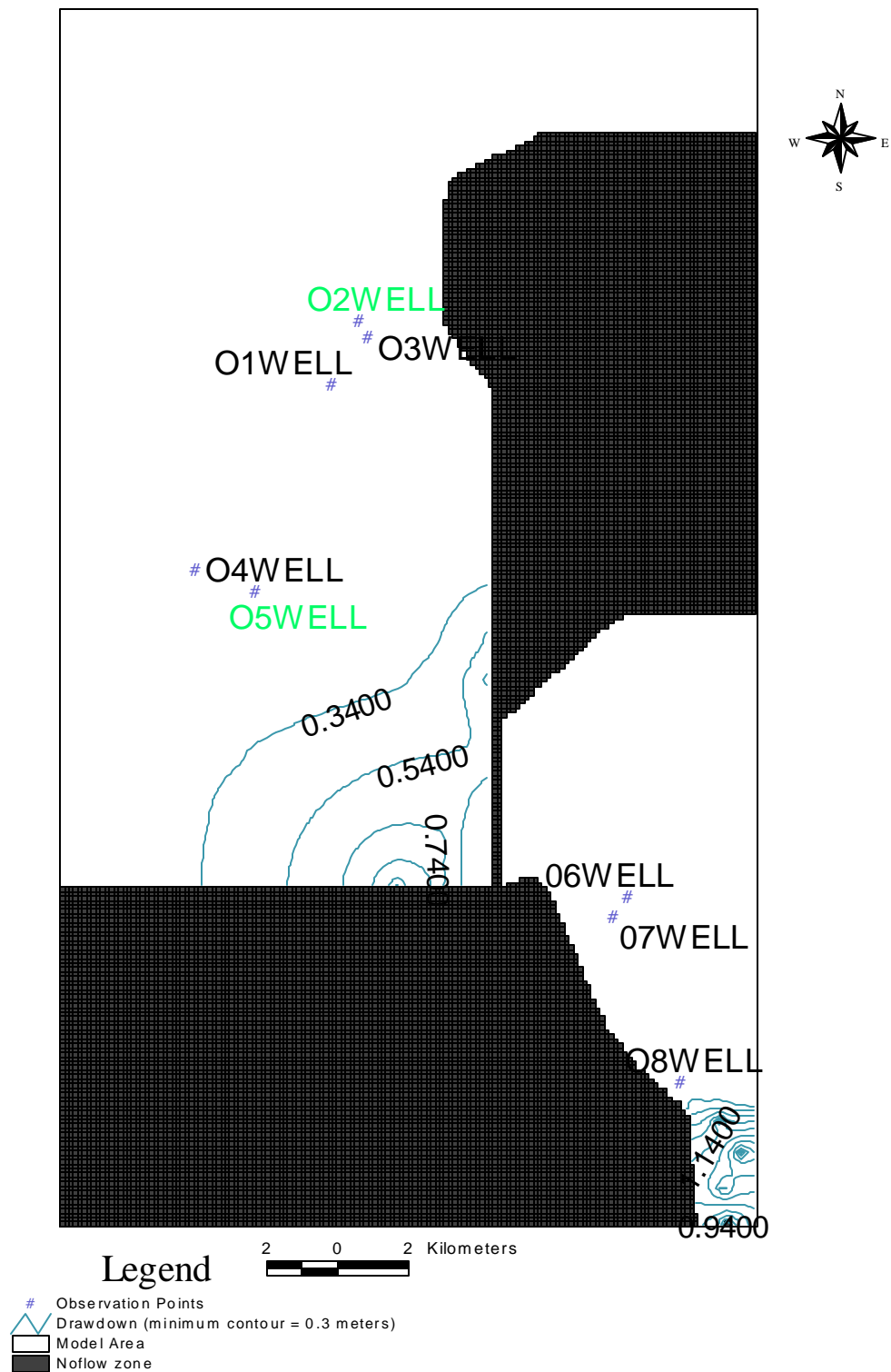
Figure 36 - Contoured model surface of drawdown after 100 years in the Current Water Use condition. Refer to Figure 21 for georeference.
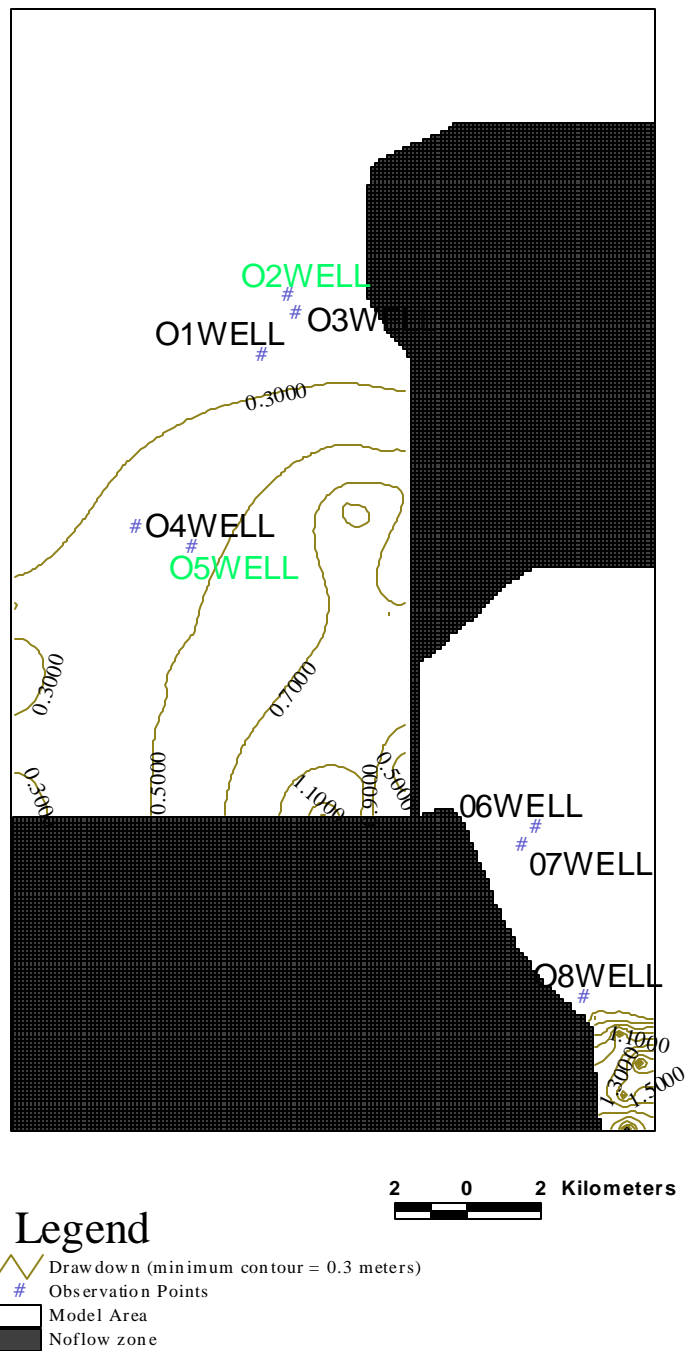
Figure 37 - Contoured model surface of drawdown after 100 years in the American Ranch Build Out condition. Refer to Figure 21 for georeference.

Table 11 - Water budgets of the calibrated current-use condition and three predictive scenarios for the MWWVS model area.

| Water Budgets | Current Water Use ($m^3$/ac-ft) | Safe Yield ($m^3$/ac-ft) | Sustainable Yield ($m^3$/ac-ft) | American Ranch Buildout ($m^3$/ac-ft) |
|---|---|---|---|---|
| **In** | | | | |
| Change in Storage | N/A | N/A | N/A | N/A |
| Flux In - Underflow | $9.1 \times 10^7$ / $7.4 \times 10^4$ | $1.2 \times 10^8$ / $9.8 \times 10^4$ | $7.9 \times 10^7$ / $6.4 \times 10^4$ | $9.2 \times 10^7$ / $7.5 \times 10^4$ |
| Recharge | $9.4 \times 10^7$ / $7.6 \times 10^4$ | $9.4 \times 10^7$ / $7.6 \times 10^4$ | $9.4 \times 10^7$ / $7.6 \times 10^4$ | $9.4 \times 10^7$ / $7.6 \times 10^4$ |
| **Out** | | | | |
| Change in Storage | 980 / 0.80 | 240 / 0.20 | $1.4 \times 10^3$ / 1.1 | 870 / 0.71 |
| Flux Out - Underflow / Drains | $1.3 \times 10^8$ / $1.1 \times 10^5$ | $1.1 \times 10^8$ / $8.9 \times 10^4$ | $1.3 \times 10^8$ / $1.1 \times 10^5$ | $1.3 \times 10^8$ / $1.1 \times 10^5$ |
| Pumping Wells | $4.2 \times 10^6$ / $3.4 \times 10^3$ | $9.8 \times 10^7$ / $8.0 \times 10^4$ | $4.9 \times 10^6$ / $4.0 \times 10^3$ | $5.6 \times 10^6$ / $4.6 \times 10^3$ |
| ET | $5.4 \times 10^7$ / $4.4 \times 10^4$ | $2.4 \times 10^6$ / $2.0 \times 10^3$ | $3.5 \times 10^7$ / $2.8 \times 10^4$ | $5.4 \times 10^7$ / $4.4 \times 10^4$ |
| **Percent Discrepancy** | -0.002% | -0.003% | -0.003% | -0.003% |

Table 12 - Water budgets of the calibrated current-use condition and three predictive scenarios for the Las Vegas Aquifer.

| Water Budgets | Current Water Use (m³/ac-ft) | Safe Yield (m³/ac-ft) | Sustainable Yield (m³/ac-ft) | American Ranch Buildout (m³/ac-ft) |
|---|---|---|---|---|
| **In** | | | | |
| Change in Storage | N/A | N/A | N/A | N/A |
| Flux In - Underflow | $6.4 \times 10^7$ / $5.2 \times 10^4$ | $8.4 \times 10^7$ / $6.8 \times 10^4$ | $5.2 \times 10^7$ / $4.2 \times 10^4$ | $6.5 \times 10^7$ / $5.3 \times 10^4$ |
| Recharge | $2.6 \times 10^7$ / $2.1 \times 10^4$ | $2.6 \times 10^7$ / $2.1 \times 10^4$ | $2.6 \times 10^7$ / $2.1 \times 10^4$ | $2.6 \times 10^7$ / $2.1 \times 10^4$ |
| **Out** | | | | |
| Change in Storage | 450 / 0.37 | 67 / 0.054 | 1000 / 0.81 | 380 |
| Flux Out - Underflow / Drains | $3.3 \times 10^7$ / $2.7 \times 10^4$ | $2.9 \times 10^7$ / $2.4 \times 10^4$ | $4.0 \times 10^7$ / $3.2 \times 10^4$ | $3.3 \times 10^7$ / $2.7 \times 10^4$ |
| Pumping Wells | $2.2 \times 10^6$ / $1.8 \times 10^3$ | $7.8 \times 10^7$ / $6.3 \times 10^4$ | $2.8 \times 10^6$ / $2.3 \times 10^3$ | $3.6 \times 10^6$ / $2.9 \times 10^3$ |
| ET | $5.4 \times 10^7$ / $4.4 \times 10^4$ | $2.4 \times 10^6$ / $2.0 \times 10^3$ | $3.5 \times 10^7$ / $2.8 \times 10^4$ | $5.4 \times 10^7$ / $4.4 \times 10^4$ |
| **Percent Discrepancy** | -0.001% | -0.003% | -0.004% | -0.002% |

Table 13 - Water budgets for the calibrated current-use condition and three predictive scenarios for the Mint Wash Aquifer.

| Water Budgets | Current Water Use (m$^3$/ac-ft) | Safe Yield (m$^3$/ac-ft) | Sustainable Yield (m$^3$/ac-ft) | American Ranch Buildout (m$^3$/ac-ft) |
|---|---|---|---|---|
| **In** | | | | |
| Change in Storage | N/A | N/A | N/A | N/A |
| Flux In - Underflow | 2.8x10$^7$ / 2.3x10$^4$ | 2.6x10$^7$ / 2.1x10$^4$ | 2.8x10$^7$ / 2.3x10$^4$ | 2.8x10$^7$ / 2.3x10$^4$ |
| Recharge | 6.8x10$^7$ / 5.5x10$^4$ | 6.8x10$^7$ / 5.5x10$^4$ | 6.8x10$^7$ / 5.5x10$^4$ | 6.8x10$^7$ / 5.5x10$^4$ |
| **Out** | | | | |
| Change in Storage | 500 / 0.41 | 160 / 0.13 | 460 / 0.37 | 470 / 0.38 |
| Flux Out - Underflow / Drains | 9.4x10$^7$ / 7.6x10$^4$ | 7.7x10$^7$ / 6.3x10$^4$ | 9.4x10$^7$ / 7.6x10$^4$ | 9.4x10$^4$ / 76 |
| Pumping Wells | 1.8x10$^6$ / 1.5x10$^3$ | 1.8x10$^7$ / 1.5x10$^4$ | 1.9x10$^6$ / 1.5x10$^3$ | 1.7x10$^6$ / 1.4x10$^3$ |
| ET | -- | -- | -- | -- |
| **Percent Discrepancy** | -0.003% | -0.002% | -0.002% | 0.0006% |

Table 14 - Water budgets for the calibrated current-use condition and three predictive scenarios for the Granite Basin Aquifer.

| Water Budgets | Current Water Use (m³/ac-ft) | Safe Yield (m³/ac-ft) | Sustainable Yield (m³/ac-ft) | American Ranch Buildout (m³/ac-ft) |
|---|---|---|---|---|
| **In** | | | | |
| Change in Storage | N/A | N/A | 2.8 / 0.0023 | N/A |
| Flux In - Underflow | $1.2 \times 10^5$ / 98 | $1.0 \times 10^6$ / 810 | $6.0 \times 10^5$ / 490 | $6.0 \times 10^5$ / 490 |
| Recharge | $5.3 \times 10^5$ / 430 | $7.7 \times 10^5$ / 630 | $8.2 \times 10^5$ / 670 | $8.2 \times 10^5$ / 670 |
| **Out** | | | | |
| Change in Storage | 14 / 0.012 | 22 / 0.018 | N/A | 16 / 0.013 |
| Flux Out - Underflow / Drains | $4.03 \times 10^5$ / 330 | $7.8 \times 10^5$ / 630 | $1.2 \times 10^6$ / 980 | $1.2 \times 10^6$ / 980 |
| Pumping Wells | $8.30 \times 10^4$ / 67 | $1.0 \times 10^6$ / 810 | $2.6 \times 10^5$ / 210 | $2.5 \times 10^5$ / 200 |
| ET | -- | -- | -- | -- |
| **Percent Discrepancy** | 0.0008% | -0.0007% | -0.003% | 0.0006% |

# CHAPTER FIVE

## SUMMARY AND CONCLUSIONS

**Geological Characterization Summary**

The geology of the MWWVS was characterized through mapping, creation of cross sections, and fracture characterization. The results of this study were combined with results from previous studies to provide a summary of the known geology of the area. Rocks that are exposed in the area range from Proterozoic granite, gneiss and schist; Paleozoic limestone; Tertiary basalt, andesite and conglomerate; and Quaternary alluvium.

Proterozoic granite is exposed in several regions within the study area (Plate 1). Granite Mountain represents a 1.72 Ga granite pluton that was emplaced during the Proterozoic (Dewitt 1999). The location of the apex of the granite pluton is at the crest of Granite Mountain (Figure 10) as indicated by the fracture orientation and the relief of the granite complex (Larsson 1976). The absolute ages provided by the granite pre-date the Yavapai Series metamorphic complex, which has been dated at 1.61 Ga +/- 85 m.y. using Rb-Sr dating (Lanphere 1968).

The Tertiary was also a time of tectonic activity for the Mint Wash and Williamson Valley area. Extensional tectonics occurred throughout the southwestern United States during middle Tertiary time. The Mint Wash and Williamson Valley area is located within the Transition Zone, an area that accomodated the transition from the highly extended Basin and Range physiographic province to the un-extended, Colorado Plateau physiographic province. The extensional tectonics within the area are represented by the inferred normal faults indicated throughout the study area (Plate 1). Most of the contacts at these faults are Tertiary deposits in contact with Proterozoic or Paleozoic rocks.

Depositional environments include a marine depositional environment represented by the Devonian Martin Formation and the Mississippian Redwall Limestone in the northeast portion of the study area (Plate 1). There are no Paleozoic deposits throughout the rest of the study area.

Sedimentary and igneous deposition occurred during the Tertiary within the study area. The Paulden Formation and the Perkinsville unit are Tertiary fluvial conglomerates which cover most of the study area (Plate 1) (Buren 1992). Tertiary igneous rocks include latite and basalt concentrated along the eastern and southern boundaries of the study area (Plate 1).

In summary, the geologic history of the area includes the emplacement of a granite pluton with subsequent metamorphism to the north and west of the granite pluton creating the Yavapai Series metamorphic complex during the Proterozoic Eon. The Paleozoic Era was characterized with a marine environment during the Devonian and Mississippian Periods in the northeast corner of the study area. The Mesozoic Era is not represented in the Mint Wash and

107

Williamson Valley area, and therefore was either a non-depositional environment, the section is

buried under Cenozoic deposits, or subsequent erosion has removed the Mesozoic section.

The Tertiary was a time of deposition and tectonic activity. A fluvial environment was

present throughout most of the field area. Extensional tectonics were responsible for the

creation of normal faults throughout the study area (Plate 1), and is assumed to be the

mechanism responsible for localized volcanic deposits of latite and basalt. The Quaternary

Period has had limited deposition, with deposits along ephemeral and perennial washes, with no

evidence of continued tectonic activity.

## Hydrogeological Characterization Summary

The ground-water system of the Mint Wash and Williamson Valley area was delineated

into three distinct aquifers. The potentiometric surface map (Figure 19) shows radial flow from

Granite Mountain into at least three aquifers.

The aquifer to the southeast of Granite Mountain is the Granite Basin Aquifer (Figure

36), and flows from Granite Mountain towards the southeast where it is assumed to discharge

into the upper Little Chino Sub-basin. The hydrostratigraphy includes the Mint Valley Basalt

overlaying Prescott Granite in the southern part of the aquifer and Paulden Conglomerate in the

northern end of the aquifer. The Mint Valley unit is unconfined. The Prescott Granite and the

Paulden Conglomerate may be confined due to the overlaying basalt, which has a lower

average hydraulic conductivity. The bottom of the granite aquifer is assumed to be 450 feet due

to the overburden weight of the rock sealing the fractures to fluid flow, and 900 feet in the

lower half where Tertiary conglomerate is present (Figure 10). Aquifer properties of the Granite

Basin Aquifer were estimated at a hydraulic conductivity of 88 meters/year and a storage

coefficient of 0.0004 (Table 3) using average specific capacity values of wells drilled into the

aquifer (Wellendorf 2000). The aquifer is assumed to be low yield relative to the other aquifers

in the MWWVS due to the aquifer property values, and the small watershed area represented

by the southeastern slope of Granite Mountain.

The aquifer that is to the east of the granite complex is the Mint Wash Aquifer (Figure

36), in which ground water flows from Granite Mountain toward the east and northeast, where

it is assumed to discharge into the mid Little Chino Sub-basin. The hydrostratigraphy includes

Prescott Granite at the upper end of the aquifer, with Paulden Conglomerate overlaying

Prescott Granite at the lower end. The bottom confining layer is assumed to be 450 feet at the

upper half based on the same assumptions that were established for the Granite Basin Aquifer,

and 900 feet at the lower half where the conglomerate is present (Plate 1). The aquifer

properties were estimated using aquifer tests. Hydraulic conductivity was estimated to be 460

meters/year. There were no valid pumping tests to estimate a value for a storage coefficient.

The aquifer is assumed to produce a higher yield than the Hobbs Aquifer due to the larger

surface area of the aquifer, a larger saturated thickness due to the shallow water table, and the

larger watershed represented by the concave east side of Granite Mountain.

The aquifer that comprises most of the study area is the Las Vegas Aquifer, to the west

and north of Granite Mountain (Figure 36). Ground water in the Las Vegas Aquifer flows from

Granite Mountain and the Santa Maria Mountains towards the north to the confluence of

Williamson Valley with Big Chino Valley. Ground-water flow then proceeds towards the east,

to the downstream end of the Little Chino Sub-basin. The hydrostratigraphy of the Las Vegas

Aquifer includes Paulden Conglomerate overlaying an assumed basement of Prescott Granite.

The Paulden Conglomerate is assumed to be 900 feet thick based on preliminary interpretation

of aero-magnetic data (Woodhouse 2000). The underlying Prescott Granite is assumed to be

the basement due to the weight of the overriding rock sealing any ground-water conduits.

Aquifer parameters were estimated using an aquifer well test within the Las Vegas Aquifer.

Hydraulic conductivity was estimated to be 990 meters/year. There was insufficient data to

estimate a value for the storage coefficient. The Las Vegas aquifer produces the highest yield of

the three aquifers within the MWWVS. The Las Vegas Aquifer is volumetrically the largest

aquifer within the MWWVS. The Las Vegas Aquifer has the largest watershed area of the

MWWVS.

**Ground-Water Flow Modeling Summary**

The ground-water flow modeling study produced some predictive results that provide insight into the transient nature of the MWWVS. The steady-state model was calibrated to less than half ( RMSE compared to head change across model area of 2.3%) of the RMSE required for the "good model" (Anderson and Woessner 1992) criteria (RMSE compared to head change across model area of 5%) with respect to measured versus calculated hydraulic head. The results of the steady-state calibration also produced a mass balance discrepancy that was over an order of magnitude less than the allowable discrepancy under the definition of a "good model". The calibrated steady-state model results showed that recharge appears slightly more sensitive than hydraulic conductivity, and that model sensitivity is more zone-dependent than parameter-dependent. The sensitivity analyses were quantified by setting a limit of change of 5% of the total head change across the model that a parameter value could have on the RMSE of the model.

The steady-state calibration was validated with a transient calibration. The transient calibration simulated a one year period during which field data was collected for the site. Hydrographs were created for wells in each of the major hydrostratigraphic units. The hydrographs were used as a basis for the transient model calibration. Both the steady-state model and the transient model remained within the calibration criteria set forth by Anderson and Woessner (1992) for a "good model".

Safe yield is a concept defined by ADWR (2000) as discharge through pumping not exceeding natural recharge. This was one of the scenarios simulated using the transient model.

The results indicate that safe yield would exceed sustainable yield by lowering the water table below land surface in areas that currently contain perennial or ephemeral springs, or lowering the water table below the root zone at areas that contain riparian vegetation, which is dependent on maintaining roots in the water table.

The transient model was run several times attempting to quantify a sustainable yield threshold. This yield would lower the water table to the limit of the sustainable yield criteria, but would not exceed a specified threshold. The results indicate that the sustainable yield threshold allows for approximately 15% more yield from the ground-water system then the current yield.

The calibrated transient model was extended to simulate the current condition 100 years into the future. The extension of the current condition for 100 years did not exceed the sustainable-yield threshold at any point during the extended simulation. This result implies that the current water use in the MWWVS is hydrologically and ecologically sustainable.

Water demand values for the American Ranch development were estimated in a study conducted by Clear Creek Associates (Glotfelty 2001). The water demand values presented in the Clear Creek study were added to the current water used scenario to simulate conditions including water use through the American Ranch development. Two of the five observation points within the Las Vegas Aquifer exceeded the 0.3 meter drawdown criteria established as an indicator of sustainable yield exceedance. The model indicates that the water use in the American Ranch Build Out scenario exceeds sustainable yield, but not safe yield.

*Model Limitations*

The model is limited by several aspects. The conceptual model was built on several values from literature as well as initial collection and analysis of data first obtained in this study. The calibration of the model to both the steady-state and transient conditions lends some confidence that the parameter values and grid setup for the model are adequate, but the lack of parameter and stress data was a limitation of the model. Data that can improve confidence in the model validation includes more aquifer tests, calculations of septic tank recharge, and a better definition of the bottom confining layer.

The predictive scenarios are limited by the lack of long-term hydrologic monitoring data. There are not enough data available to represent the climatic fluctuations of the area, nor are there exact data on the amount of water use. The predictive scenarios are more properly titled extended interpretive scenarios. Scenarios that simulate potential water use assuming that all of the remaining variables including climate are constant. Additional calibration is necessary to use this model for predictive purposes because of the influence of constant-head and general-head boundaries on the solution.

**Implications**

The predictive simulations imply that the MWWVS is within the sustainable yield criteria at present, and can allow for more water consumption. The scenarios also imply that the ADWR defined "safe yield" does not account for hydrological and ecological sustainability.

The model developed through this study should be used as a framework for future

113

modeling efforts. This model was constructed from scratch, and needs to be revisited and updated in the future. The most powerful step in the use of a model of a natural system is a post-audit to quantify the accuracy of the model, and make improvements as more data becomes available.

**Future Work**

Several boundaries of the MWWVS need to be further developed. The bottom confining surface for all three aquifers needs to be better defined. Final interpretation of the aeromagnetic data should provide insight on the bottom confining surface of the Las Vegas Aquifer. Geophysics can possibly help determine the bottom confining surface for the Mint Wash and Granite Basin Aquifers. The boundary across the Sullivan Buttes needs to be better defined. The deep water table underneath the crest of the Sullivan Buttes has made it difficult to analyze ground-water flow across this boundary.

More aquifer tests would benefit the aquifer parameter estimation. The aquifer tests should be conducted with an observation well allowing for the estimation of storage coefficients. Several aquifer tests within each aquifer will allow for statistical validation of the aquifer parameter values used in the ground-water flow model. Variograms could be created using the results from several aquifer tests to set error limits to parameter values. The error limits would provide insight into the "goodness" of the calibrated parameter values.

Water level data, pumping averages, and precipitation data should be collected continually through several years to develop the predictive capabilities of a ground-water flow

114

model. Data should be collected through at least one El Nino cycle to account for multi-annual climatic fluctuations. The model will need a post-audit of the transient condition to improve predictive modeling.

Individual models for each aquifer identified through this study should be produced. The models will be able to address smaller scale questions regarding ground-water flow and supply. Individual models for each aquifer should provide sensitivity analyses and sustainable yield estimates for each aquifer, which may vary between the aquifers.

REFERENCES

ADWR, 2000 Arizona Department of Water Resources, Well Registry CD, Phoenix Arizona.

ALRIS, 2000. Arizona Land Resource Information System, geographic information system database, Phoenix, Arizona.

Anderson, M.P., and W.W. Woessner, 1992. *Applied groundwater modeling, simulation of flow and advective transport*, Academic Press, San Diego, CA, 381 p.

Arizona Department of Economic Security, 1999. *Yavapai County census data*, internet site, http://www.de.state.az.us/links/economic/webpage/popweb/BETTY70-97.HTML.

Briggs, M.K., 1996. Riparian Ecosystem Recovery in Arid Lands, Univ. Arizona Press, Tucson, AZ, 159 p.

Buren, M.R., 1992. *Definition and paleogeographic significance of Cenozoic stratigraphic units, Chino-Lonesome Valley, Yavapai County, Arizona*, Master's thesis, Northern Arizona University, 153 p.

Castro, Antonio, 1984. Emplacement fractures in granite plutons, *Geologische Rundschau*, 73, 3, pp. 869-880.

Celestian, S.M., 1979. *A faunal analysis of the Devonian Martin Formation in the Verde Valley, Arizona*, Master's thesis, Northern Arizona University, 68 p.

Corkhill, E.F., and D.A. Mason, 1995. *Hydrogeology and simulation of groundwater flow, Prescott Active Management Area*, Arizona Department of Water Resources, 143 p.

Dewitt, E., 1999. *Personal communication regarding absolute dates for the Iron Springs Granite*, U. S. Geological Survey, Denver, Colorado.

Domenico, P.A., and F.W. Schwartz, 1998. *Physical and chemical hydrogeology*, John Wiley and Sons, Inc., New York, NY, 506 p.

Driscoll, F.G., 1986. *Groundwater and wells*, Johnson Filtration Systems Inc., St. Paul, MN, 1089 p.

ESI, 1998. Groundwater Vistas, version 2.x, Ground-water flow modeling software, Herndon, Virginia.

ESRI, Inc., 1999. ArcView, version 3.2, Geographic Information System Software, Redlands, California.

Fetter, C.W., 1994. *Applied Hydrogeology*, 3rd edition. Prentice Hall, Inc., Upper Saddle River, NJ, 691 p.

Freeze, R.A. and J.A. Cherry, 1979. *Groundwater*, Prentice Hall, Inc., Englewood Cliffs, New Jersey, 604 p.

Gee, G.W. and D. Hillel, 1988. Groundwater recharge in arid regions: review and critique of estimation methods. *Hydrological Processes*, v. 2, pp. 255-266.

Gleick, P.H., 1998. The World's Water: The Biennial Report on Freshwater Resources, Island Press, Washington, DC, 307 p.

Glotfelty, M.A., 2001. Hydrologic Analysis of Proposed American Ranch Development, Yavapai County, Arizona, Clear Creek Associates.

Golden Software, 2000. Surfer 7.0 and Grapher 2.0 plotting and graphing software, Golden, Colorado.

Gutschick, R.C., 1943. The Redwall limestone (Mississippian) of Yavapai County, Arizona, *Plateau*, vol. 16, no. 1, pp. 1-11.

Kent, W.N., 1975. *Facies analysis of the Mississippian Redwall Limestone in the Black Mesa region*, Master's thesis, Northern Arizona University, 186 p.

Krieger, M.H. 1967a. *Reconnaissance geologic map of the Simmons quadrangle Yavapai County, Arizona*, U.S. Geological Survey miscellaneous geologic investigations, map I-503.

Krieger, M.H., 1967b. *Reconnaissance geologic map of the Iron Springs quadrangle Yavapai County, Arizona*, U.S. Geological Survey miscellaneous geologic investigations, map I-504.

Krieger, M.H., S.C. Creasey, and R.F. Marvin, 1971. *Ages of some Tertiary andesitic and latitic volcanic rocks in the Prescott-Jerome area, North -Central Arizona*, U.S. Geological Survey miscellaneous paper, v. 750-B, p. B157-160.

Lanphere, M.A., 1968. Geochronology of the Yavapai Series of central Arizona, *Geochronology of Precambrian stratified rocks*, Canadian Journal of Earth Sciences, Ottawa, Canada, p. 757-762.

Larsson, I., 1972. Ground water in granite rocks and tectonic models, *Nordic Hydrology*, 3, 3, pp. 111-129.

Maslansky, Steven P., 2000. Personal communication from a resident and registered geologist / hydrogeologist, Prescott, Arizona, USA.

Matlock, W.G., and P.R. Davis, 1972. *The groundwater supply of Little Chino Valley*, Hydrogeology and water resources in Arizona and the southwest, proceedings of the 1972 meetings of the Arizona section, A.W.R.A. and the hydrology section, Arizona Academy of Science, p.67-86.

McDonald, M.G., and A.W. Harbaugh, 1988. *A modular three-dimensional finite-difference ground-water flow model*, Techniques of Water-Resources Investigations of the United States Geological Survey, 498 p.

Meader, N.M., 1977. *Paleoecology and paleoenvironments of the Upper Devonian Martin Formation in the Roosevelt Dam-Globe area, Gila County, Arizona*, Master's Thesis, University of Arizona, 124 p.

Meinzer, O.E., 1923. *The occurrence of ground water in the United States*, U S. Geological Survey, Water Supply Paper 489. 321 p.

Microsoft, 2000. Microsoft Windows 2000, computer platform, Redmond, Washington.

Neuman, S.P., 1975. Analysis of pumping test data from anisotropic unconfined aquifers considering delayed gravity response. *Water Resources Research*, v. 11, pp. 329-342.

NFS, 2000. National Foerst Service, Personal communication regarding land access and GIS support.

Rabinowitz, D.D., G.W. Gross and C.R. Holmes, 1977. Environmental tritium as a hydrometeorologic tool in the Roswell basin, New Mexico, I. Tritium input function and precipitation-recharge relation. *Journal of Hydrology*, v. 32, pp. 3-17.

Sanders, L.L., 1998. *A Manual of Field Hydrogeology*, Prentice Hall, Inc, Upper Saddle River, New Jersey, 381 p.

Schwalen, H.C., 1967. *Little Chino Valley Artesian Area and Groundwater Basin*, Agricultural Experiment Station, The University of Arizona, Technical Bulletin 178, 63 p.

Semmens, B.A., 1999. *Hydrogeologic characterization and numerical transport simulations of a reattachment-bar aquifer in the Colorado River*, Master's thesis, Northern Arizona University, 189 p.

Simmers, I., 1997. *Recharge of phreatic aquifers in (semi-) arid areas*, A.A. Balkema, Rotterdam, Netherlands, 277 p.

Smith, J.W., 1974. *The petrology of the Mississippian Redwall Limestone in northern Yavapai County, Arizona*, Master's thesis, Northern Arizona University, 88 pages.

Soilmoisture Equipment Corp., 1986, 2800KI Operating Instructions, Guelph Permeameter, Santa Barbara, California.

Solinst, 2000. Solinst model 101 Water Level Meter, Georgetown, Ontario, Canada.

Springer, A.E., 1998. *Geology 451: Hydrogeology - class lecture*, Northern Arizona University.

Theis, C.V., 1935. The relation between the lowering of the piezometric surface and the rate and duration of discharge of a well using ground water storage, *American Geophysical Union*, Washington D.C., pp. 518-524.

Wallace, B.L., and R.L. Laney, 1976. *Maps showing ground-water conditions in the Lower Big Chino Valley and Williamson Valley areas Yavapai and Coconino counties, Arizona*. Water-Resources Investigations number 76-0078, United States Geological Survey.

Watson, P., P.Sinclair and R.Waggoner, 1976. Quantitative evaluation of a method for estimating recharge to the desert basins of Nevada. *Journal of Hydrology*, vol. 31, pp. 335-357.

Wellendorf, W.G., 1999. *Personal communication regarding the MWWVS and Little Chino Valley areas*: Southwestern Ground-water Consultants, Inc.

Wendt, G.E., P. Winkelaar, C.W. Wiesner, R.A. Bither, B.A. Whitney, and K.N. Larson, 1976. *Soil survey of Yavapai County, Arizona, western part*, United States Department of Agriculture Soil Conservation Service and Forest Service, 121 p.

Woessner, W.W., 1998. *Evaluation of two groundwater models of the Prescott Active Management Area*, report prepared for Arizona Department of Water Resources. internet site, http://www.adwr.state.az.us/annc/press005.html.

Woodhouse, B., 2000. *Personal communication regarding analysis of aeromagnetic data available for the MWWVS*: USGS.

Wright, J. M., 1997. *Coupling ground-water and riparian vegetation models to simulate impacts of a reservoir release,* Master's thesis, Northern Arizona University, 111 p.

Appendix 1:

Location and elevation of the monitoring and synoptic wells, and the 95% confidence interval

for the horizontal and vertical precision

Table 15 - Location and elevation of the monitor and synoptic wells in the MWWVS.

| well ID | UTM (Easting zone12) | UTM (Northing) | Elevation (meters) | horizontal 95% confidence (meters) | vertical 95% confidence (meters) |
|---|---|---|---|---|---|
| 1 | 361092.442 | 3834311.145 | 1608.110 | 1.470 | 3.024 |
| 2 | 358952.667 | 3836680.034 | 1554.853 | 1.404 | 1.660 |
| 3 | 359249.728 | 3838115.416 | 1547.315 | 1.563 | 1.821 |
| 4 | 358963.285 | 3839114.035 | 1538.466 | 1.585 | 1.803 |
| 5 | 358061.043 | 3839949.101 | 1520.602 | 2.267 | 2.523 |
| 6 | 352691.153 | 3851845.254 | 1422.965 | 1.280 | 2.411 |
| 7 | 352549.263 | 3854547.457 | 1427.348 | 1.174 | 2.072 |
| 8 | 352800.094 | 3848649.489 | 1413.076 | 1.657 | 2.672 |
| 9 | 352814.555 | 3847666.947 | 1417.578 | 0.887 | 1.602 |
| 10 | 351992.850 | 3847014.430 | 1444.887 | 1.449 | 3.726 |
| 11 | 351262.255 | 3847892.171 | 1423.408 | 1.337 | 2.478 |
| 12 | 348400.332 | 3847375.046 | 1406.467 | 1.323 | 2.484 |
| 13 | 348205.199 | 3847654.541 | 1406.362 | 1.304 | 2.384 |
| 14 | 351413.521 | 3851964.512 | 1402.598 | 1.218 | 2.080 |
| 15 | 351069.094 | 3854036.361 | 1386.556 | 1.138 | 2.062 |
| 16 | 352179.071 | 3856519.615 | 1381.938 | 0.982 | 1.665 |
| 17 | 351101.872 | 3855981.749 | 1391.781 | 1.366 | 2.078 |
| 18 | 357958.298 | 3842735.108 | 1575.992 | 1.042 | 1.742 |
| 19 | 360688.846 | 3838865.963 | 1555.882 | 1.136 | 2.202 |
| 20 | 360831.050 | 3838340.175 | 1556.356 | 1.010 | 1.609 |
| 21 | 360314.419 | 3838335.154 | 1556.154 | 1.212 | 1.875 |
| 22 | 362087.691 | 3834419.732 | 1592.166 | 1.501 | 1.942 |

| well ID | UTM (Easting zone12) | UTM (Northing) | Elevation (meter) | horizontal 95% confidence (meters) | vertical 95% confidence (meters) |
|---|---|---|---|---|---|
| 23 | 362045.835 | 3833562.247 | 1605.259 | 1.248 | 1.8047 |
| 24 | 361407.005 | 3835896.812 | 1582.496 | 80.79 | 127.3 |
| 25 | 362219.334 | 3832976.161 | 1627.497 | 80.94 | 127.5 |
| 26 | 352920.582 | 3848320.650 | 1415.768 | 0.958 | 1.796 |
| 27 | 354121.263 | 3852487.395 | 1475.920 | 0.986 | 1.428 |
| 28 | 352381.648 | 3854469.583 | 1420.240 | 1.237 | 2.156 |
| 29 | 358267.549 | 3852887.199 | 1533.965 | 1.067 | 1.788 |
| 30 | 358218.998 | 3852860.300 | 1532.024 | 0.980 | 1.721 |
| 31 | 358724.926 | 3852793.250 | 1526.168 | 0.912 | 1.666 |
| 32 | 357996.205 | 3852474.756 | 1518.536 | 0.881 | 1.606 |
| 33 | 357862.607 | 3842807.415 | 1576.549 | 1.076 | 2.041 |
| 34 | 357703.241 | 3842553.281 | 1574.093 | 0.975 | 1.599 |
| 35 | 360163.447 | 3845813.776 | 1516.989 | 0.868 | 1.255 |
| 36 | 359012.358 | 3836880.485 | 1539.662 | 1.241 | 2.257 |
| 37 | 353821.874 | 3860651.968 | 1355.761 | 1.043 | 1.312 |
| 38 | 358976.372 | 3836611.965 | 1552.715 | 1.111 | 1.953 |

Appendix 2:

Water level data for monitoring wells

Table 16 - Ground water elevation data (meters above sea-level) collected at the monitor wells from Aug'99 to Sep'00.

| Well ID | Aug-99 | Sep-99 | Oct-99 | Nov-99 | Dec-99 | Jan-00 | Feb-00 |
|---------|--------|--------|--------|--------|--------|--------|--------|
| 1 | 1554.12 | 1553.91 | 1553.88 | 1553.74 | 1553.59 | 1553.46 | 1553.34 |
| 2 | 1535.64 | 1535.98 | 1536.36 | 1536.51 | 1536.46 | 1536.30 | 1536.11 |
| 3 | 1532.75 | 1531.16 | 1531.44 | 1531.59 | 1531.79 | 1531.74 | 1531.88 |
| 4 | 1524.20 | 1523.78 | 1523.71 | 1523.68 | 1523.59 | 1523.52 | 1523.45 |
| 5 | 1519.12 | 1519.45 | 1519.22 | 1519.70 | 1519.65 | 1519.64 | 1519.58 |
| 6 | 1392.09 | 1392.02 | 1392.05 | 1392.02 | 1391.94 | 1391.89 | 1391.81 |
| 7 | 1379.87 | 1379.72 | 1379.92 | 1379.99 | 1379.95 | 1379.95 | 1379.94 |
| 8 | 1407.46 | 1407.38 | 1407.39 | 1407.29 | 1407.22 | 1407.14 | 1407.09 |
| 9 | -------- | -------- | -------- | 1384.64 | 1384.27 | 1384.06 | 1384.9 |
| 10 | 1411.27 | -------- | 1411.28 | 1411.27 | 1411.19 | 1411.21 | 1411.22 |
| 11 | -------- | 1408.23 | 1408.28 | 1408.27 | 1408.24 | 1408.26 | 1408.26 |
| 12 | 1406.26 | 1406.47 | 1406.32 | 1406.18 | 1406.44 | 1406.40 | 1406.39 |
| 13 | -------- | 1406.01 | 1406.28 | 1406.35 | 1406.66 | 1406.36 | 1406.35 |
| 14 | 1390.07 | 1389.98 | 1390.01 | 1388.93 | 1389.85 | 1389.79 | 1389.72 |
| 15 | 1382.14 | 1382.21 | 1382.24 | 1382.23 | 1382.22 | 1382.23 | 1382.22 |
| 16 | -------- | 1374.50 | 1374.52 | 1374.50 | 1374.50 | 1374.50 | 1374.50 |
| 17 | 1374.26 | 1374.33 | 1374.36 | 1374.05 | 1374.34 | 1374.37 | 1374.4 |
| 18 | -------- | -------- | -------- | 1517.68 | 1517.55 | 1517.19 | 1516.56 |

| Well ID | Mar-00 | Apr-00 | May-00 | Jun-00 | Jul-00 | Aug-00 | Sep-00 |
|---------|--------|--------|--------|--------|--------|--------|--------|
| 1 | 1553.32 | 1553.12 | 1552.94 | 1552.75 | 1552.52 | 1552.43 | 1552.27 |
| 2 | 1536.02 | 1536.04 | 1535.95 | 1535.67 | 1535.42 | 1535.27 | 1535.19 |
| 3 | 1531.91 | 1531.97 | 1532.00 | 1531.89 | 1531.79 | 1535.73 | 1531.76 |
| 4 | 1523.40 | 1523.29 | 1523.22 | 1523.12 | 1522.97 | 1522.87 | 1522.78 |
| 5 | 1519.84 | 1519.56 | 1519.40 | 1519.02 | 1518.82 | 1518.72 | 1518.79 |
| 6 | 1391.77 | 1391.68 | 1391.61 | 1391.54 | 1391.45 | --------- | 1391.30 |
| 7 | 1379.96 | 1379.93 | 1379.92 | 1379.90 | 1379.86 | --------- | 1379.79 |
| 8 | 1407.05 | 1406.97 | 1406.90 | 1406.84 | 1406.78 | 1406.76 | 1406.70 |
| 9 | 1383.81 | 1383.70 | 1383.62 | 1383.51 | 1383.42 | 1383.33 | 1383.24 |
| 10 | 1411.27 | 1411.22 | 1411.18 | 1411.18 | 1411.04 | 1411.00 | 1410.91 |
| 11 | 1408.30 | 1408.26 | 1408.21 | 1408.15 | 1408.06 | 1408.02 | 1407.97 |
| 12 | 1406.40 | 1406.39 | 1406.25 | --------- | -------- | -------- | -------- |
| 13 | 1406.35 | 1406.36 | -------- | -------- | -------- | 1405.60 | -------- |
| 14 | 1389.68 | 1389.60 | 1389.52 | 1389.39 | 1389.27 | 1389.19 | 1389.07 |
| 15 | 1382.26 | 1382.18 | 1382.12 | 1382.05 | 1381.99 | --------- | 1381.86 |
| 16 | 1374.52 | 1374.50 | 1374.47 | 1374.46 | 1374.42 | 1374.40 | --------- |
| 17 | 1374.45 | 1374.32 | 1374.37 | -------- | 1373.81 | -------- | --------- |
| 18 | 1516.61 | 1516.52 | 1517.02 | 1516.74 | 1515.63 | 1514.49 | 1513.92 |

Appendix 3:

Precipitation data used for the MWWVS

Table 17 - Precipitation data collected at the rain gauge stations in the MWWVS.

| Date[1] | Rain Station 1 (inches) | Rain Station 2 (inches) | Rain Station 3 (inches) | Soil Survey Averages[2] (inches) |
|---|---|---|---|---|
| Sep. 15, 1999 | 1.76 | 3.78 | 3.16 | 1.61 |
| Oct. 15, 1999 | 3.98 | 2.9 | 5.44 | 1.08 |
| Nov. 15, 1999 | 0.00 | 0.00 | 0.00 | 0.95 |
| Dec. 15, 1999 | 0.00 | 0.00 | 0.00 | 1.93 |
| Jan. 15, 2000 | 0.08 | 0.15 | 0.15 | 1.71 |
| Feb. 15. 2000 | 0.20 | 0.05 | 2.69 | 1.67 |
| Mar. 15, 2000 | 2.46 | 3.23 | 0.30 | 1.48 |
| Apr. 15, 2000 | 0.46 | 0.29 | 0.07 | 0.92 |
| May 15, 2000 | 0.12 | 0.25 | 0.00 | 0.35 |
| Jun. 15, 2000 | 0.00 | 0.00 | 0.00 | 0.46 |
| Jul. 15, 2000 | 1.66 | 0.57 | 1.04 | 2.72 |
| Aug. 15, 2000 | 2.8 | 4.47 | 0.99 | 3.36 |
| **Total** | **13.52** | **15.69** | **13.84** | **18.24** |

Notes:

[1] Precipitation includes total precipitation measured during the preceding month.

[2] Soil survey averages are for a rain gauge in Prescott, AZ from 1936-1965.

Appendix 4:

Hydrographs for the transient targets

# Observed vs. Simulated heads for Well 1
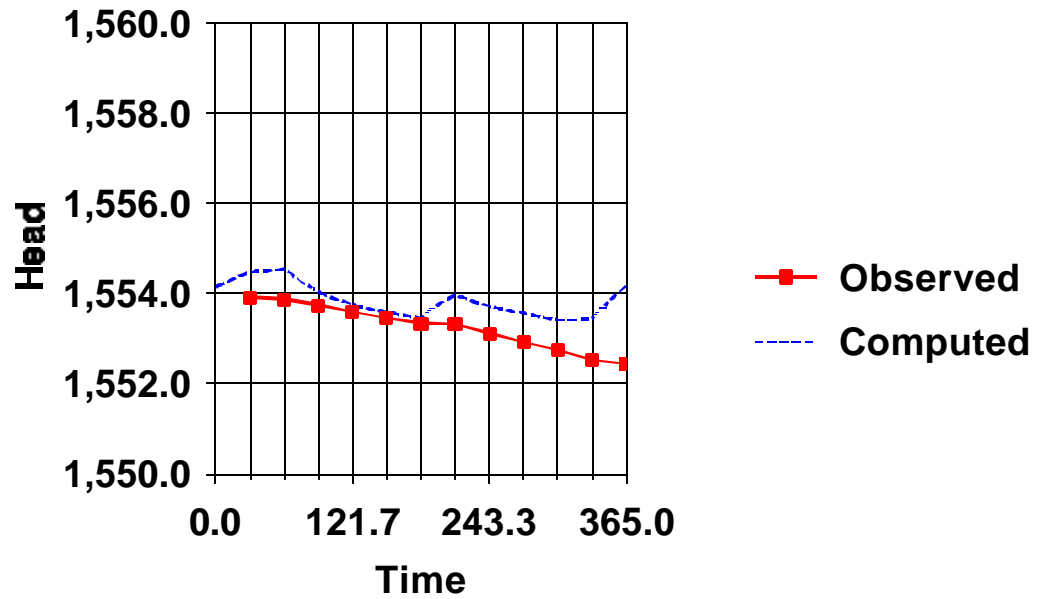


# Observed vs. Simulated heads for Well 3
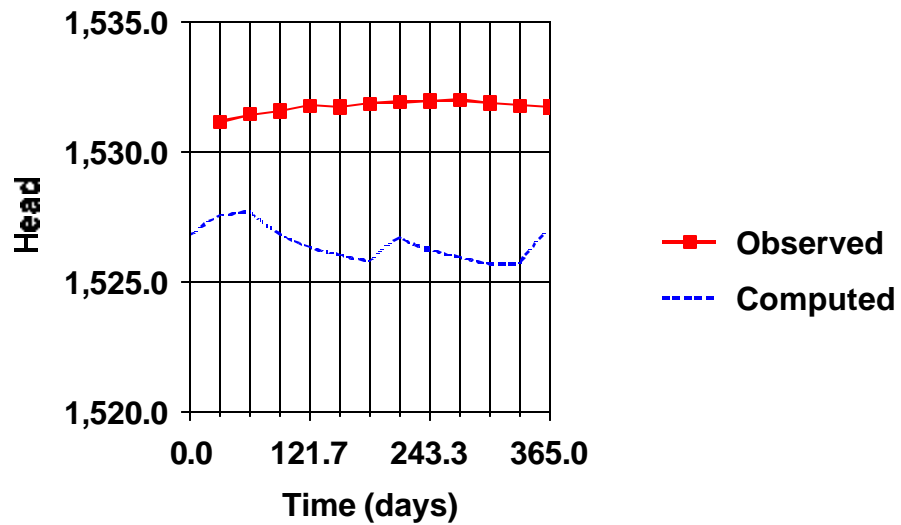
# Observed vs. Simulated heads for Well 4
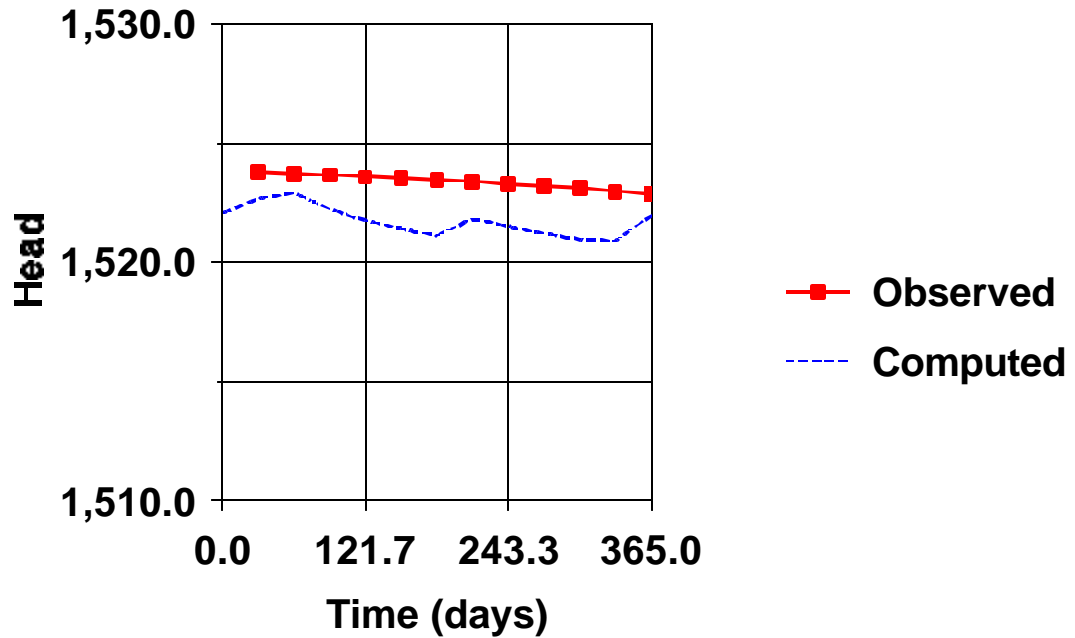


# Observed vs. Simulated heads for Well 5
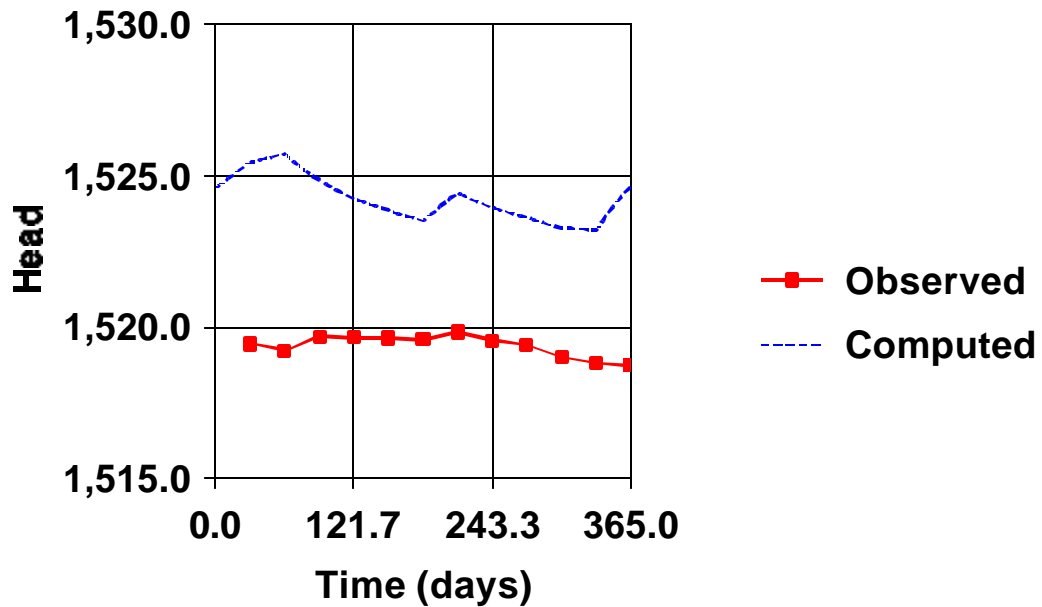
## Observed vs. Simulated heads for Well 6
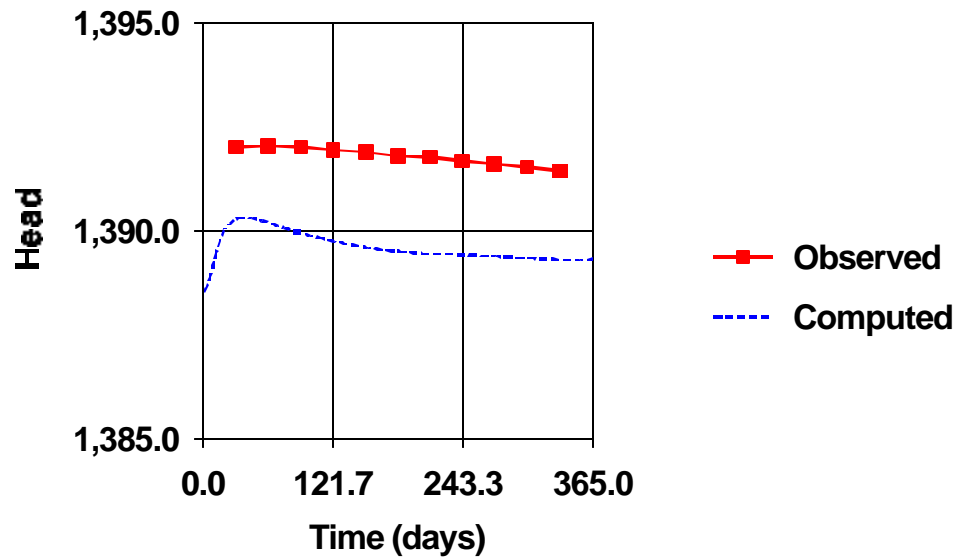


## Observed vs. Simulated heads for Well 7
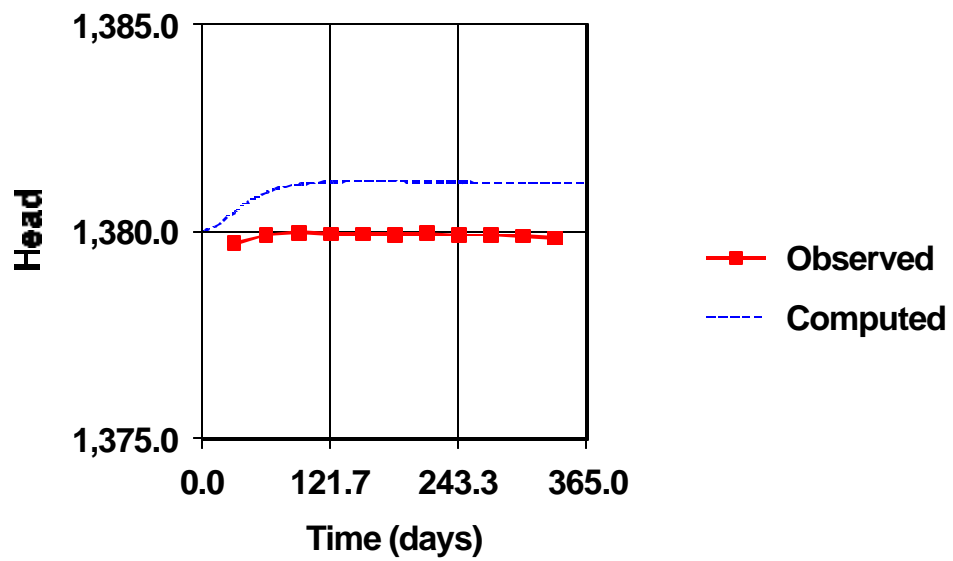
# Observed vs. Simulated heads for Well 8
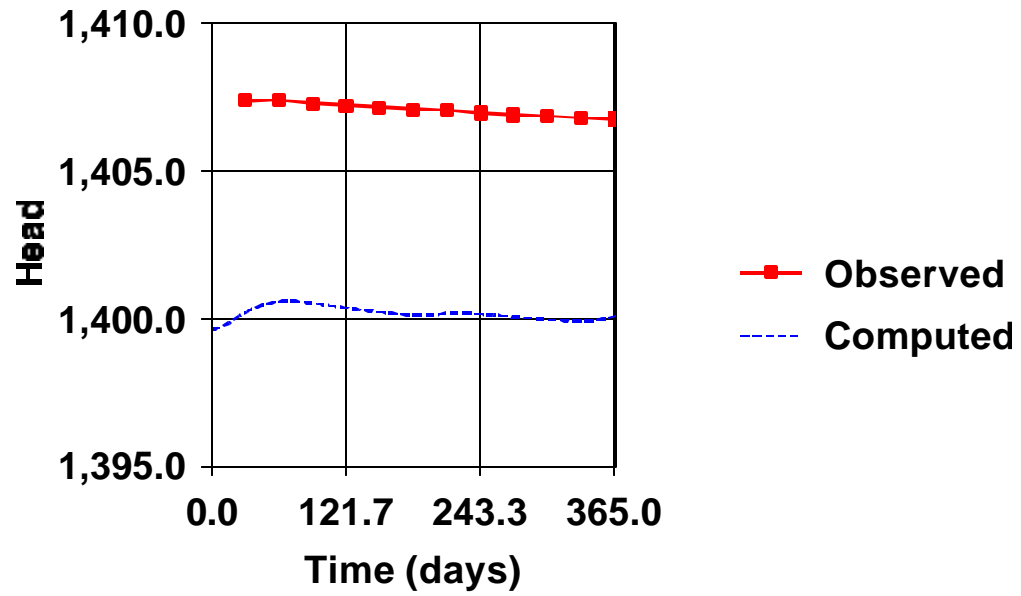


# Observed vs. Simulated heads for Well 9
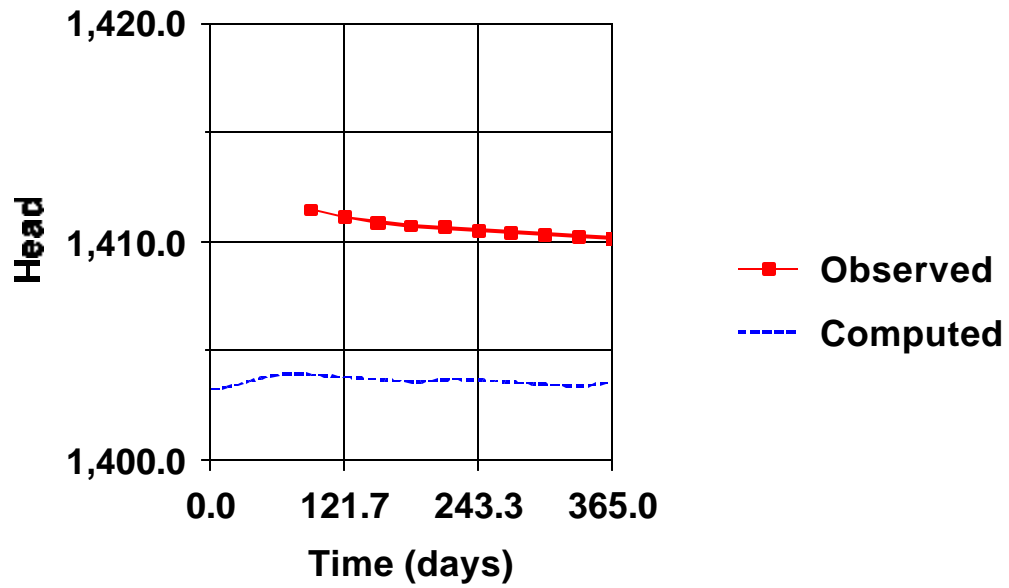
# Observed vs. Simulated heads for Well 10
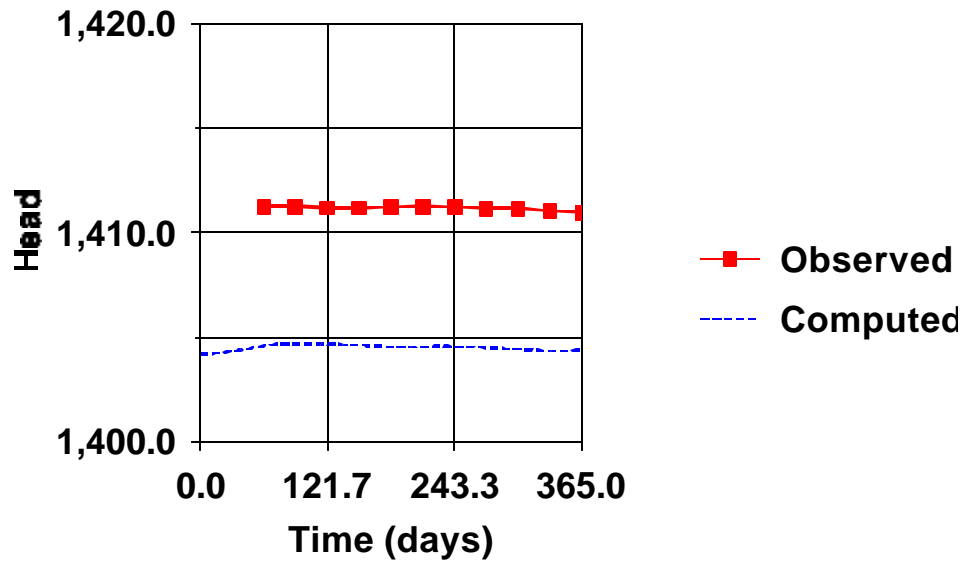


# Observed vs. Simulated heads for Well 11



134
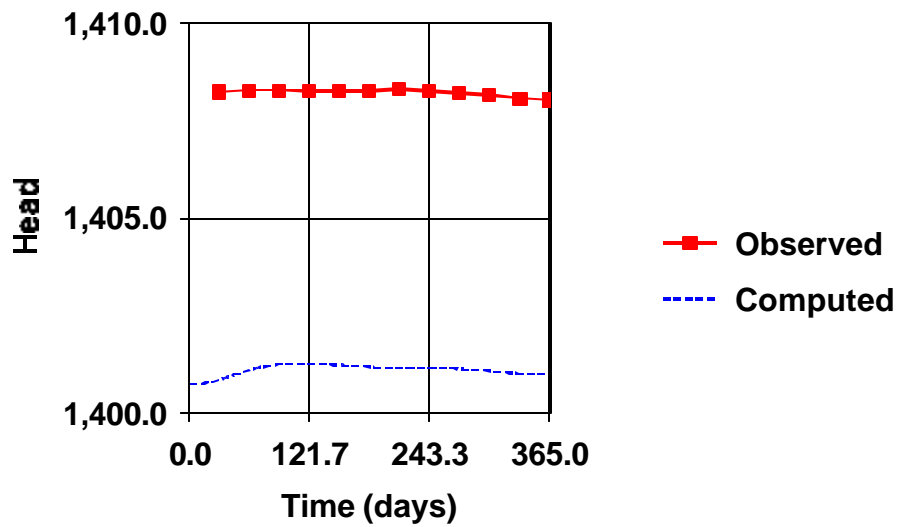
# Observed vs. Simulated heads for well 12
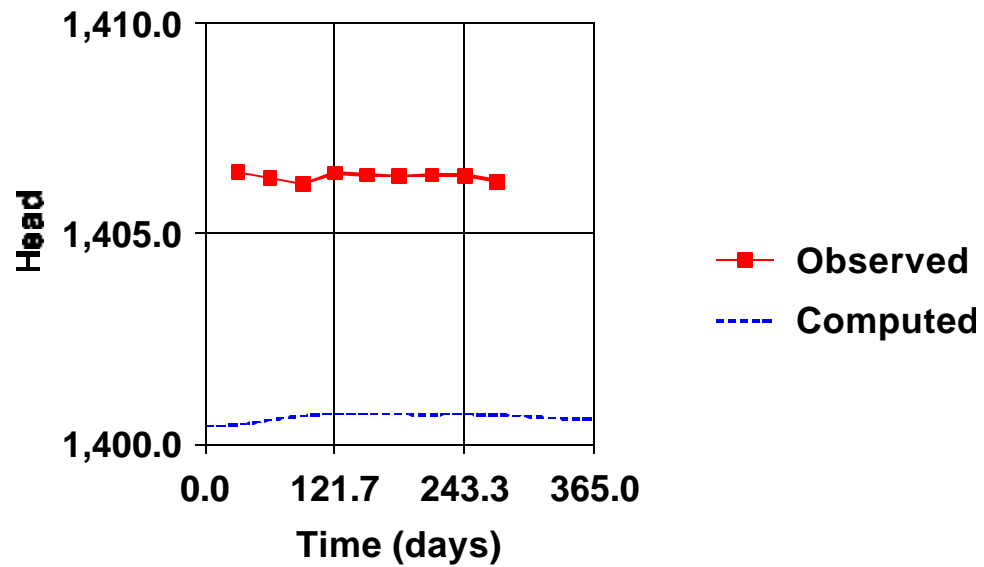


# Observed vs. Simulated heads for Well 13
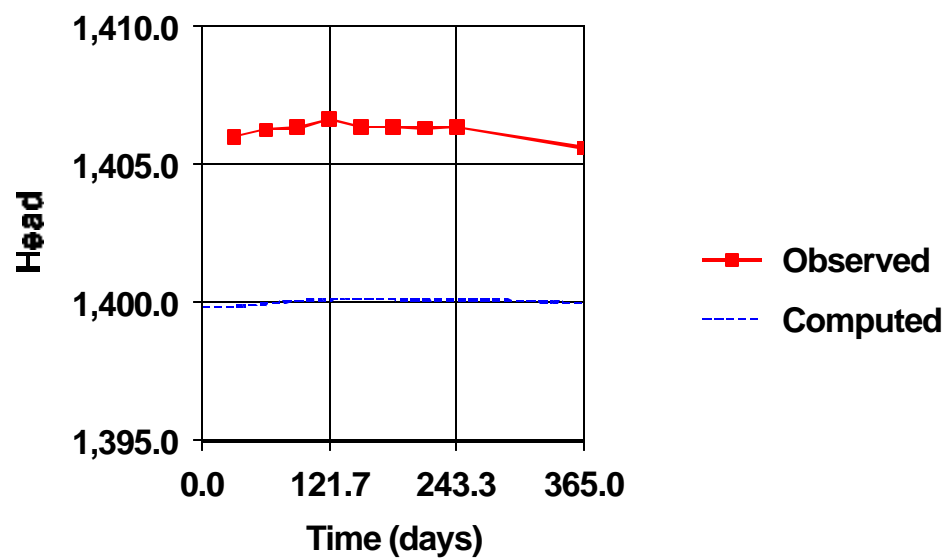
# Observed vs. Simulated heads for Well 14
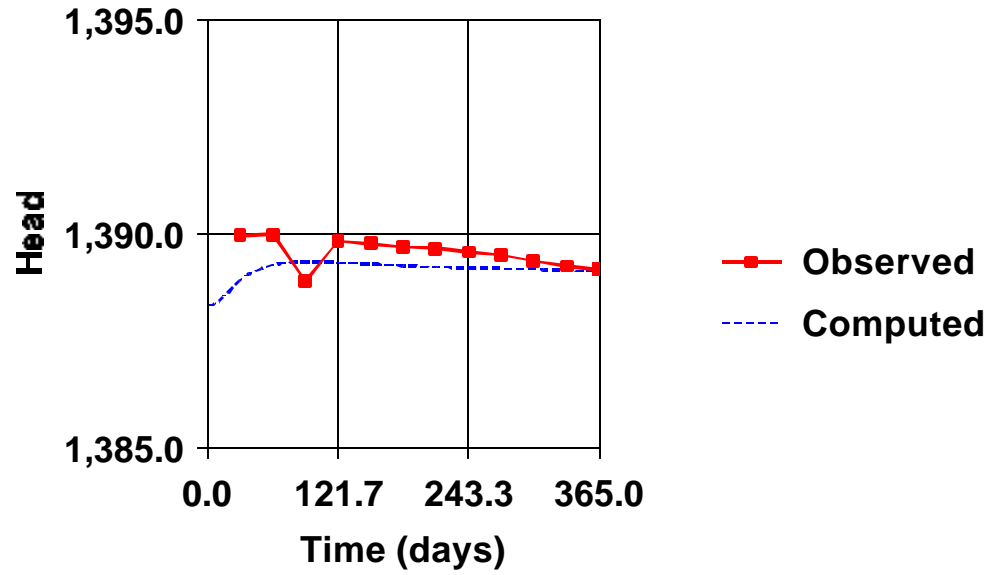
## Observed vs. Simulated heads for Well 16





137
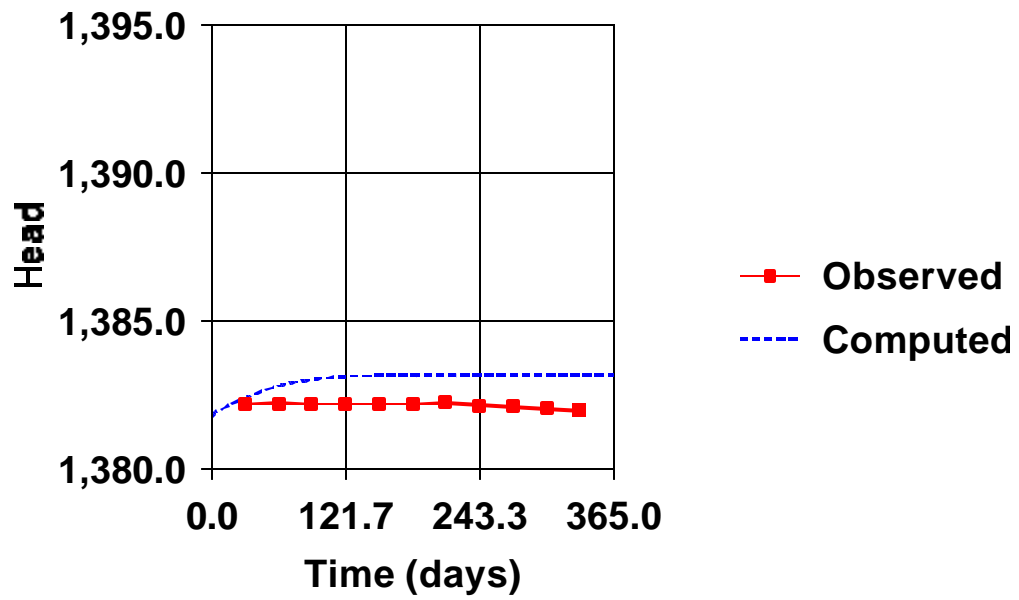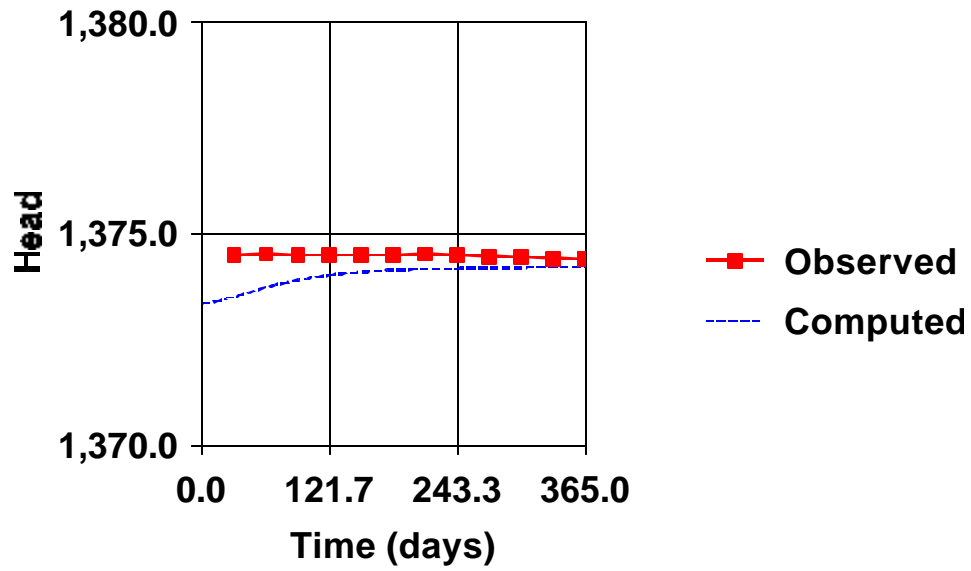
**Observed vs. Simulated heads for Well 17**
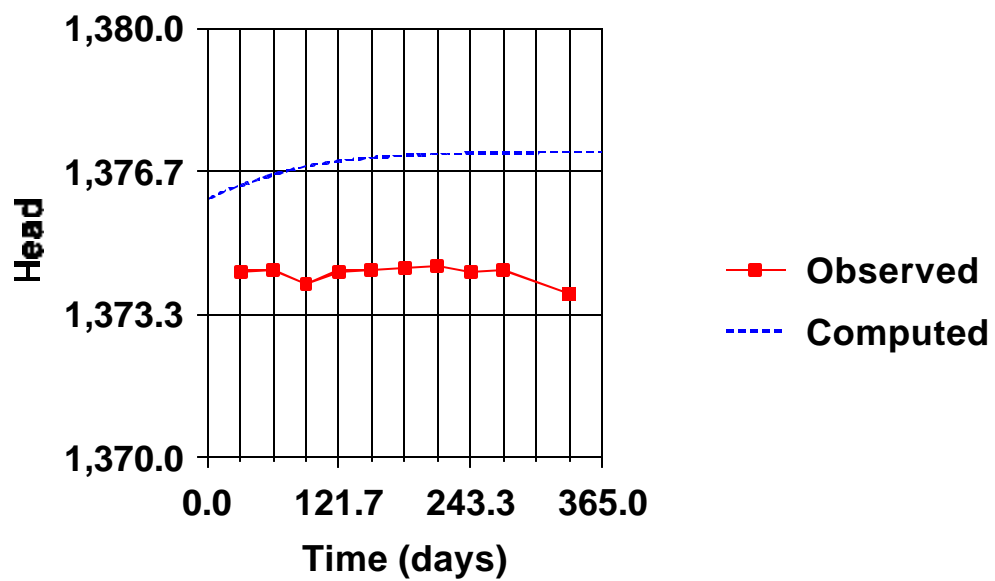
# Observed vs. Simulated heads for Well 18
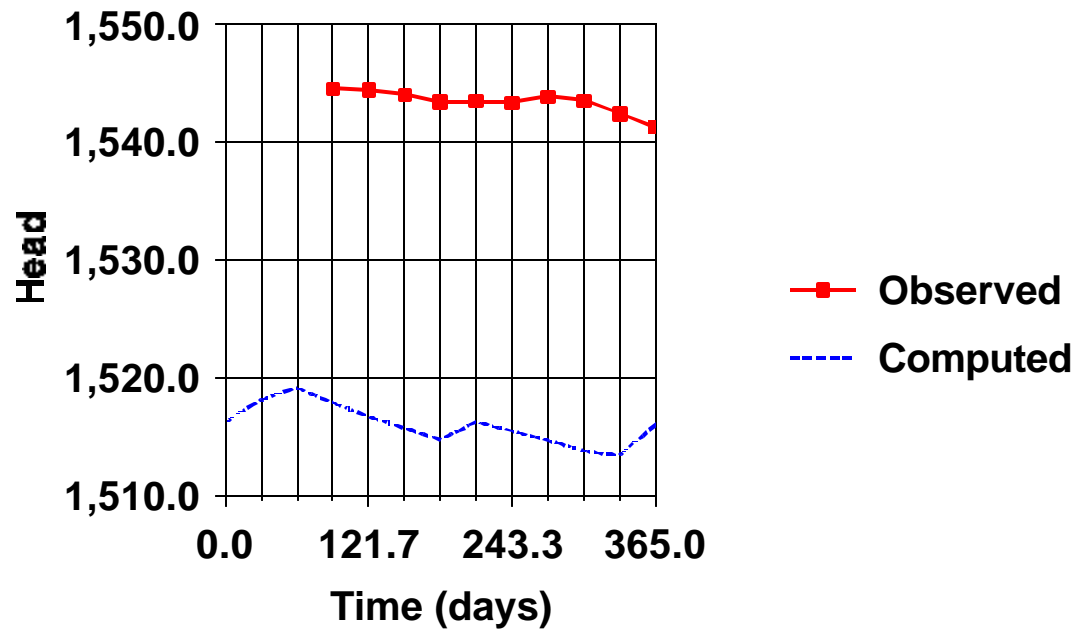
Appendix 5:

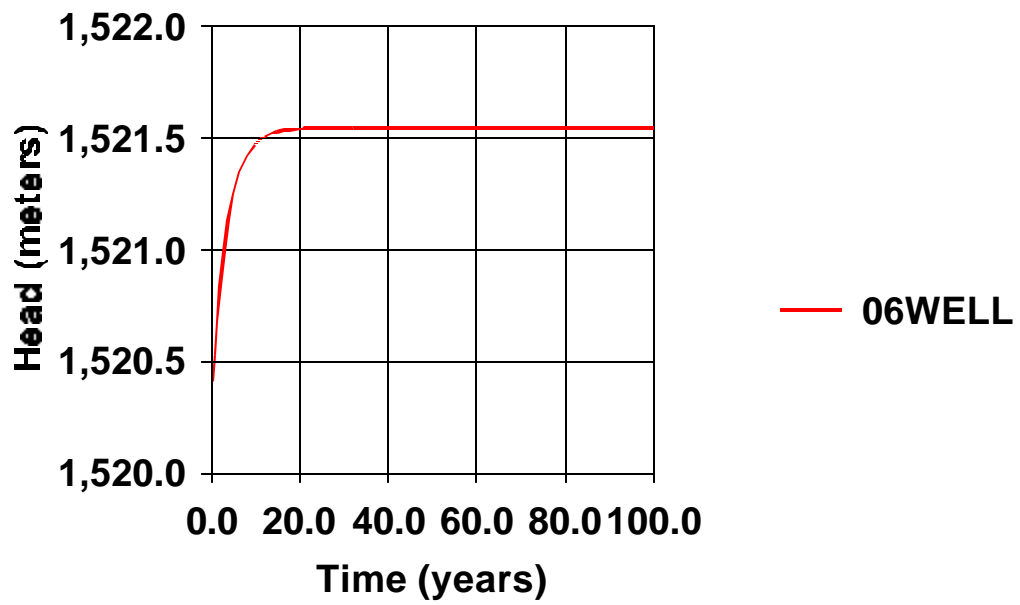Hydrographs of the observation points for the extended current water use scenario
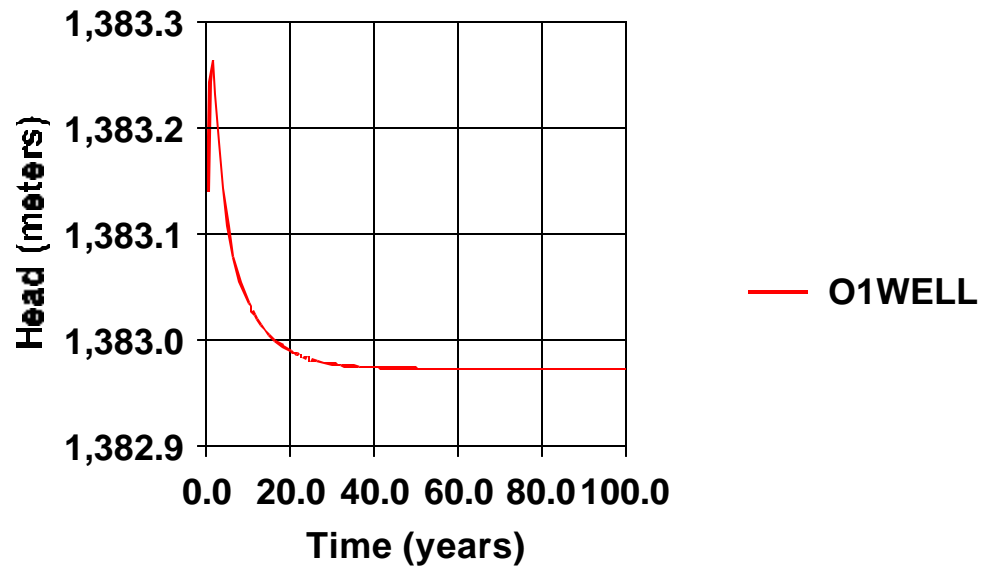
# Head vs. Time at Observation Point 1



# Head vs. Time at Observation Point 2
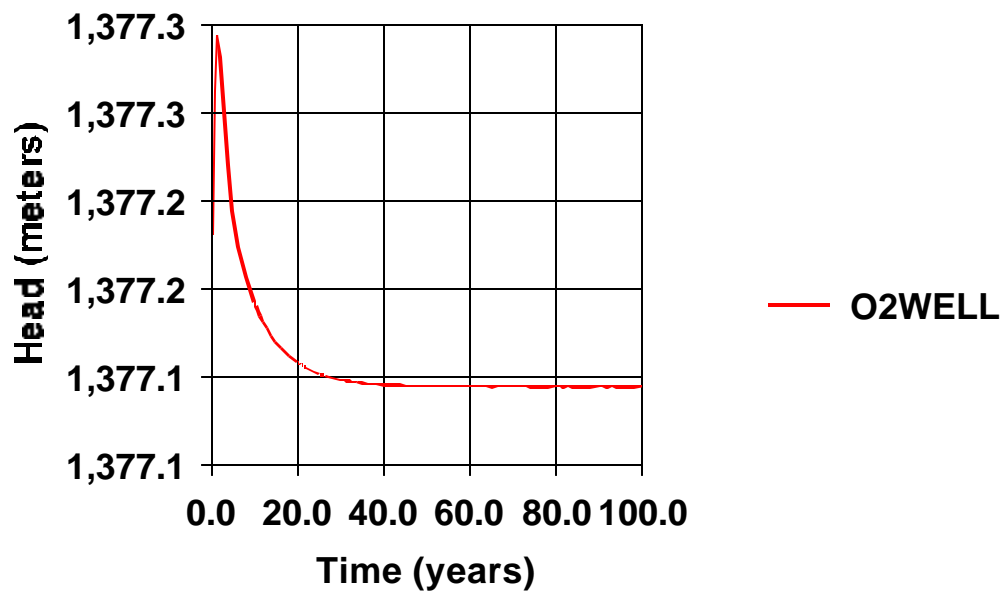
# Head vs. Time at Observation Point 3
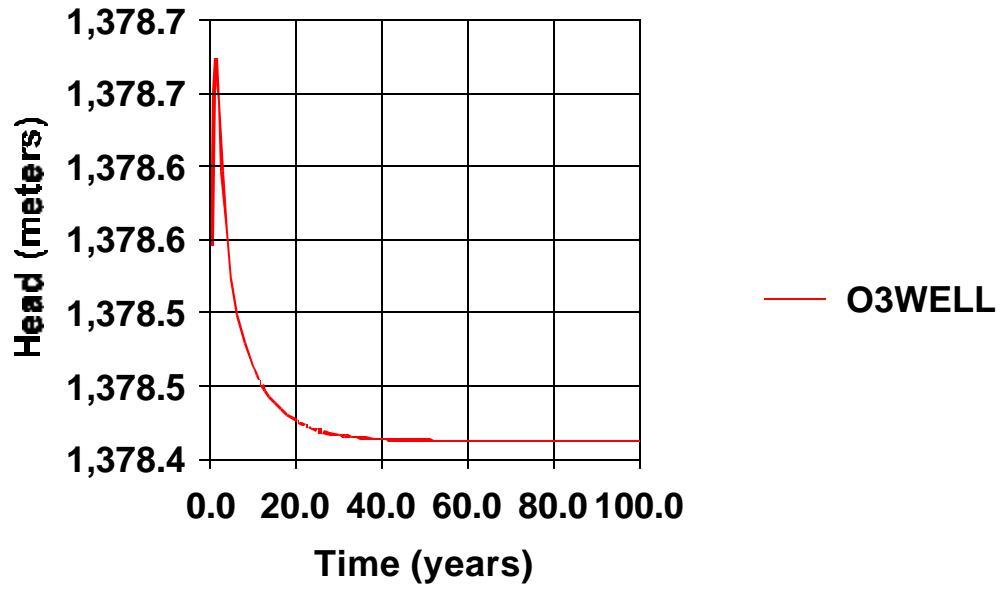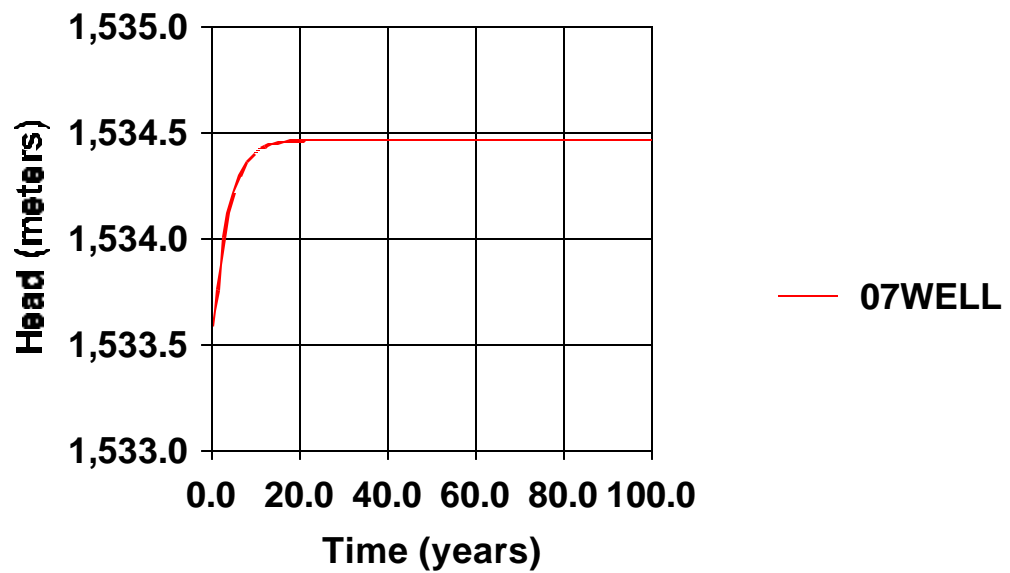


# Head vs. Time at Observation Point 4
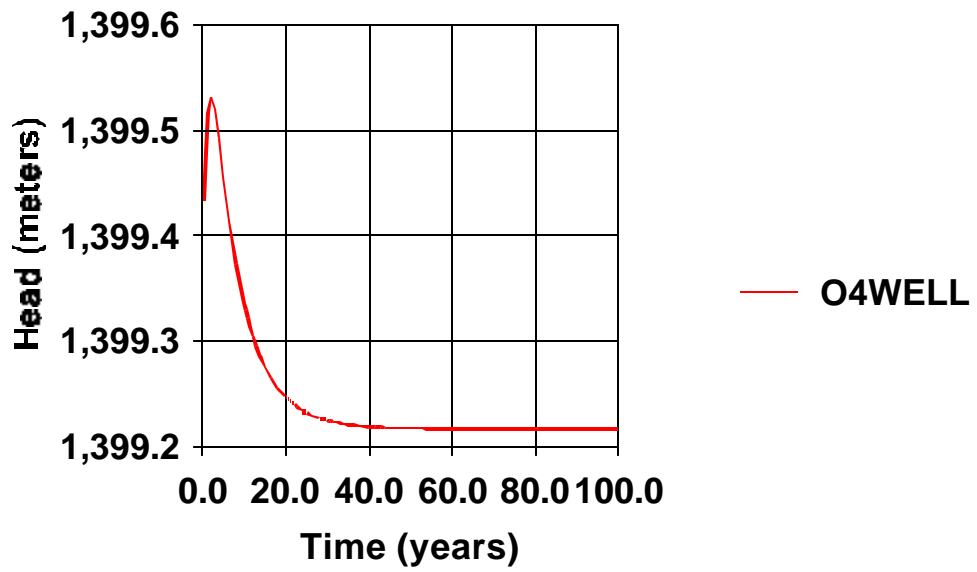
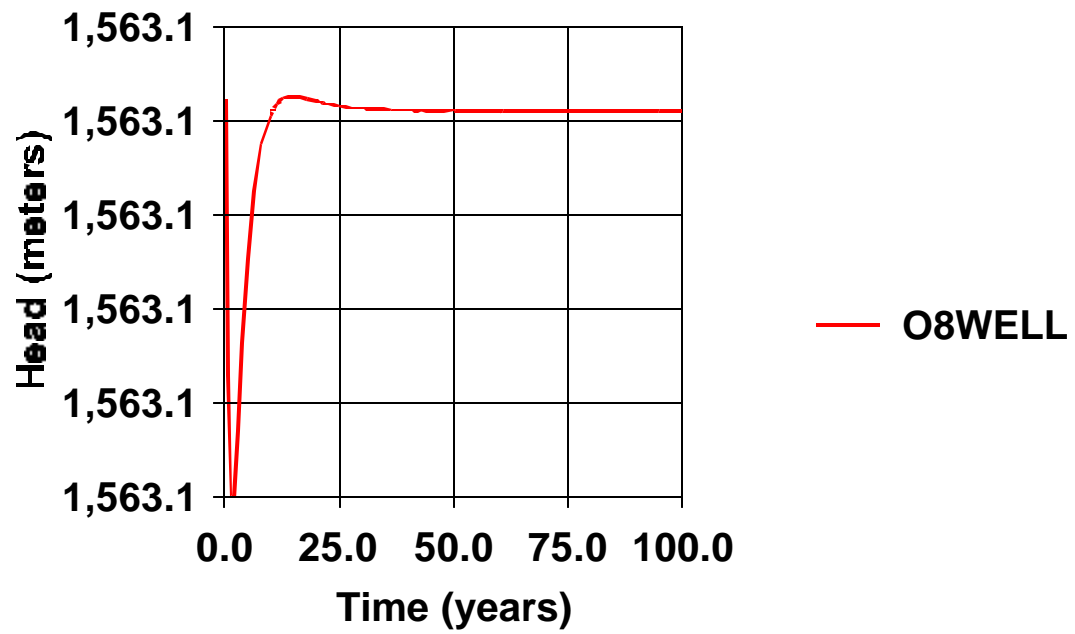# Head vs. Time at Observation Point 5
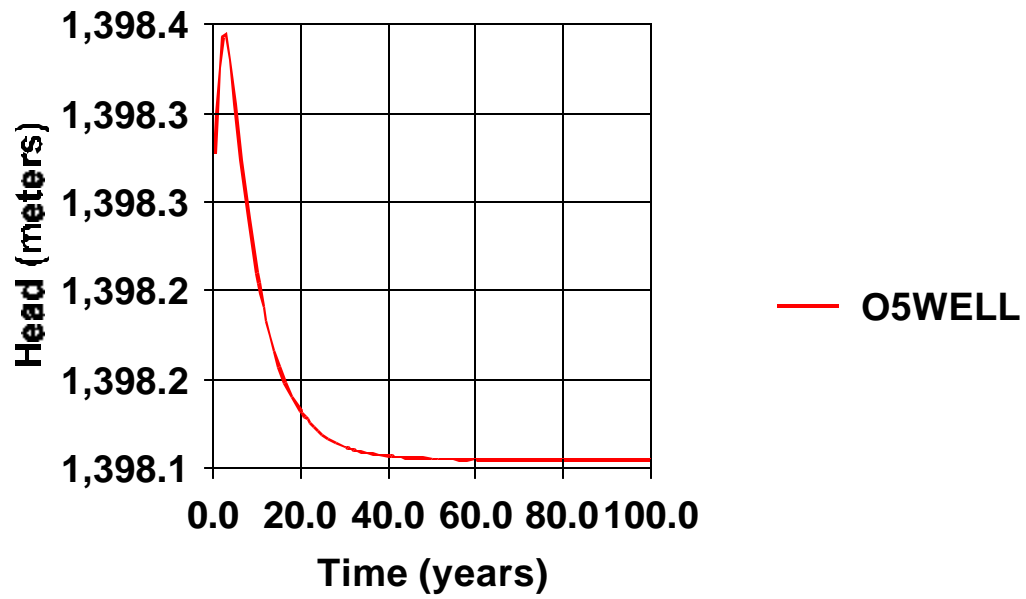


# Head vs. Time at Observation Point 6
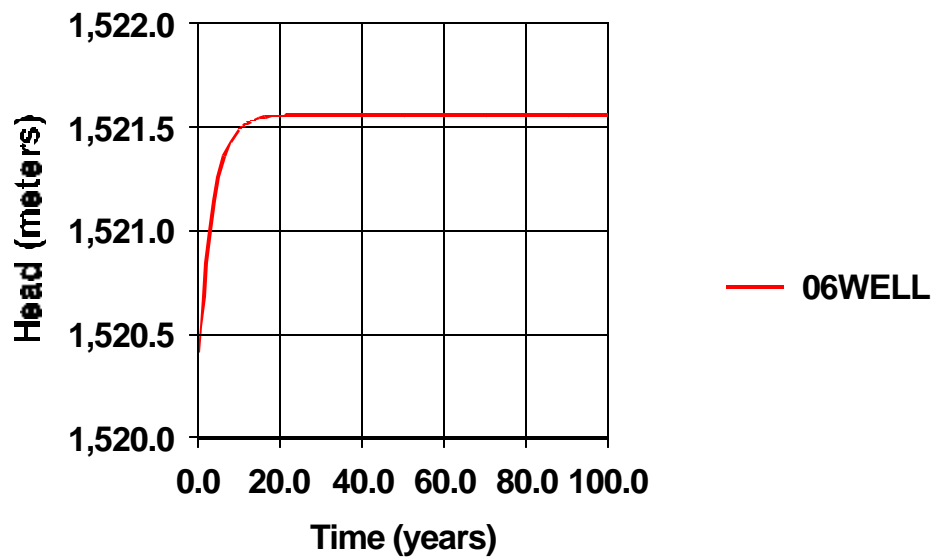
# Head vs. Time at Observation Point 7
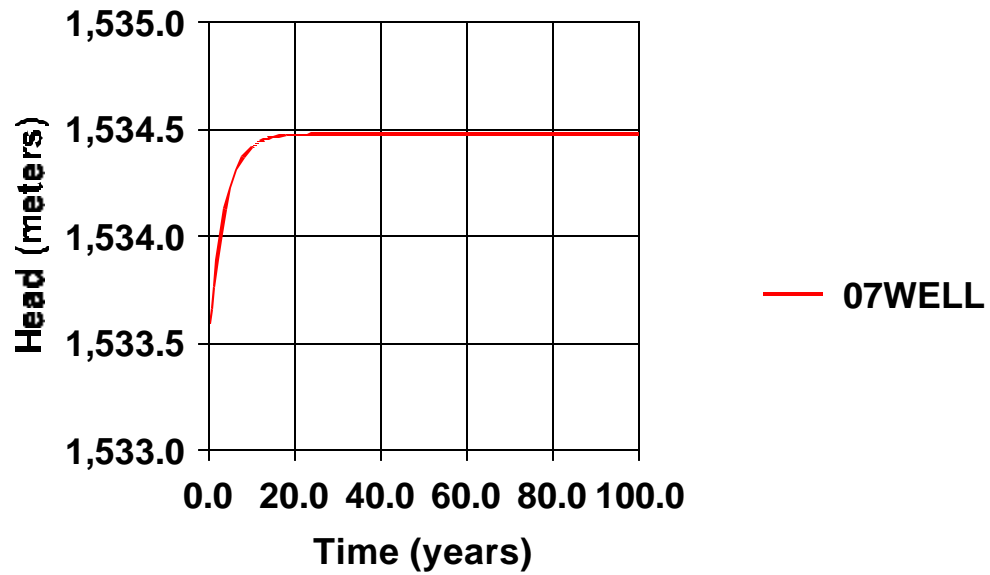


# Head vs. Time at Observation Point 8
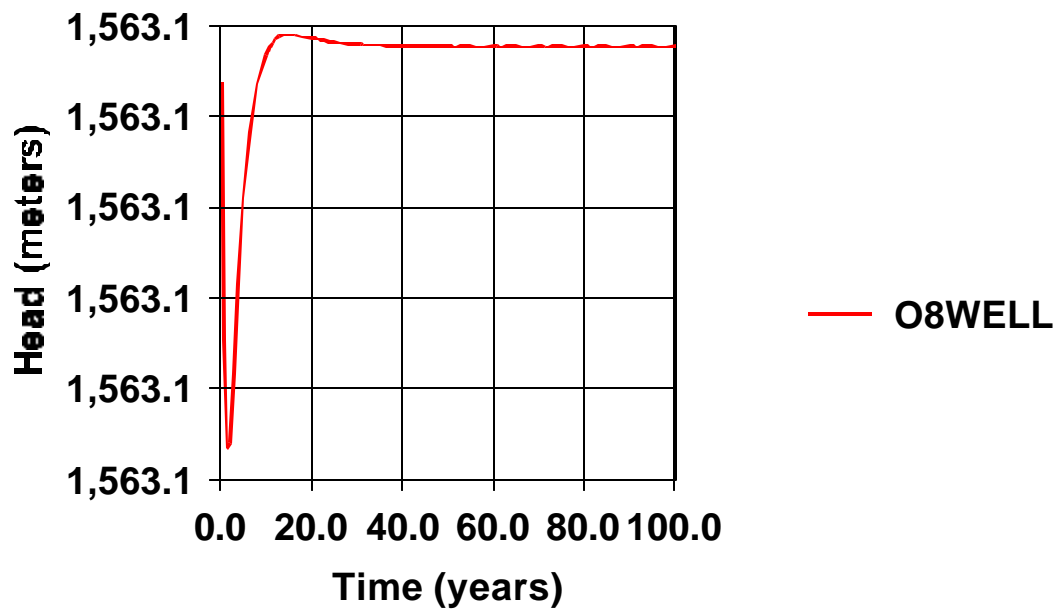
Appendix 6:

Hydrographs of the observation points for the extended safe yield water use scenario
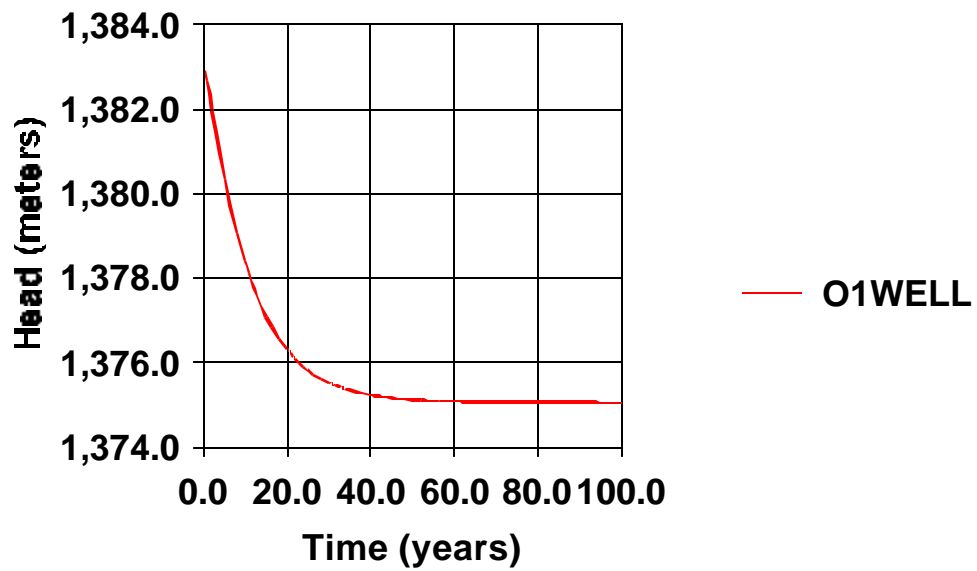
## Head vs. Time at Observation Point 1



## Head vs. Time at Observation Point 2



146

## Head vs. Time at Observation Point 3



## Head vs. Time at Observation Point 4

# Head vs. Time at Observation Point 5
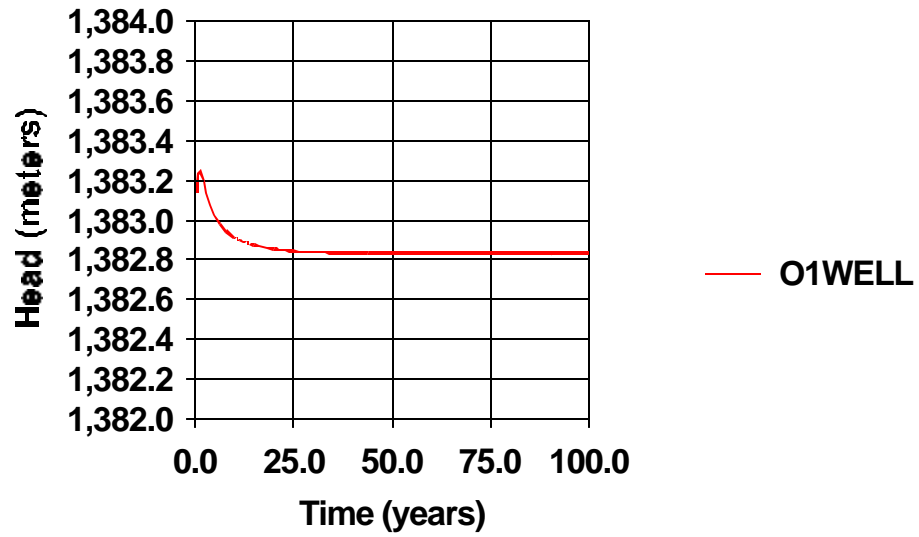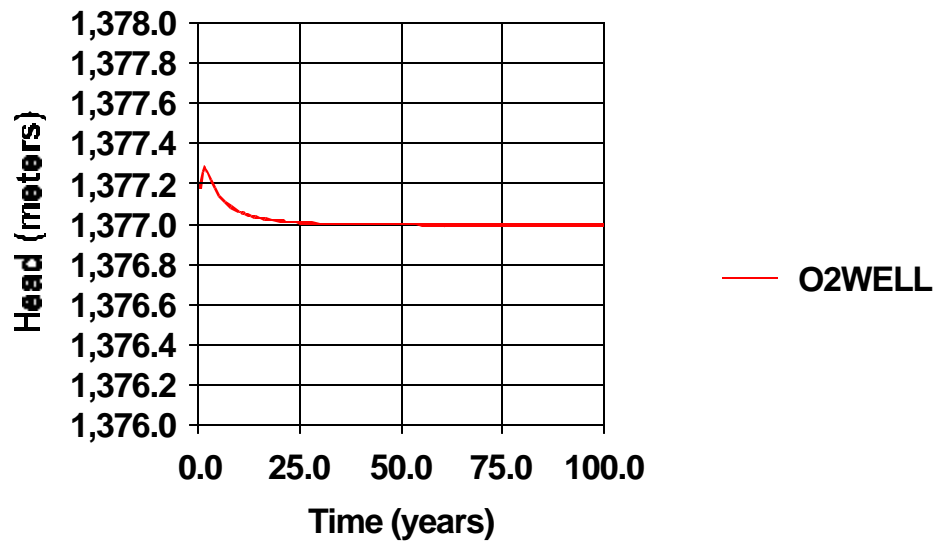
# Head vs. Time at Observation Point 7



Head (meters) vs. Time (years)

— 07WELL

# Head vs. Time at Observation Point 6



Head (meters) vs. Time (years)

— 06WELL
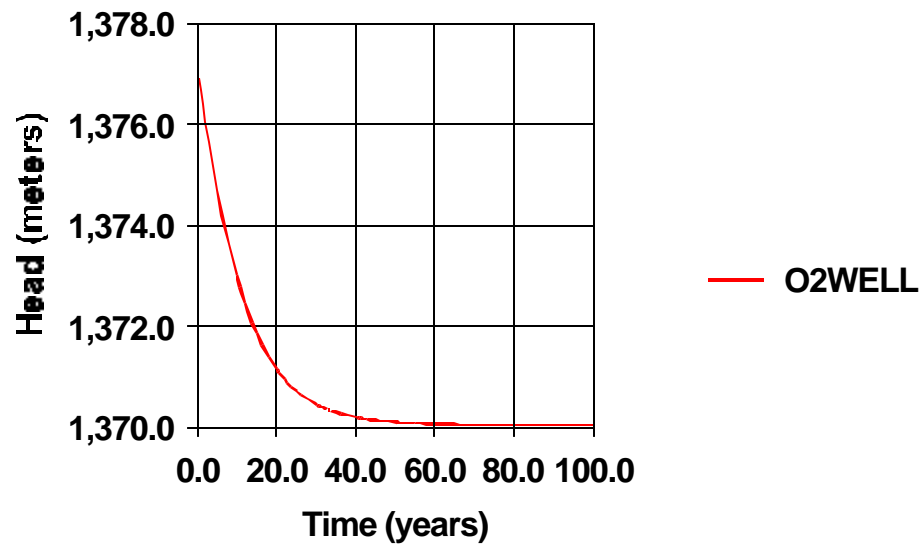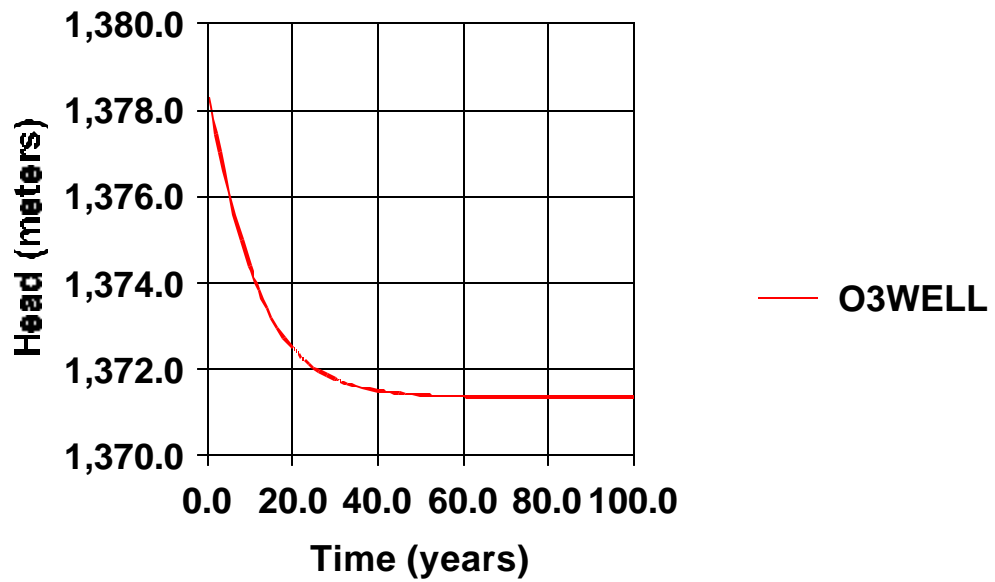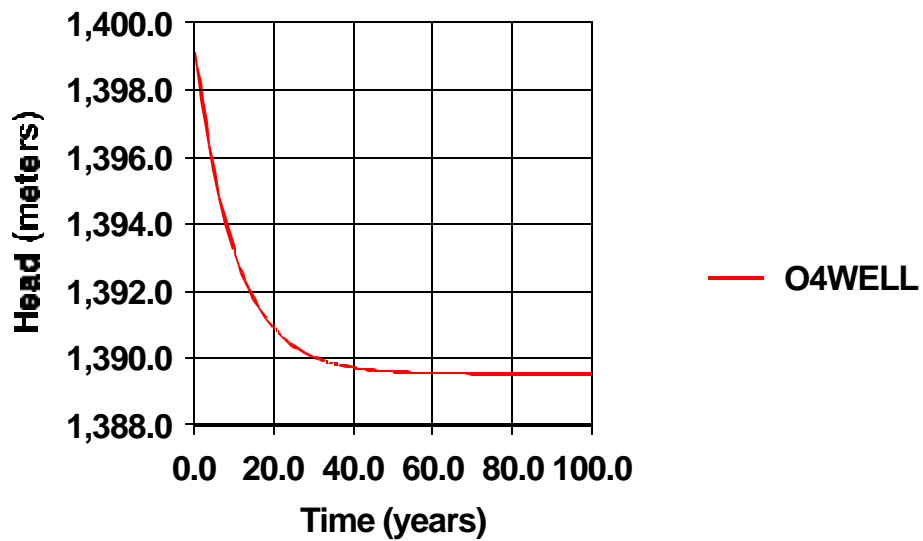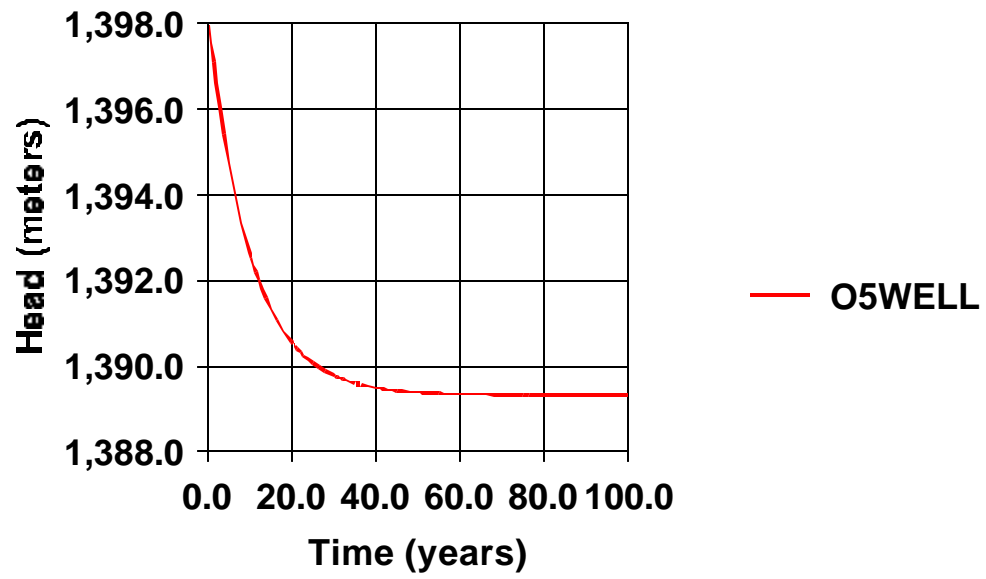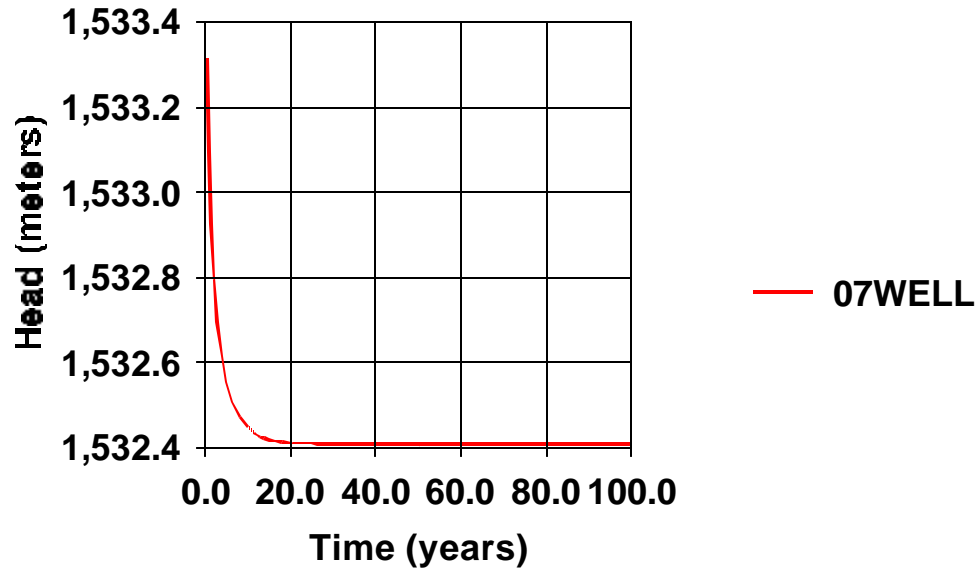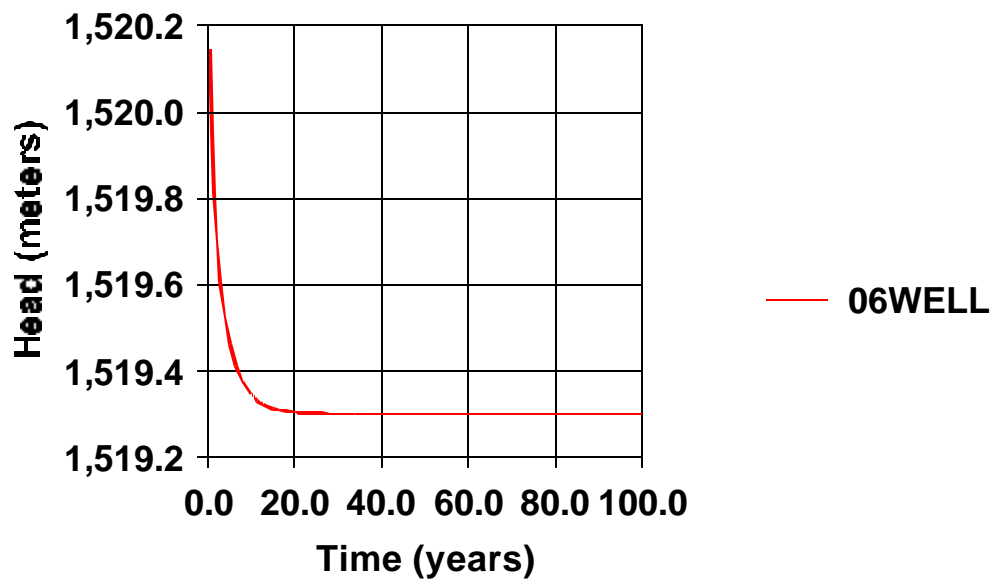
# Head vs. Time at Observation Point 8
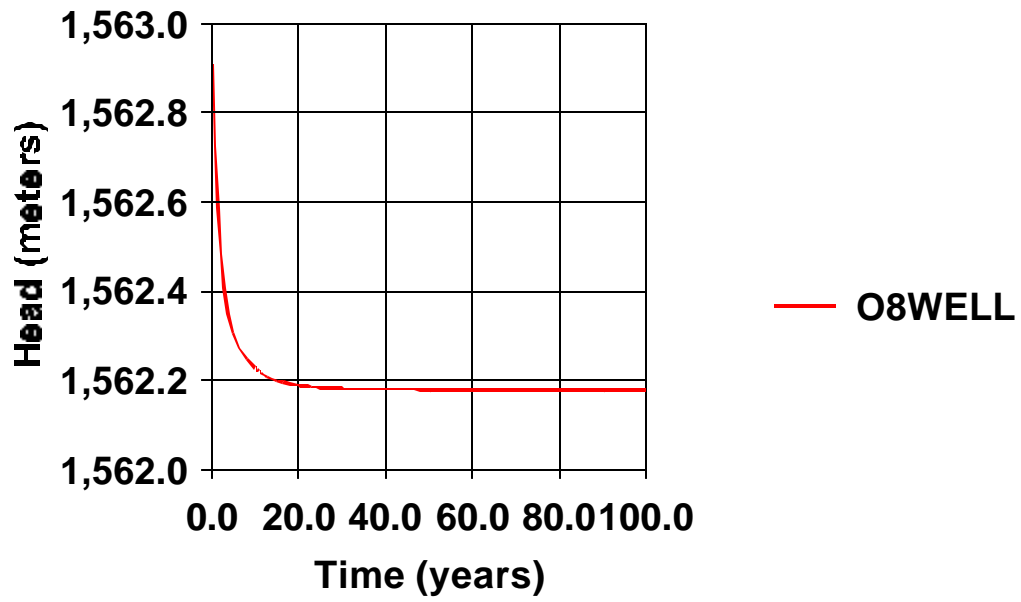
Appendix 7:

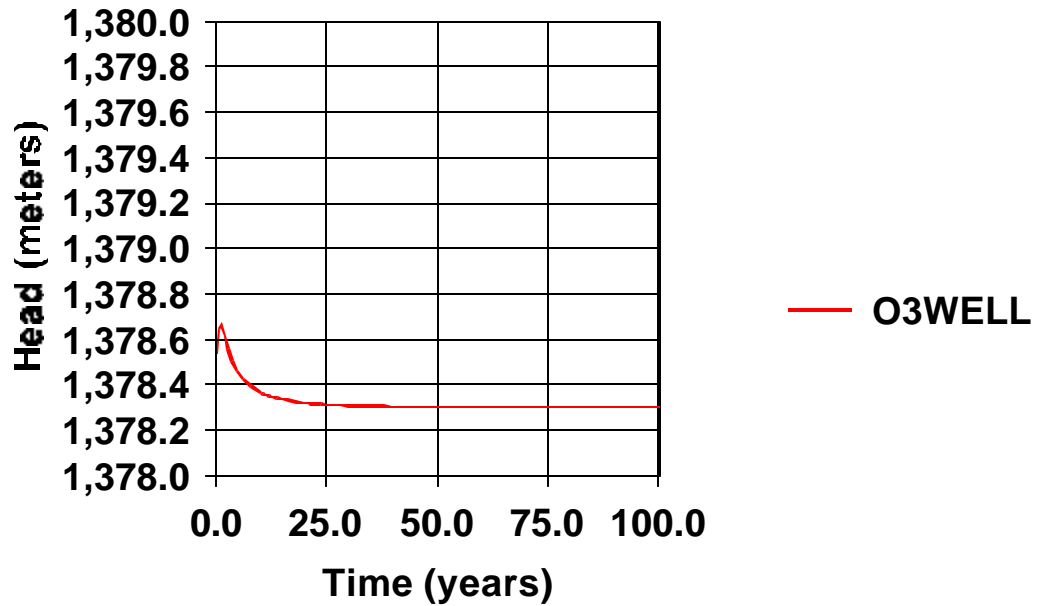Hydrographs of the observation points for the extended sustainable yield water use scenario
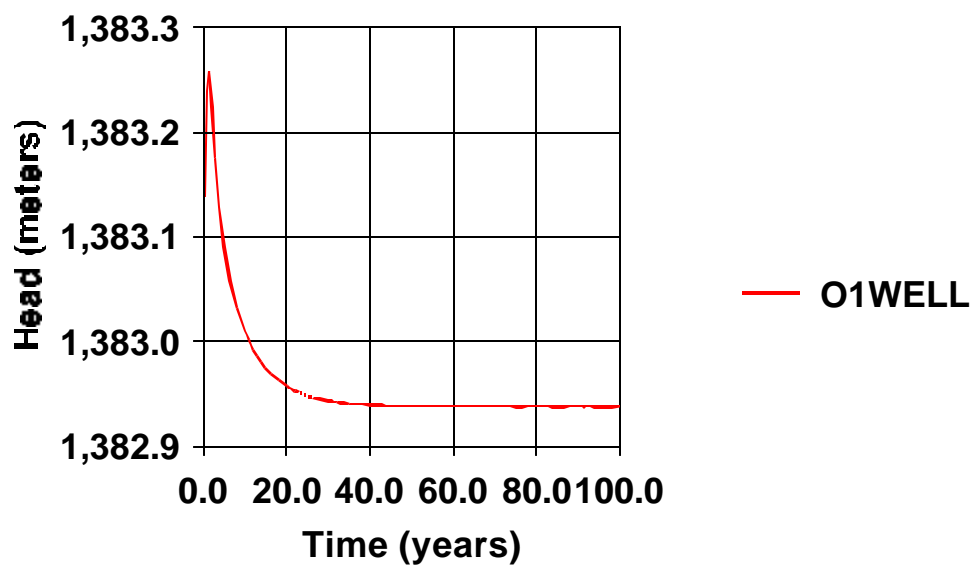
## Head vs. Time at Observation Point 1



## Head vs. Time at Observation Point 2

Head vs. Time at Observation Point 4



Head vs. Time at Observation Point 5

## Head vs. Time at Observation Point 6



## Head vs. Time at Observation Point 7



154
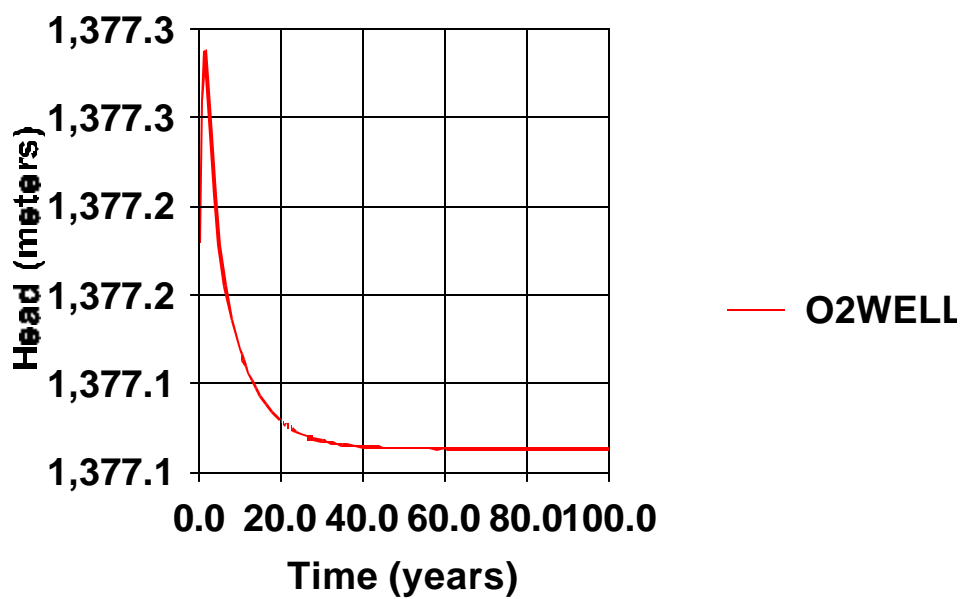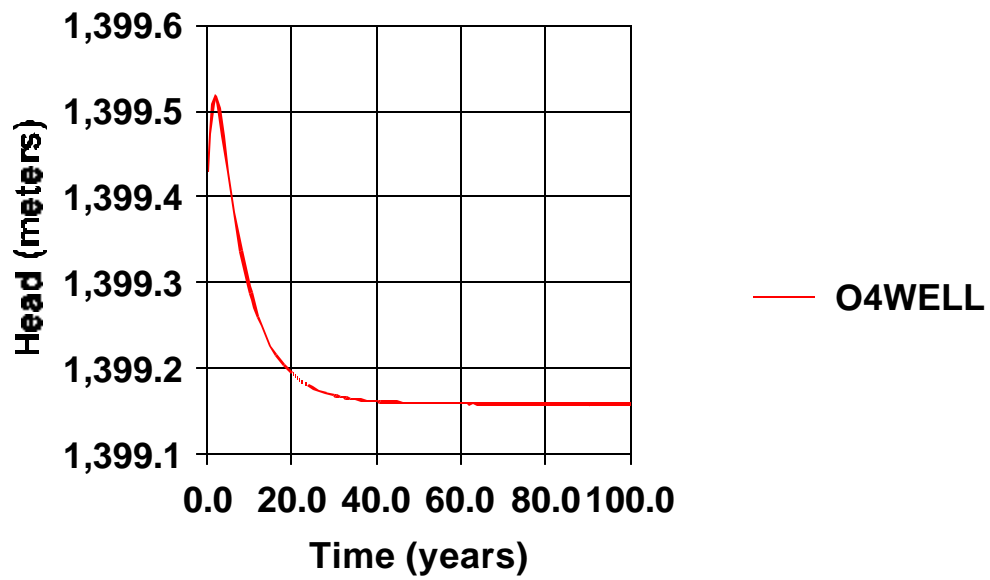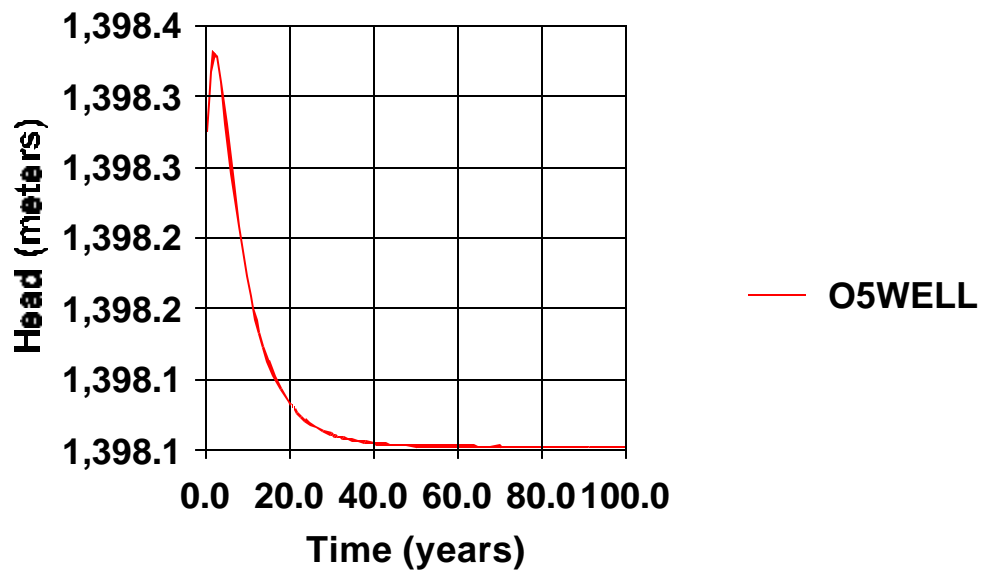
# Head vs. Time at Observation Point 8

Appendix 8:

Hydrographs of the observation points for the American Ranch Build Out scenario
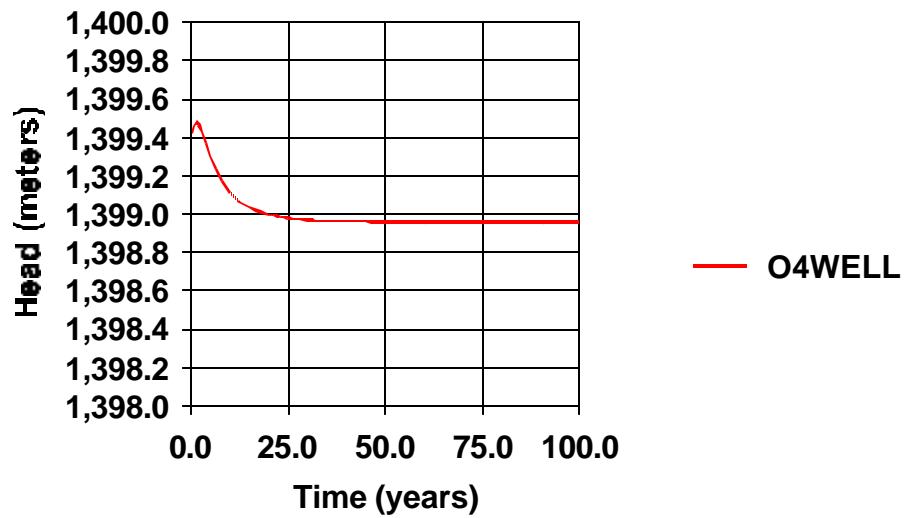
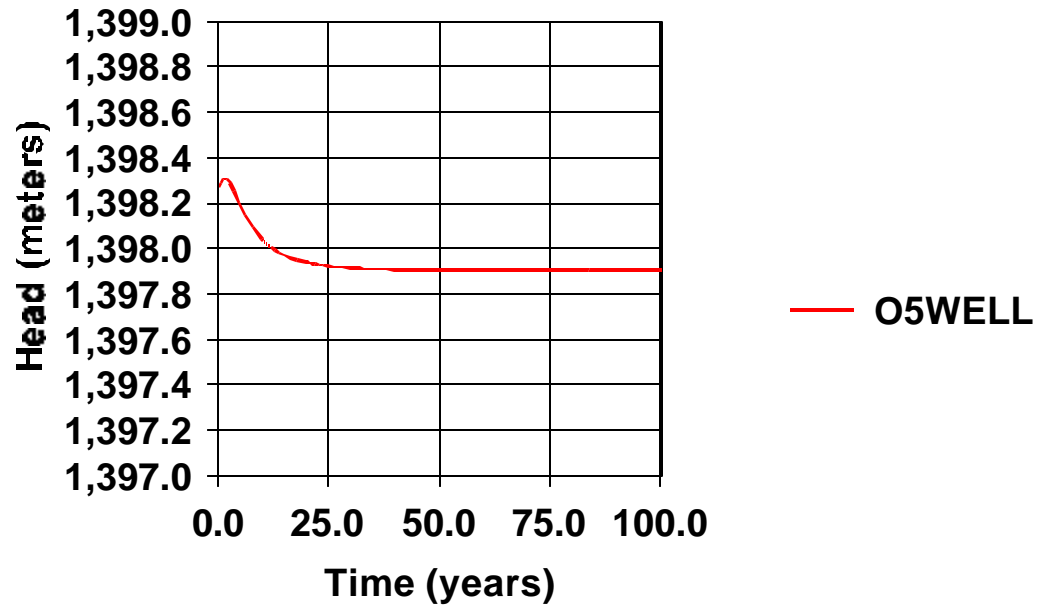## Head vs. Time at Observation Point 1



## Head vs. Time at Observation Well 2

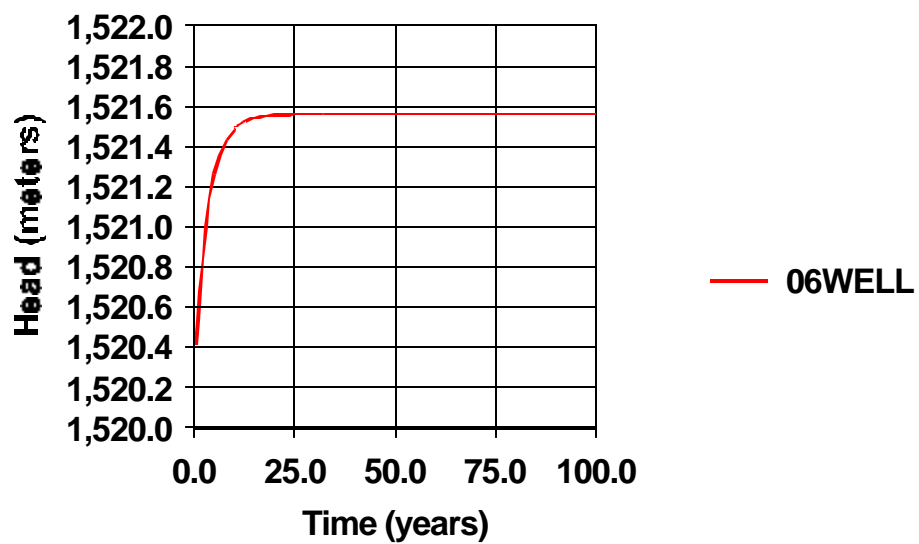# Head vs. Time at Observation Well 3



--- O3WELL

# Head vs. Time at Observation Well 4



--- O4WELL

## Head vs. Time at Observation Well 5



O5WELL

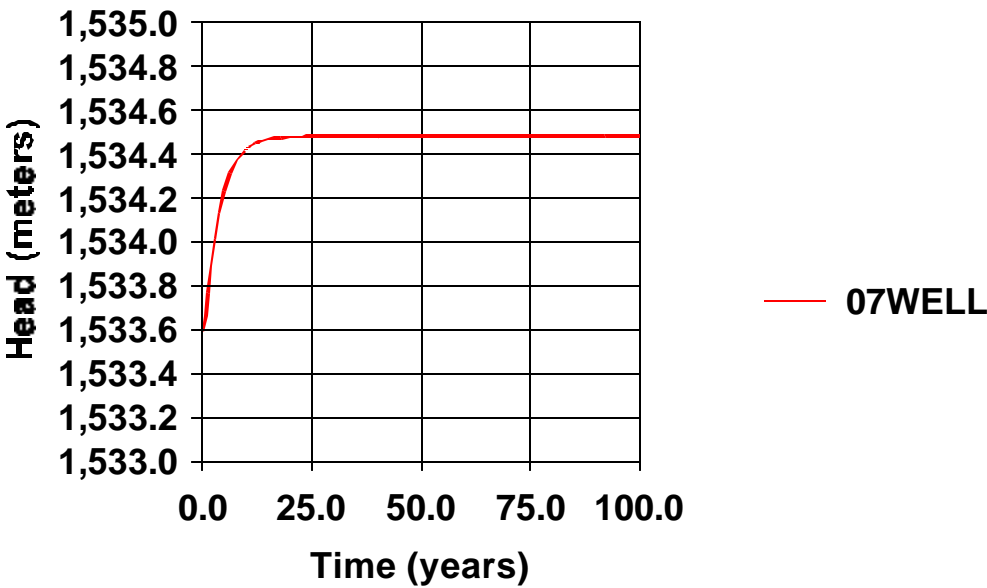## Head vs. Time at Observation Well 6



06WELL

## Head vs. Time at Observation Point 7



## Head vs. Time at Observation Point 8